THE SYNTHESIS OF HYPERBRANCHED EPOXY RESIN FOR IMPROVEMENT OF THERMAL, MECHANICAL, AND ADHESION PROPERTIES OF EPOXY ADHESIVE

Mr. Tossapol Boonlert-uthai

จุฬาลงกรณ์มหาวิทยาลัย
CHULALONGKORN UNIVERSITY

A Dissertation Submitted in Partial Fulfillment of the Requirements
for the Degree of Doctor of Engineering in Chemical Engineering
Department of Chemical Engineering
FACULTY OF ENGINEERING
Chulalongkorn University
Academic Year 2019

การสังเคราะห์ไฮเปอร์บรานซ์อิพ็อกซีเรซิน สำหรับการปรับปรุงสมบัติเชิงความร้อน สมบัติเชิงกล
และสมบัติการยึดติดของกาวอิพ็อกซี

นายทศพล บุญเลิศอุทัย

วิทยานิพนธ์นี้เป็นส่วนหนึ่งของการศึกษาตามหลักสูตรปริญญาวิศวกรรมศาสตรดุษฎีบัณฑิต
สาขาวิชาวิศวกรรมเคมี ภาควิชาวิศวกรรมเคมี
คณะวิศวกรรมศาสตร์ จุฬาลงกรณ์มหาวิทยาลัย
ปีการศึกษา 2562

Thesis Title	THE SYNTHESIS OF HYPERBRANCHED EPOXY RESIN FOR IMPROVEMENT OF THERMAL, MECHANICAL, AND ADHESION PROPERTIES OF EPOXY ADHESIVE
By	Mr. Tossapol Boonlert-uthai
Field of Study	Chemical Engineering
Thesis Advisor	Associate Professor Anongnat Somwangthanaroj, Ph.D.

Accepted by the FACULTY OF ENGINEERING, Chulalongkorn University in Partial Fulfillment of the Requirement for the Doctor of Engineering

.... Dean of the FACULTY OF ENGINEERING
(Associate Professor Supot Teachavorasinskun, D.Eng.)

DISSERTATION COMMITTEE

.... Chairman
(Associate Professor Tharathon Mongkhonsi, Ph.D.)

.... Thesis Advisor
(Associate Professor Anongnat Somwangthanaroj, Ph.D.)

.... Examiner
(Associate Professor Tawatchai Charinpanitkul, D.Eng.)

.... Examiner
(Associate Professor Varong Pavarajarn, Ph.D.)

.... External Examiner
(Assistant Professor Wanchai Lerdwijitjarud, Ph.D.)

ทศพล บุญเลิศอุทัย : การสังเคราะห์ไฮเปอร์บรานซ์อิพ็อกซีเรซิน สำหรับการปรับปรุงสมบัติเชิงความร้อน สมบัติเชิงกล และสมบัติการยึดติดของกาวอิพ็อกซี. (THE SYNTHESIS OF HYPERBRANCHED EPOXY RESIN FOR IMPROVEMENT OF THERMAL, MECHANICAL, AND ADHESION PROPERTIES OF EPOXY ADHESIVE) อ.ที่ปรึกษาหลัก : รศ. ดร.อนงค์นาฏ สมหวังธนโรจน์

งานวิจัยนี้สังเคราะห์และศึกษาคุณลักษณะของไฮเปอร์บรานซ์อิพ็อกซีเรซินด้วยปฏิกิริยาพอลิคอนเดนเซชัน A_2 + B_4 ที่มีบิสฟีนอลเอ (BPA) และพอลิเอทิลีนไกลคอล (PEG) เป็นมอนอเมอร์ A_2 และเพนตะอีริทริทอลเป็นมอนอเมอร์ B_4 สำหรับการแตกกิ่งและมีหมู่อิพ็อกซีเป็นหมู่ปลาย โดยมีการเปลี่ยนแปลงปริมาณของโพลิเอทิลีนไกลคอลที่ 0, 5, 10 และ 15 เปอร์เซ็นต์โดยน้ำหนักของ BPA พบว่าเรซินที่สังเคราะห์นั้นสามารถถูกยืนยันด้วยพันธะเคมีที่สำคัญและโครงสร้างที่น่าจะเป็นไปได้ด้วยเทคนิคฟูเรียร์ทรานส์ฟอร์มอินฟราเรดสเปกโตรสโคปี (FTIR) และเทคนิคโปรตรอนและคาร์บอน-13 นิวเคลียร์แมกเนติกเรโซแนนซ์สเปกโตรสโคปี (H NMR และ ^{13}C NMR) และเทคนิค ^{13}C NMR สามารถหาระดับการแตกแขนงของเรซินที่ถูกสังเคราะห์ได้ พบว่าระดับการแตกแขนงของทุกเรซินที่ถูกสังเคราะห์มีค่ามากกว่า 0.5 ซึ่งหมายความว่าเป็นไฮเปอร์บรานซ์พอลิเมอร์ทั้งหมด มีระดับการแตกแขนงเพิ่มขึ้นเมื่อมีปริมาณของพอลิเอทิลีนไกลคอลเพิ่มขึ้นตั้งแต่ 0.82 – 0.90 การศึกษาการบ่มด้วยความร้อนโดยมีไดเอทิลีนไตรเอมีน (DETA) เป็นสารบ่ม พบว่าทั้งระบบไฮเปอร์บรานซ์พอลิเมอร์ที่สังเคราะห์ทุกชนิดและระบบเรซินผสมระหว่างไฮเปอร์บรานซ์พอลิเมอร์ที่สังเคราะห์และไดไกลซิดิลอีเทอร์ของบิสฟีนอลเอ (DGEBA) มีพฤติกรรมการบ่มแบบปฏิกิริยาออโตแคทตาไลติกของสมการ Šesták-Berggren และพบว่าไฮเปอร์บรานซ์อิพ็อกซีที่มีพอลิเอทิลีนไกลคอล 10 เปอร์เซ็นต์โดยน้ำหนัก (HBE10P) และระบบเรซินผสมระหว่างไดไกลซิดิลอีเทอร์ของบิสฟีนอลเอและไฮเปอร์บรานซ์อิพ็อกซีที่มีพอลิเอทิลีนไกลคอล 10 เปอร์เซ็นต์โดยน้ำหนัก (DH10P) ให้พฤติกรรมการบ่มด้วยความร้อนและสมบัติเชิงความร้อนที่เหมาะสมที่สุด จากการศึกษาพบว่าอัตราส่วนเรซินผสมระหว่าง DGEBA และ HBE10P เท่ากับ 90:10 (D90H10) ที่มีความเข้มข้นของตัวกระตุ้นปฏิกิริยาด้วยรังสีอัลตราไวโอเลตที่ 5 เปอร์เซ็นต์โดยน้ำหนักของเรซิน ให้ระดับการบ่มด้วยรังสีอัลตราไวโอเลตสูง เวลาการเกิดเจลต่ำ และมีสมบัติกระแสวิทยากับสมบัติเชิงความร้อนที่เหมาะสม นอกจากนี้อุณหภูมิและเวลาในการฉายรังสีที่มากขึ้นจะทำให้ระดับการบ่มสูงขึ้น แต่เมื่อให้เวลาในการฉายรังสีมากเกินไปจะทำให้ระดับการบ่มลดลง นอกจากนี้ความเข้มข้นของรังสีอัลตราไวโอเลต กลไกการเกิดปฏิกิริยา และโครงสร้างของเรซินมีผลต่ออุณหภูมิเปลี่ยนสถานะคล้ายแก้ว ซึ่งถูกยืนยันโดยรัศมีไจเรชันของโครงสร้างตาข่ายที่มากขึ้น โดยวัดจากเทคนิค small-angle X-ray scattering (SAXS)

สาขาวิชา	วิศวกรรมเคมี	ลายมือชื่อนิสิต ....
ปีการศึกษา	2562	ลายมือชื่อ อ.ที่ปรึกษาหลัก ....

5771411021 : MAJOR CHEMICAL ENGINEERING

KEYWOR   thermal cure, UV cure, thermal property, rheological property,
D: hyperbranched epoxy resin

Tossapol Boonlert-uthai : THE SYNTHESIS OF HYPERBRANCHED EPOXY RESIN FOR IMPROVEMENT OF THERMAL, MECHANICAL, AND ADHESION PROPERTIES OF EPOXY ADHESIVE. Advisor: Assoc. Prof. Anongnat Somwangthanaroj, Ph.D.

This research aimed to synthesize and characterize the hyperbranched epoxy resin synthesized by $A_2 + B_4$ polycondensation reaction consisting of bisphenol A (BPA) and polyethylene glycol (PEG) as A_2 monomers, pentaerythritol as B_4 branching monomer, and epoxide end group. There were varying PEG contents of 0, 5, 10, and 15 wt% of BPA. It was found that the synthesized resins could be confirmed by identifying the important chemical bond and possible structure by Fourier-transform infrared spectroscopy (FTIR) and H- and ^{13}C-nuclear magnetic resonance (H-NMR and ^{13}C-NMR) techniques. The ^{13}C-NMR technique could identify the degree of branching (DB) of the synthesized resins. It was found that the degree of branching of the synthesized resins was higher than 0.5 in which it meant they were the hyperbranched polymers. There was a high degree of branching when the content of PEG increased from 0.82 to 0.90. The study of thermal cure with diethylenetriamine (DETA) as a curing agent, both the synthesized hyperbranched epoxy systems and combined resins between the hyperbranched polymer and diglycidyl ether of bisphenol A (DGEBA) had the curing behavior following auto-catalytic reaction of Šesták-Berggren equation. The hyperbranched epoxy resin system with 10 wt% PEG (HBE10P) and the combined resin system between DGEBA and hyperbranched epoxy with 10 wt% PEG (DH10P) provided thermal curing behavior and thermal properties appropriately. The ratio of DGEBA to HBE10P of 90:10 (D90H10) with 5 wt% photoinitiator provided high UV conversion, low gelation time, and suitable rheological and thermal properties. Furthermore, high temperature and high irradiation time provided the conversion; however, when the irradiation time was too much, the conversion decreased. Besides, UV intensity, reaction mechanism, and structure of resin affected glass transition temperature in which it was confirmed by the radius of gyration of the network segment measured by small-angle X-ray scattering (SAXS) technique.

Field of Study:	Chemical Engineering	Student's Signature
		....
Academic Year:	2019	Advisor's Signature
		....

ACKNOWLEDGEMENTS

TABLE OF CONTENTS

Page

LIST OF TABLES

จุฬาลงกรณ์มหาวิทยาลัย

CHULALONGKORN UNIVERSITY

LIST OF FIGURES

CHAPTER 1
INTRODUCTION

1.1. General Introduction

The Head gimbals assembly (HGA) is an important part of a hard disk drive because it performs reading and writing the data on a disk. The HGA consists of a slider or read-write head and suspension. The slider is held on suspension by an adhesive as shown in Figure 1.1.
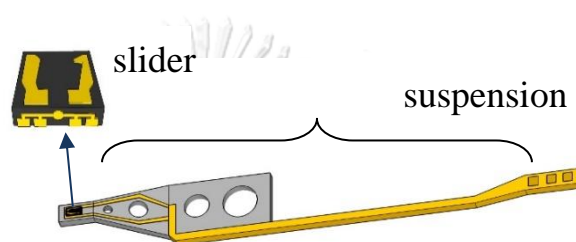
Figure 1.1 Head gimbals assembly (HGA)

Generally, the adhesives used in the HGA process in Western Digital (Bang Pa-in) Co., Ltd. (WD), Thailand, is an epoxy adhesive. The adhesive should be cured by UV- and thermal-curing and its properties: namely, thermal and mechanical properties, have to be appropriate with the HGA. The characterization of the adhesive for the HGA as shown in Table 1.1. Interestingly, glass transition temperature (T_g) of the adhesive used in the HGA process is very low in which the physical property of adhesive likes rubber. Generally, there are widely use diglycidyl ether of bisphenol A (DGEBA) as a base commercial epoxy resin in adhesive because of its overall good properties, such as high thermal and mechanical properties, low shrinkage, excellent adhesion, good chemical resistant, and high reactivity [1-3]. However, there are restrictions of advanced applications due to their inherent brittleness and low toughness. Therefore, it should have ingredients acting as toughener, flexibilizer, and plasticizer in the adhesive. Normally, the structure of the resin molecule most affects the properties of UV-cured adhesive because of homopolymerization reactions in

which there are only epoxy resin molecules in this reaction, as shown in Figure 1.2. Moreover, the physical properties of the cured epoxy depend on the structure of the crosslinking network, curing temperature, and curing time [4-7]. Therefore, the final cured properties of the epoxy system are primarily due to the nature of the epoxy resin.

Several studies added polyethylene glycol (PEG) in the DGEBA resin to develop impact resistance of DGEBA thermoset by decreasing its glass transition temperature [8-11]. However, the crystallization can occur when PEG content increases, and it can hinder and decrease the cure reaction. Besides, the melting, which reduces the thermal stability of the thermoset, can occur when the PEG is excessively added in the system [11, 12].

Table 1.1 Characterization of adhesive for HGA process

Property	Characterization
UV curing condition behavior (Photoinitiator)	• Absorb UVA ray (300 – 400 nm) • Curing time ~ 2 – 3 min
Thermal curing behavior (Curing agent)	• Onset temperature ~ 80 – 100 °C • Peak temperature ~ 120 – 130 °C • Curing time ~ 10 min (at 100 °C)
Glass transition temperature (fully cured by DSC)	• ~ 5 – 10 °C
Viscosity (uncured adhesive)	• ~ 400,000 cP
Pull strength (WD's test)	• ~ 300 gf

$$Ar_3S^+PF_6^- + RH \xrightarrow{h\nu} Ar_2S + Ar\bullet + R\bullet + H^+PF_6^-$$
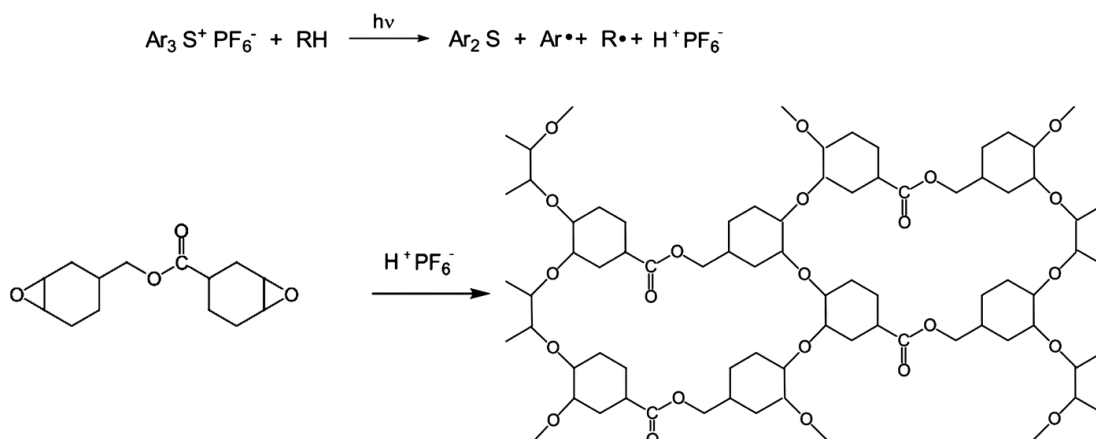
Figure 1.2 Homopolymerization reactions of cycloaliphatic epoxy resins [13]

Hyperbranched epoxy (HBE) resins are one of the special interesting resins because of their easy synthesis accessibility in the one-step procedure, low viscosity, and high solubility. Moreover, it can design an epoxy with unique features, such as a combination of aliphatic-aromatic moieties, as shown in Figure 1.3, and this feature can improve toughness, adhesion strength, elongation at break, and impact strength of the epoxy adhesive. Also, it can reduce curing time and glass transition temperature because of a large number of end functional groups and free volume, respectively [14-16].

Therefore, this research aims to synthesize and characterize hyperbranched epoxy resin by $A_2 + B_4$ polycondensation reaction. Afterward, the research aims to study the relationship of curing behavior, rheological and thermal properties, and adhesive strength of DGEBA modified with HBE resin through photo-initiated cationic polymerization.
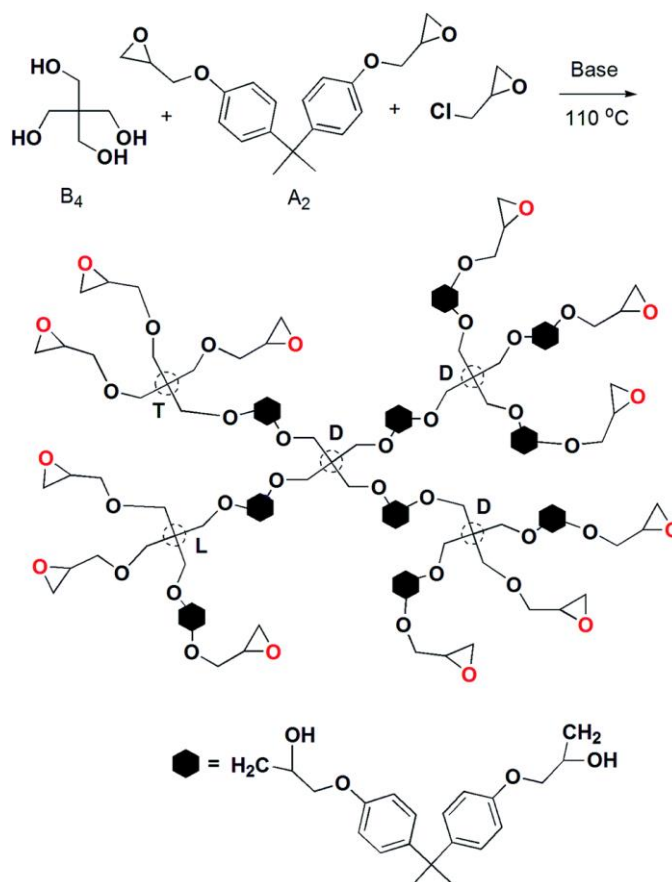
Figure 1.3 Hyperbranched epoxy resin with a combination of aliphatic-aromatic moieties [15]

1.2. Objectives

1.2.1 To synthesize and characterize hyperbranched epoxy resins by $A_2 + B_4$ polycondensation reaction

1.2.2 To study the effects of curing agent, photoinitiator, and hyperbranched epoxy resin on curing and flow behaviors, thermal and mechanical properties, and adhesive strength.

1.3. Scopes of the research

1.3.1 Effects of components for synthesizing hyperbranched epoxy resins, namely, bisphenol A and polyethylene glycol on architectural features and physical properties

1.3.2 Effects of epoxy resin, diethylenetriamine as curing agent, and triarylsulfonium hexafluorophosphate salt photoinitiator, on curing behavior and thermal property by differential scanning calorimetry (DSC) technique

1.3.3 Investigate rheological properties of an uncured epoxy adhesive by rheometer technique

1.4. The procedure of the research

1.4.1 Study HGA process and characterization of commercial adhesive in the process

1.4.2 Study related theory and conduct a literature review

1.4.3 Design the experimental procedure

1.4.4 Synthesize and characterize hyperbranched epoxy resins

1.4.5 Test and analyze the properties of epoxy adhesive

1.4.6 Analyze and conclude the acquired data

1.4.7 Write the thesis and prepare for publication

จุฬาลงกรณ์มหาวิทยาลัย
CHULALONGKORN UNIVERSITY
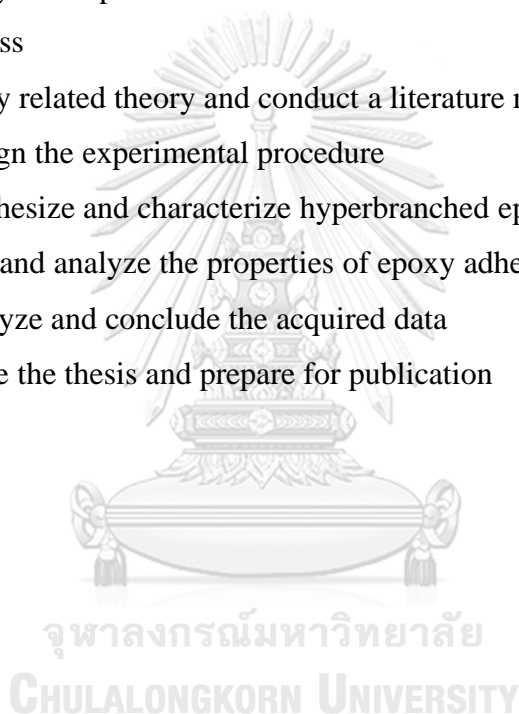
CHAPTER 2
THEORY AND LITERATURE REVIEWS

2.1 Adhesive

Adhesive is a material joining between two surfaces of two substrates permanently by an adhesive bonding process. Generally, the adhesive is a plastic thermoset and it will be dried by curing reaction. The curing reaction is that the adhesive molecules crosslink together and form to a network structure, as shown in Figure 2.1.
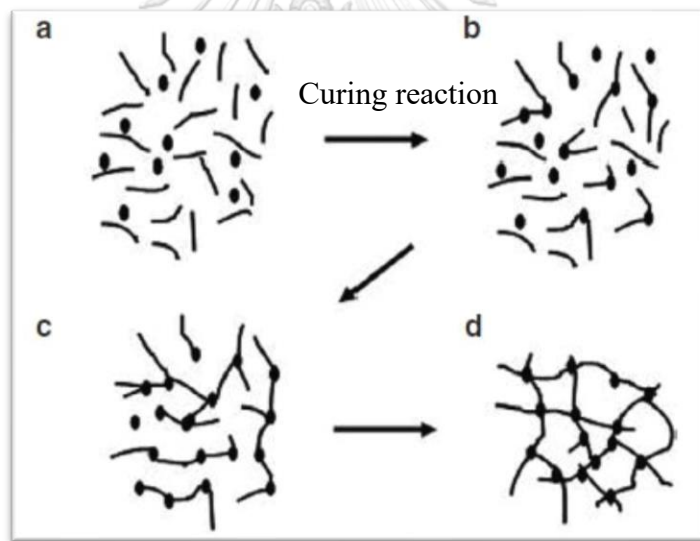
Figure 2.1 The adhesive molecules crosslink together and form to a network structure

2.2 Types of adhesive

The types of adhesive can be classified into three main categories, viz. by source, by physical form, and by type of curing process [17], as shown in Table 2.1 – 2.3, respectively.

Table 2.1 Classification of adhesive by source

Natural adhesive	Synthesis adhesive
• Gelatins	• Thermosetting adhesives
➢ Animal glue	• Thermoplastic adhesives
➢ Fish glue	• Elastomeric adhesives
➢ Casein- and protein-based adhesives	• Alloy adhesives
• Natural rubber adhesives	
• Asphalt & Bitumen	

Table 2.2 Classification of adhesive by physical form

Physical Form	
Liquid Adhesives	Be easily applied using mechanical spreaders such as rolls, by spraying, or by brushing
Paste Adhesives	Have high viscosities to allow application on vertical surfaces with little tendency to sag or drip and can serve as gap fillers and sealants
Tape and Film Adhesives	Provide a bond line with uniform thickness and offer the advantages of no need for metering and ease of dispensing
Powder or Granule Adhesives	Must be heated or dissolved in a solvent to be converted into a liquid form, to enable their application to a surface

Table 2.3 Classification of adhesive by type of curing process

Chemical Curing Adhesives		Physical Curing Adhesives
Polyaddition adhesives:	Polycondensation adhesives:	• Hot melts
• Epoxy adhesives	• Silicones	• Solvent-based adhesives
• Polyurethane adhesives	• Silanes (modified)	• Waterborne adhesives
• Silicone adhesives	• Phenolic adhesives	• Contact adhesives
• Hot curing rubber adhesives	• Polyamides	• Dispersion adhesives
Polymerization adhesives:		• Plastisol adhesives
• Methacrylate adhesives		• Pressure-sensitive adhesives
• Cyanoacrylates		
• Anaerobic adhesives		
• Unsaturated polyester adhesives		
• Acrylates (radiation cure)		
• Epoxy adhesives (radiation cure)		

2.3 Theories of adhesion

There are various theories to explain adhesion between adhesive and substate: mechanical anchoring, contact charging, diffusion, dipole-dipole interaction, chemical cross-linking, hydrogen bridging bonds, and mirror forces in metals, as shown in Figure 2.2 [18].
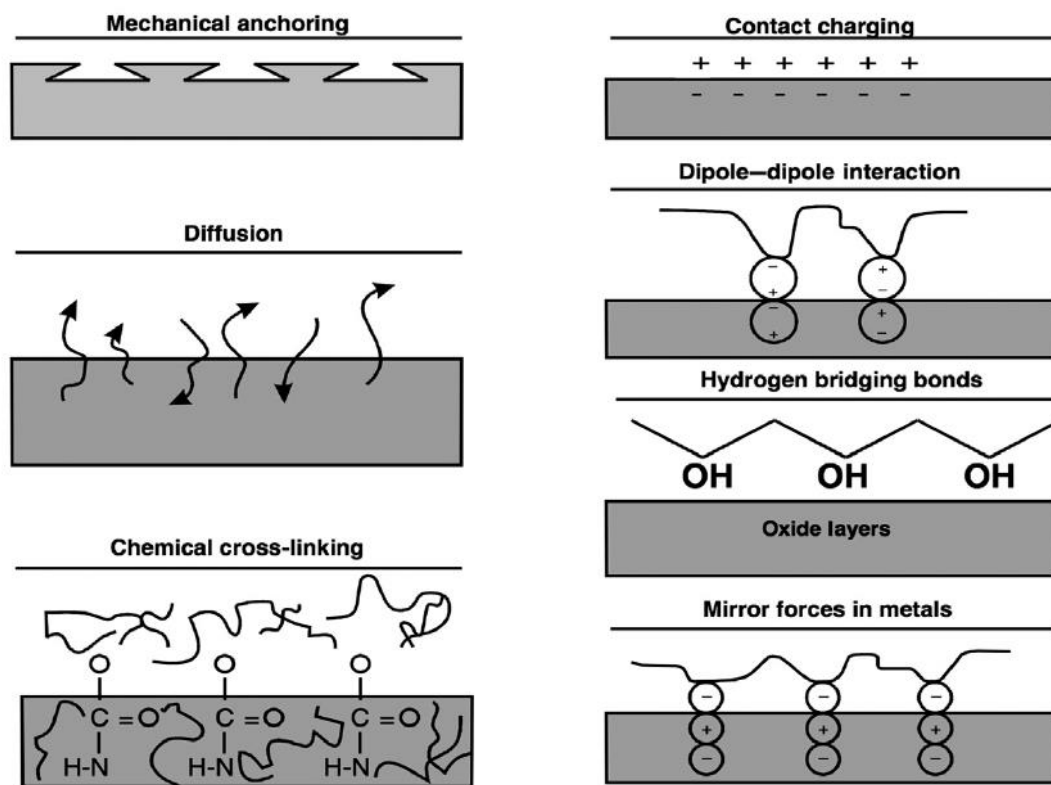
Figure 2.2 Physical and chemical causes for the adhesion between adhesive and substrate [18]

2.3.1 Mechanical theory

According to the mechanical theory (mechanical anchoring or mechanical interlocking), mechanical adhesion occurs by that adhesives penetrate into pores, cavities, and other surfaces of the substrate. Due to high surface area in rough surfaces, the penetration of adhesives into the rough surfaces can frequently form stronger bonds than the penetration into smooth surfaces. However, this theory is not universally appropriate because there is good adhesion between smooth surfaces.

2.3.2 Electrostatic (contact charging) theory

The electrostatic theory proposes that adhesion occurs due to electrostatic effects between the adherend and the adhesive by electron transfer. Electrostatic forces in an electrical double layer are formed at the interface of adhesive and adherend. This theory is supported by the fact that when an adhesive is peeled from a substrate, electrical discharges have been observed. The electrostatic theory is a suitable explanation for polymer-metal adhesion bonds. However, the electrostatic forces in nonmetallic systems to adhesion is small when compared with chemical bonding.

2.3.3 Diffusion theory

The diffusion theory suggests that adhesion takes place due to the interdiffusion of molecules in between the adhesive and the substrate. The theory is primarily applied when both the adhesive and the substrate are polymers with relatively long-chain molecules. The nature of materials (i.e. molecular weight and polarity) and bonding conditions (i.e. temperature and diffusion time) can affect the interdiffusion of molecules. Typically, a thickness of the diffuse interphase layer is in the range of 10 – 100 Å (1 – 100 nm).

2.3.4 Wetting theory

The wetting theory proposes that adhesion is developed by molecular contact between two materials and the surface forces. The formation of bonds firstly generates interfacial forces between the adhesive and the substrates. The process of developing continuous contact between the adhesive and the adherend is called wetting. The wetting means a liquid spreading over and intimately contacting a solid surface, as displayed in Figure 2.3 [19]. For good wetting of an adhesive on a solid surface, the surface free energy (surface tension, γ_{LV}) of the liquid adhesive should be lower than the critical surface tension γ_C of the solid adherend. Figure 2.4 exhibits a simple view of the relationship of wetting and surface energies. The expected bond strength of an epoxy adhesive should increase when the contact angle of a drop of the epoxy adhesive decreases, followed by polyvinyl chloride, polyethylene,

polytetrafluoroethylene in that order. Good wetting is necessary for the formation of bonds; however, it is not the main criterion for strong adhesion.
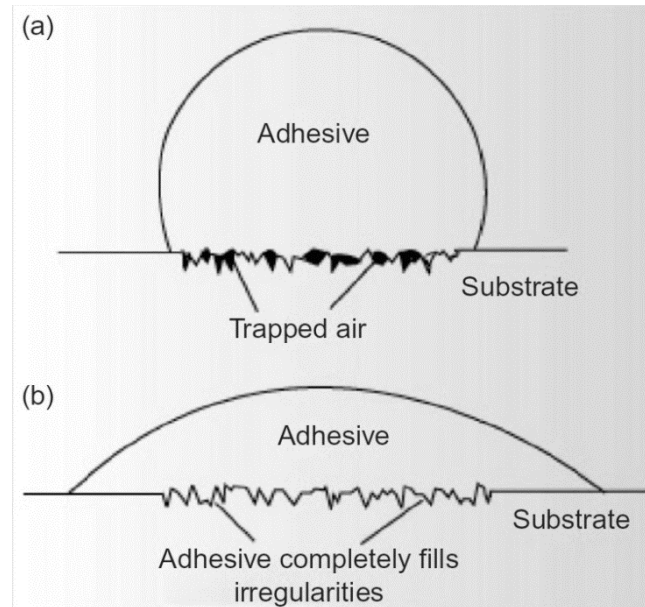
Figure 2.3 Illustration of poor (a) and good (b) wetting by adhesive spreading over a surface [19]
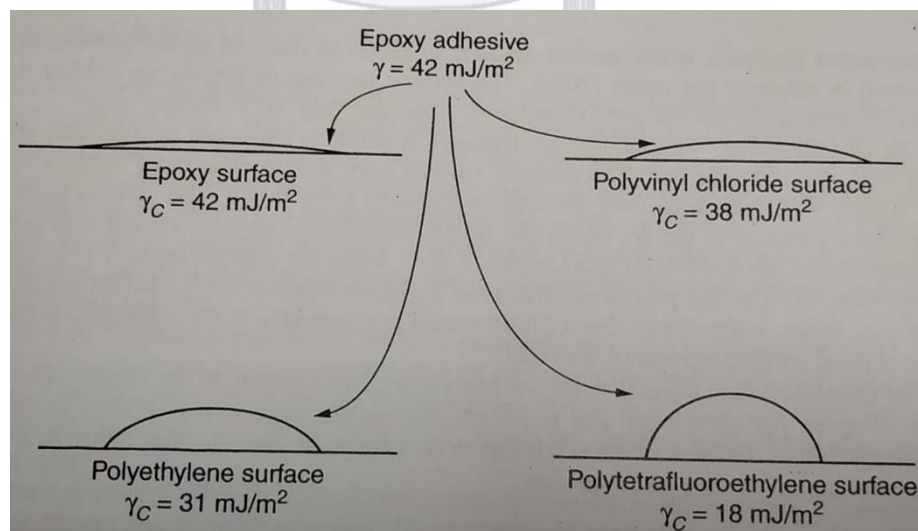
Figure 2.4 Contact angle of an uncured epoxy adhesive on various substrates of varying critical surface tension [19]

2.3.5 Chemisorption theory

The chemisorption theory proposes that adhesion bond is formed by surface chemical forces. Generally, there are four types of chemical interactions: covalent bonds, hydrogen bonds, Lifshitz-van der Waals forces, and acid-base interactions. The covalent chemical bonds are usually the strongest and most durable. Table 2.4 lists examples of these bonds and their magnitudes.

Table 2.4 Examples of energies of chemical bonds and Lifshitz-van der Waals forces

Type	Example	Energy (kJ/mol)
Covalent	C-C	350
Ion – Ion	Na+ … Cl-	450
Ion – dipole	Na+ … CF3H	33
Dipole – dipole	CF3H … CF3H	2
London dispersion	CF4 … CF4	2
Hydrogen bonding	H2O … H2O	24

2.3.6 Weak boundary layer theory

The adhesive, the adherend, the environment, or a combination of any of these three factors can initiate weak boundary layers. For example, if the air is trapped in the bounding surface, a weak boundary layer can occur and result in poor wetting, as shown in Figure 2.3.

2.4 Epoxy adhesive

An epoxy adhesive has become the most recognizable structural adhesive type and is widely used in demanding industries, such as aerospace, automotive, building and construction, and electrical and electronics [19]. Typically, a general formula of epoxy resin can be represented by a linear polyether with a terminal oxirane ring or epoxide group whose reactivity is very high, as shown in Figure 2.5.
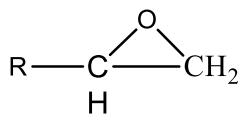
Figure 2.5 The epoxy or oxirane ring structure

Generally, diglycidyl ether of bisphenol A (DGEBA), as shown in Figure 2.6, is based on commercial epoxy adhesive because of their high thermal and mechanical properties, high chemical resistance, low shrinkage, and high adhesive strength [1]. Moreover, for the UV curing process, cycloaliphatic epoxy derivatives, such as 3, 4-epoxycyclohexylmethyl 3', 4'-epoxycyclohexanecarboxylate as displayed in Figure 2.7, are almost used in the formulation of epoxy adhesive because of its excellent adhesion, good chemical resistance, high reactivity, low shrinkage, and a good balance of hardness and toughness than other forms.
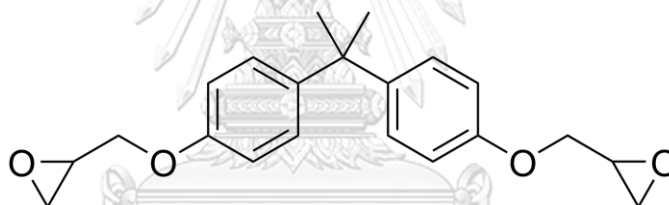
Figure 2.6 The formula structure of diglycidyl ether of bisphenol A (DGEBA)
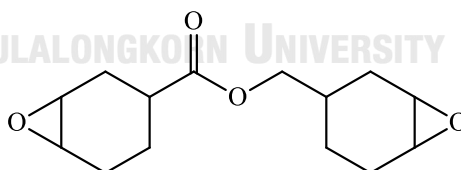
Figure 2.7 The formula structure of 3, 4-epoxycyclohexylmethyl

3', 4'-epoxycyclohexanecarboxylate

2.5 UV-radiation and thermal curing of the adhesive

In the present, the UV-radiation is extensively applied in electronics industries because of several advantages of UV-curable adhesives, such as high curing rate, curable ambient temperature, good adhesion, low energy, one component, solvent-free, and high stability at any storage [1, 20]. The mechanism of the UV curing is

initiated by UV radiation and there are very high polymerization rates and transformation of a liquid phase into a solid phase as a network within a fraction of a second as shown in following scheme [21, 22]:
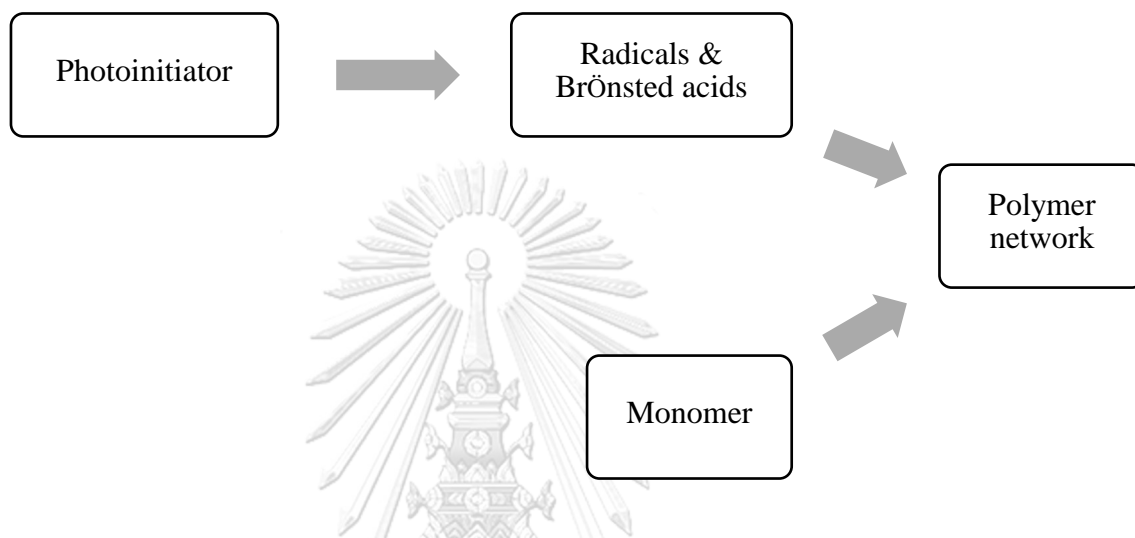
Photoinitiator is an initiator for the UV curing. The photoinitiator is activated to be radical and acid by UV rays and is cleaved to be radicals and protonic acids or BrÖnsted acids. These active molecules can initiate cross-linking polymerization with an adhesive monomer and then polymer network is formed.

There are two main types of UV-curing reactions based on polymerization mechanisms which are photoinitiated radical polymerization and photoinitiated cationic polymerization [22].

The first reaction, photoinitiated radical polymerization, the free radicals from aromatic ketones, or aromatic carbonyl compounds are produced upon UV irradiation. There are three main UV-curable adhesive classes in the radical mechanism i.e. unsaturated polyester/styrene, thiol-polyene, and acrylate monomers.

The second reaction, photoinitiated cationic polymerization, is the efficient process to react inactive monomers toward protonic acids generated by UV irradiation. Photoinitiators for this reaction are onium salts, such as diazonium salt, diaryliodonium salt, diarylbromonium salt, triarylsulfonium salt, triarylselenonium

salt, and ferrocenium salt. However, the diaryliodonium salt or the triarylsulfonium salt is widely used because of their good absorption in UV range and availability when compared with other types, as shown in Figure 2.8 [23]. Moreover, the onium salt consists of cation and anion. There are several types of anions, such as SbF_6^-, $(C_6F_6)_4B^-$, AsF_6^-, PF_6^-, BF_6^-, and ClO_4^-. Moreover, the anions directly affect polymerization rate, for example, SbF_6^- most affects the polymerization rate. Also, the photoinitiators absorb different UV wavelengths; therefore, it should inspect what wavelengths the photoinitiators can absorb.

(a)   (b)
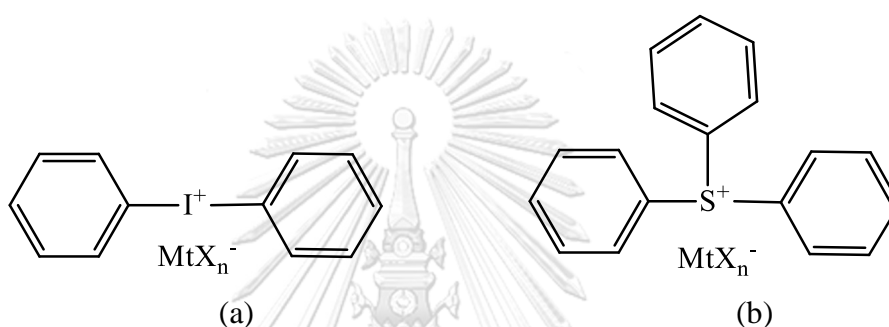
Figure 2.8 The formula structure of (a) diaryliodonium salt and (b) triarylsulfonium salt

The photoinitiated cationic polymerization has the main advantages compared with the radical polymerization in which curing reaction can continuously occur in the dark or after switching off UV light and it is not sensitive with oxygen [24, 25].

Because of this research formulating epoxy-based adhesive, only the photoinitiated cationic polymerization mechanism is mentioned in this chapter.

Crivello [23] proposed the overall mechanism of photolysis of a diaryliodonium salt as depicted in Eqs. (2.1) – (2.4). At initial reaction, the diaryliodonium salt absorbs UV light and then there are homolytic and heterolytic cleavages of carbon-iodine (C–I) bond, as in Eq. (2.1). The products of the first reaction are cationics, cationic-radicals, and free radicals species. Then they react with solvent or monomer to form strong protonic acids or strong BrÖnsted acids (HMtX$_n$), as in Eq. (2.2). When the strong BrÖnsted acid is produced and it reacts with a monomer (M), the initiated cationic polymerization rapidly occurs, as in Eq. (2.3).

The propagation steps, as in Eq. (2.4), are occurred by the addition of monomer molecules, resulting in polymer chains or networks. Interestingly, both reactions in Eqs. (2.3) and (2.4) proceed spontaneously without UV light: namely, dark reaction.

$$Ar_2I^+MtX_n^- \xrightarrow{h\nu} \begin{bmatrix} ArI^{\cdot +}MtX_n^- + Ar\cdot \\ Ar^+MtX_n^- + ArI \end{bmatrix}$$

(2.1)

$$\begin{bmatrix} ArI^{\cdot +}MtX_n^- + Ar\cdot \\ Ar^+MtX_n^- + ArI \end{bmatrix} \xrightarrow[\text{monomer}]{\text{solvent or}} HMtX_n$$

(2.2)

$$HMtX_n + M \longrightarrow HM^+ MtX_n^-$$

(2.3)

$$HM^+ MtX_n^- + nM \longrightarrow H(M)_{n-1} M^+ MtX_n^-$$

(2.4)
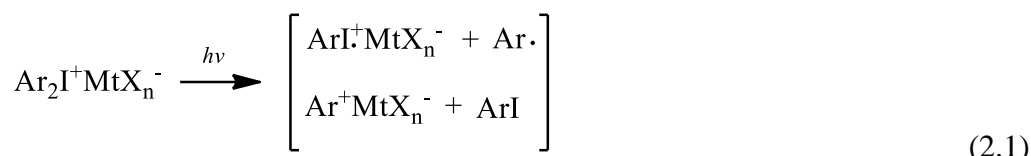
The polymerization rate of photoinitiated cationic polymerization depends on the type of photoinitiator bearing anions or MtX_n^-. The order of increasing polymerization rates for a series of photoinitiators are as follows: $SbF_6^- >$ $(C_6F_6)_4B^- > AsF_6^- > PF_6^- > BF_6^- > ClO_4^-$ [1, 21-23].

Furthermore, there are generally two mechanisms of the ring-opening cationic polymerization for the epoxy system with alcohol functional group: the activated chain end (ACE) and the activated monomer (AM) mechanisms [26], as depicted in Figure 2.9. Commonly, there is the ACE mechanism in the ring cationic polymerization of the epoxy system. The acid initiator can react with an epoxy monomer and then the activated monomer or propagating center is formed. The activated monomer can react with a monoalcohol by transfer reaction and it can result in the formation of a dead end. Consequently, the growing polymer chain was terminated but it can continue to react with the activated monomer. Repetition of this mechanism regenerates a hydroxyl-terminated chain that continues the termination

and transfers reactions. Thus, each time the OH group reacts, another OH group is produced; and this condition is called the AM mechanism.
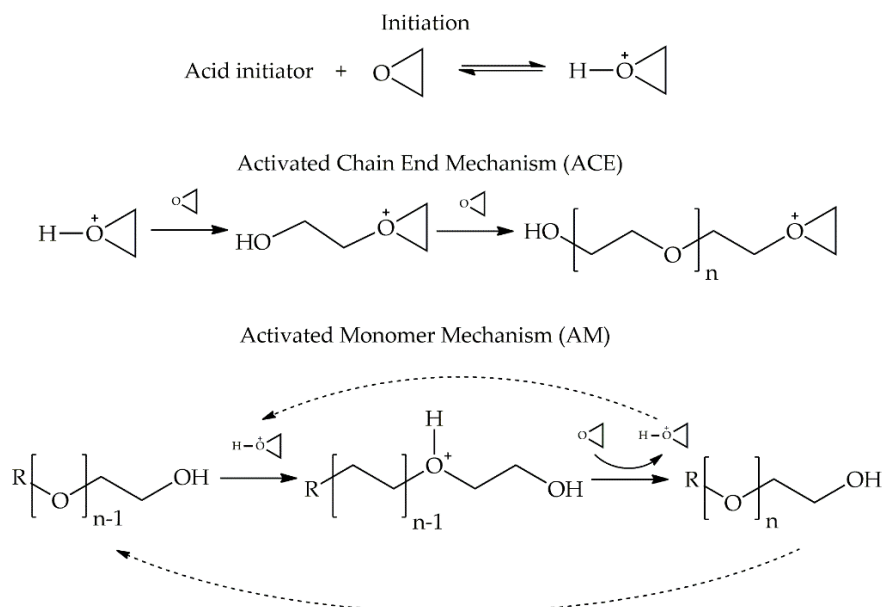
Figure 2.9 The mechanisms of the ring-opening cationic polymerization for an epoxy system with alcohol functional group: the activated chain end (ACE) and the activated monomer (AM) mechanisms [26]

Besides, adhesive's thickness, UV intensity and time of UV irradiation affect the rate of reaction and conversion (α) [1, 24, 27, 28]. If adhesive is too thick, the UV irradiation cannot penetrate through deep layers of the adhesive. Hence, the photoinitiators in the deep layers are not initiated by UV light and UV curing does not occur in the deep layers.

UV intensity is one of the most important factors affecting the degree of cure or conversion of curing reaction. If the UV intensity is high, the rate of reaction is increased. On the contrary, if low UV light intensity is selected, the rate reaction is slow, resulting in a low conversion.

Also, UV irradiation time affects the penetration of UV light through the layers of adhesive. If irradiation time is long enough, the UV light can penetrate through the deep layers.

Ficek et al [24] studied the effects of UV radiation time and UV intensity on the thick adhesive. Figure 2.10 displays profiles of light intensity and photoinitiator concentration for UV irradiation times from 0 to 5 minutes. Figure 2.10A shows penetrable light intensity through sample depth. The intensity gradient falls off according to the sample depth if there is longer UV radiation time. The initial photoinitiator concentration is uniform at 21 g/L. The concentration of photoinitiator at the irradiated surface of the sample was completely consumed; however, the concentration of photoinitiator was unchanged in the deeper layers, as shown in Figure 2.10B.
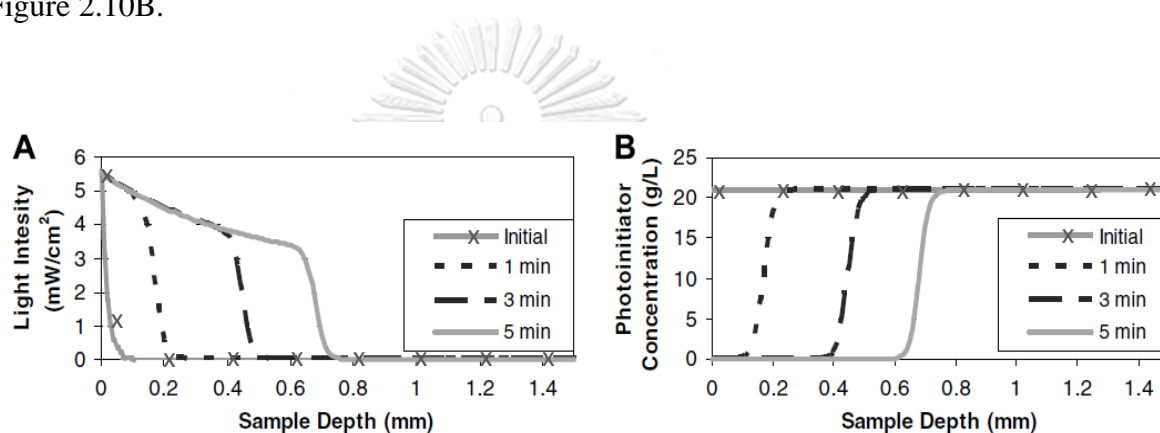
Figure 2.10 Profiles of (A) the light intensity and (B) the photoinitiator concentration at irradiation time of 0, 1, 3 and 5 min. at 25°C, light intensity of 50 mW/cm^2 [24]

Chiang and Hsieh [29] studied and demonstrated the UV curing of 3, 4-epoxycyclohexylmethyl 3', 4'-epoxycyclohexanecarboxylate using triarylsulfonium salts as photoinitiators and thermal curing using tertiary amines as curing agents [30]. They proposed the dual-cure mechanism as shown in Eqs. (2.5) – (2.8). For the initiation of photoinitiated cationic polymerization in Eq. (2.5), triarylsulfonium salts undergo rapid photolysis when they are irradiated by UV light and become aryl radicals, aryl cationic radicals, aryl cations, and super acid (BrÖnsted acid), H^+SbF_6. The superacid induces the cationic polymerization to produce oxiranium ion as shown in Eq. (2.6). The cationic polymerization takes place by the attack of protonated epoxide on other epoxy molecules as presented in Eq. (2.7). The oxiranium ions react with amines to induce cationic thermal polymerization as shown in Eq. (2.8).

Nevertheless, there is an effect of tertiary amine on UV conversions whereas the tertiary amine can inhibit the UV-radiation curing because of nitrogen atoms of tertiary amines, whose a lone pair of electrons can react with MtX_n^- to produce ammonium salts [30]. Figure 2.11 shows UV conversion versus the irradiation time of epoxy samples containing various concentrations of a tertiary amine. When the amount of concentration of tertiary amine increases, the UV conversion decreases.
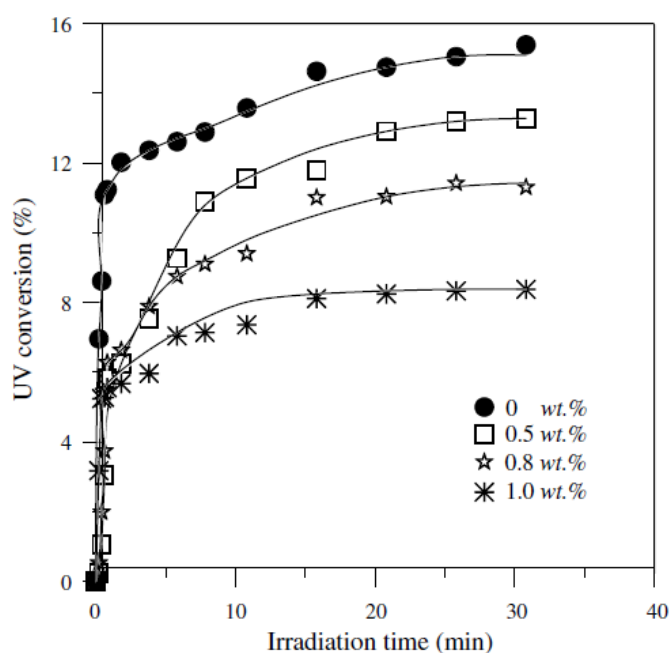
Figure 2.11 UV conversion as a function of the irradiation time of epoxy samples containing various concentration of a tertiary amine [30]

(2.5)

(2.6)

(2.7)

$$(2.8)$$
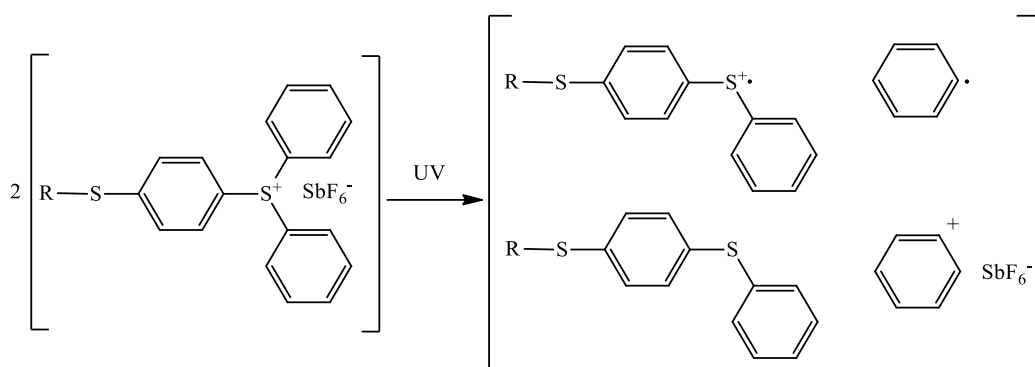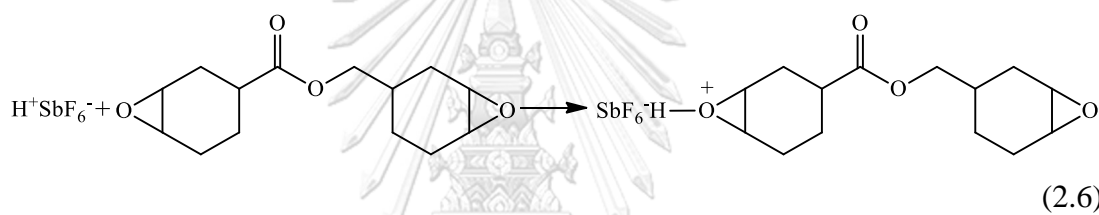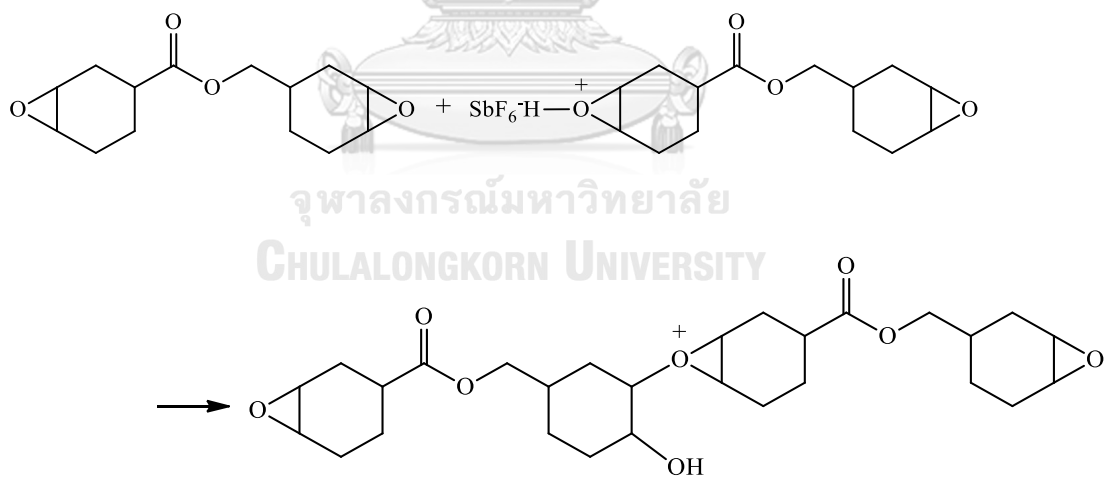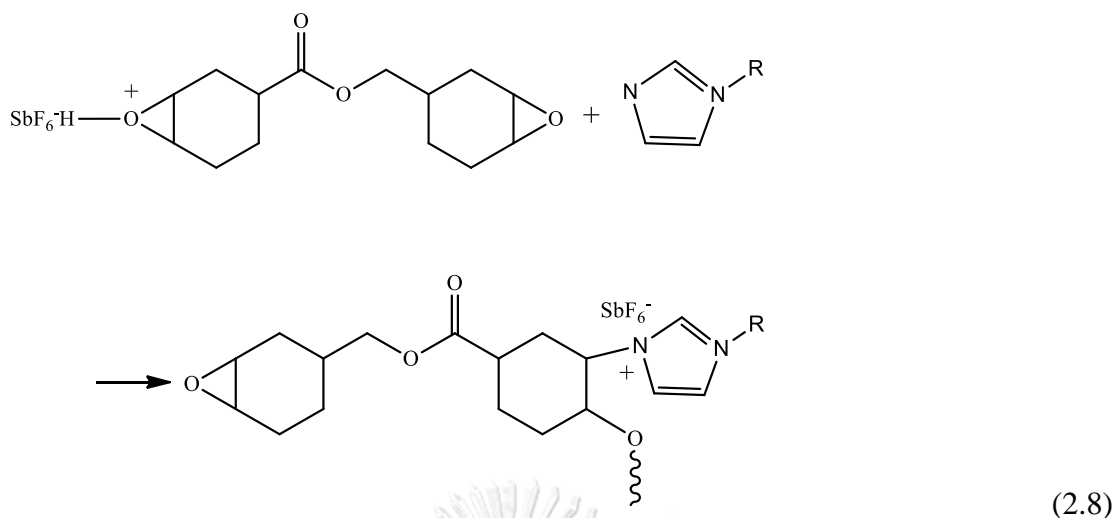
Furthermore, there are effects of temperature on the polymerization rate [1]. The adhesive's viscosity decreases when curing temperature increase because the temperature can accelerate the polymerization rate due to the higher mobility of adhesive molecules.

However, in complex area or shape, the UV-curing reaction of adhesive may be incomplete because some are of adhesive cannot be irradiated by UV light. Therefore, it should have a thermal curing unit and use a curing agent as a thermal accelerator, in order to completely curing reaction [31, 32].

2.6 Thermal curing kinetics

The thermal curing under isothermal condition is a conventional method to monitor the curing kinetics, which includes pre-exponential factor (A), activation energy (E_a), and reaction order (n) [33]. The curing kinetics can be expressed in the following equation:

$$\frac{dQ}{dt} = Q_r \frac{d\alpha}{dt} = Q_r k(T) f(\alpha) \tag{2.9}$$

where dQ/dt is the heat flow, Q_r is the total heat released after the reaction was complete, $d\alpha/dt$ is the rate of reaction or curing rate, α is the degree of cure or conversion, $k(T)$ is the rate constant, T is the absolute temperature, and $f(\alpha)$ is the

function of reaction model. The degree of cure at a time (t) from the isothermal analysis is defined as in Eq. (2.10):

$$\alpha = \frac{\Delta H(t)}{\Delta H_{total}}; \qquad \Delta H_{total} = \Delta H(t) + \Delta H_{res} \tag{2.10}$$

when H(t) is the heat of reaction at a certain time t, ΔH_{res} is residual heat of reaction in the second scan and H_{total} is the total heat of reaction.

The rate constant can be determined by an Arrhenius equation. Therefore, Eq. (2.9) can be rearranged as shown in Eq. (2.11):

$$\frac{d\alpha}{dt} = A\exp(-\frac{E_a}{RT})f(\alpha) \tag{2.11}$$

where A is the pre-exponential factor, E_a is the activation energy, and R is the gas constant (8.314 kJ kmol^{-1} K^{-1}).

The kinetic parameters will be meaningless unless the reaction model is suitably fitted with the curing reaction [34]. Generally, three reaction models are classified by the characteristic of the reaction profile. The suitable reaction model can be decided to use by visually inspecting the isothermal reaction profile [35]. Firstly, the accelerating model is the first model. The rate increases exponentially with a rising degree of cure and approaches maximum at the end of the cure state. This model can be expressed by a power law model:

$$f(\alpha) = n\alpha^{(n-1)/n} \tag{2.12}$$

where n is a constant. The second model is the decelerating model in which there is the maximum rate at the initial reaction, and it decreases continuously whereas the degree of cure increases. This model is a common reaction model as expressed in Eq. (2.13):

$$f(\alpha) = (1-\alpha)^n \tag{2.13}$$

where n is the reaction order. The third model is a sigmoidal model in which the rate consists of the accelerating and decreasing patterns at the initial and final stages, respectively. The last model is called the auto-catalyzed reaction, which is commonly known as Šesták–Berggren model [36] as shown in Eq. (2.14):

$$f(\alpha) = \alpha^m (1-\alpha)^n \tag{2.14}$$

where n and m are the reaction orders and they can relate to the effects of unreacted reactants and catalytic effect of the product of the reaction, respectively.

The curing kinetics of the epoxy system can be generally explained by the autocatalytic model [37] as expressed by Kamal's equation:

$$\frac{d\alpha}{dt} = (k_1(T) + k_2(T)\alpha^m)(1-\alpha)^n \tag{2.15}$$

where $k_1(T)$ and $k_2(T)$ are the rate constants and m and n are the reaction orders. When combining Eqs. (2.11), (2.14) and (2.15) and simplifying the calculations [40], the curing kinetics could be expressed by Šesták–Berggren model [41] and the kinetic model is shown in Eq. (2.16).

$$\frac{d\alpha}{dt} = k(T)\alpha^m (1-\alpha)^n \tag{2.16}$$

k(T), m and n can be calculated by MATLAB program (version: R2018b) and the activation energy (E_a) is determined by taking natural logarithm to Arrhenius's equation as shown in Eq. (2.17):

$$\ln k(T) = \ln A - \frac{E_a}{RT} \tag{2.17}$$

E_a and lnA are evaluated from the slope and y-intersection of the graph plotted between lnk(T) and reciprocal T.

2.7 The gel point of cross-linking polymer

The transformation of a liquid state to a solid state is based on the hypothesis that power law behavior for the dynamic moduli at the time at the critical extent of reaction (t_c) [38, 39].

$$G'(\omega) = G'_c \omega^n \tag{2.18}$$

$$G^n(\omega) = G^n_c \omega^m, \quad 0 < \omega < \infty \tag{2.19}$$

where G'_c and G^n_c are two material constants (values of complex moduli at $\omega = 1$ s^{-1}), and the exponent m and n are about equal in value.

Introducing Eqs. (18) and (19) into Kramers-Kroning relation [38]

$$\frac{G'(\omega)}{\omega^2} = \frac{2}{\pi} \int_0^\infty \frac{G''(x)/x}{\omega^2 - x^2} \, dx \tag{2.20}$$

when n = m

$$G_c' = \frac{G_c''}{\tan\left(\frac{n\pi}{2}\right)}, \quad n < 1 \tag{2.21}$$

Therefore, the complex moduli are related by

$$G' = \frac{G''}{\tan\left(\frac{n\pi}{2}\right)} = G_c'\omega^n, \quad n < 1 \text{ and } 0 < \omega < \infty \tag{2.22}$$

if $G' = G''$, $n = 1/2$; $r = r_e$ (excess of cross-linker)

$G' > G''$, $n < 1/2$

$G' < G''$, $n > 1/2$; $r < r_e$ (lack of cross-linker)

where r is a stoichiometric ratio (cross-linker group/monomer group) and r_e is the stoichiometric ratio causing the highest modulus (not to chemical stoichiometric). Moreover, when n is not equal ½, both of modulus will not intersect and will be like parallel.

For gel point (GP) determination without stopping the curing reaction, in this case, the gelation can be observed at the crossover of G" and G' on the modulus curve: namely, gelation point, as shown in Figure 2.12. Generally, the method to detect the gelation point may be based on the observation at a critical reaction and independent of frequency, as shown in Eq. (2.23).

$$\tan(\delta) = \tan\left(\frac{n\pi}{2}\right) = \frac{G''(\omega)}{G'(\omega)}, \quad 0 < n < 1 \tag{2.23}$$
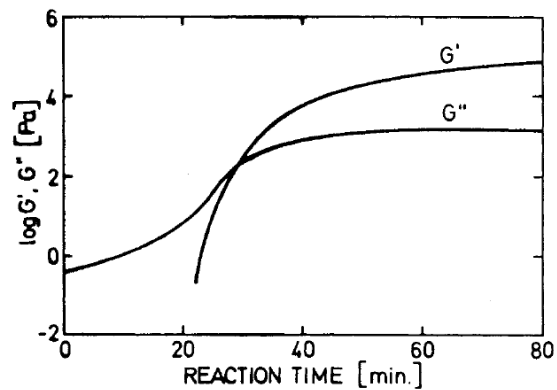
Figure 2.12 Storage modulus (G') and loss modulus (G'') as a function of reaction time

2.8 Molecular weight between crosslinking points

The molecular weight between crosslinking points (M_c), as shown in Figure 2.13, is the average molecular weight of the monomer (M_{av}) divided by the number of cross-links per molecule (c):

$$M_c = \frac{M_{av}}{c} \tag{2.24}$$
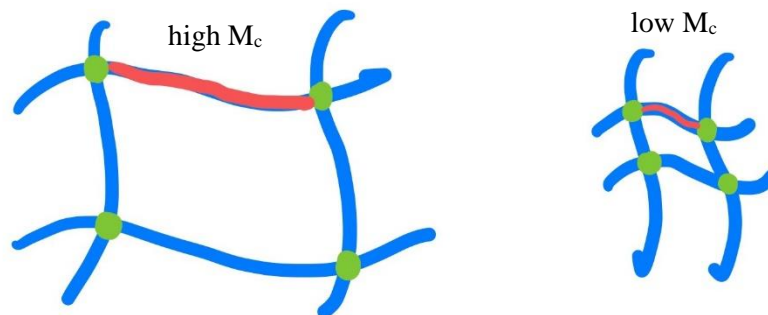
Figure 2.13 The size of network segment varying by M_c

There is a relationship between network structure and gelation, even though it is hard to determine the number of cross-links per molecule, [40]. The modulus of the entangled polymer network can be simply approximated as a simple sum as shown in Eq. (2.25).

$$G \cong G_x + G_e \approx \rho RT \left(\frac{1}{M_x} + \frac{1}{M_e} \right) \tag{2.25}$$

where G_x is the modulus of all classic models, G_e is the rubbery plateau modulus of high molar mass polymer, ρ is the density of the cured sample, R is the gas constant (8.314 m^3Pa K^{-1} mol^{-1}), T is the temperature (K), M_x is the apparent molar mass, and M_e is the entanglement molar mass. At the gel point, there are no effects of entanglement; therefore, the G'_{gel} can be expressed as shown in Eq. (2.26).

$$G'_{gel} \approx \frac{\rho RT}{M_c}$$

(2.26)

where G'_{gel} is the storage modulus at the gel point and the ρ of each sample was determined by the density kit MS-DNY-54 (Mettler Toledo, USA).

2.9 Hyperbranched epoxy resin

Hyperbranched polymers are a novel kind of three-dimensional macromolecules and are produced in a one-step procedure by multiplicative growth from a multi-functional core to form repeated branching units: namely, polycondensation of AB_x monomers [14-16]. If $x \geq 2$ and functional group of A reacts only with a functional group of B of another molecule, the highly branched polymers are ensured to produce.

Hyperbranched epoxy resins are easily synthesized, low viscosity, high solubility and a large number of end functional groups; therefore, they are widely produced and developed in several industrial-scale production and applications in the present as shown in Figure 2.14 [16].
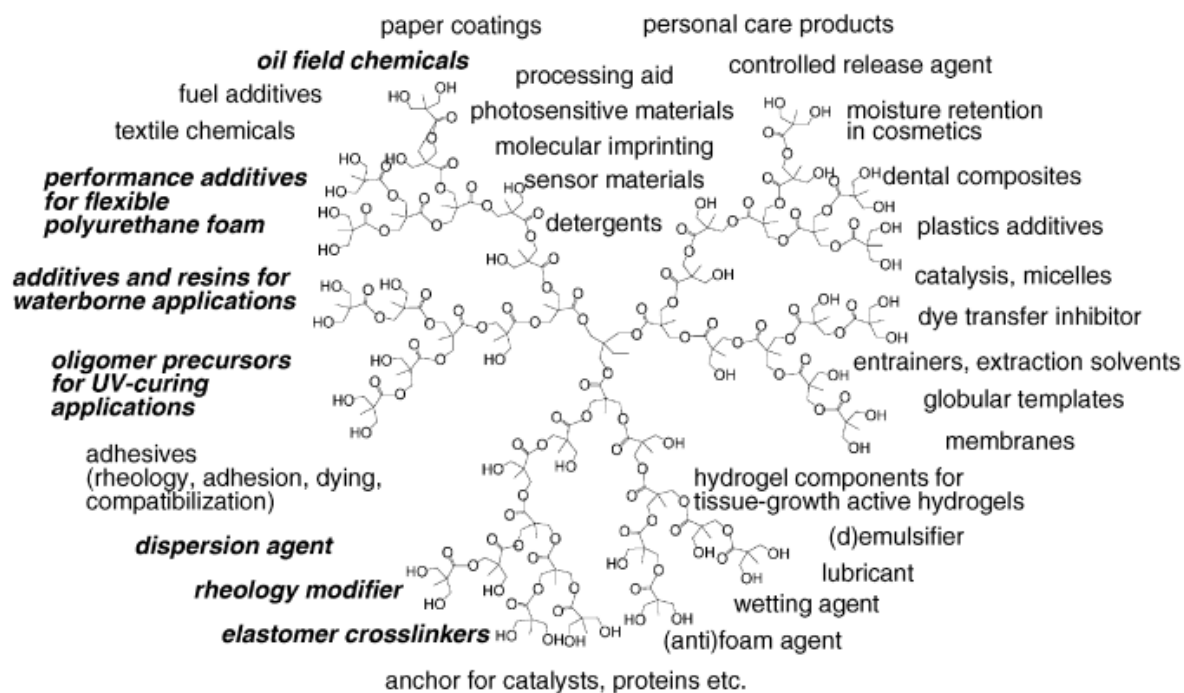
Figure 2.14 Applications of hyperbranched polymers

(bold italic: commercial applications of hyperbranched polymers) [16]

The most important feature of hyperbranched polymer is their "degree of branching" DB or "branching factor". It defines of dendritic (D), linear (L), and terminal (T) units in macromolecular structure [16]. The segment types of hyperbranched macromolecule are shown in Figure 2.15.
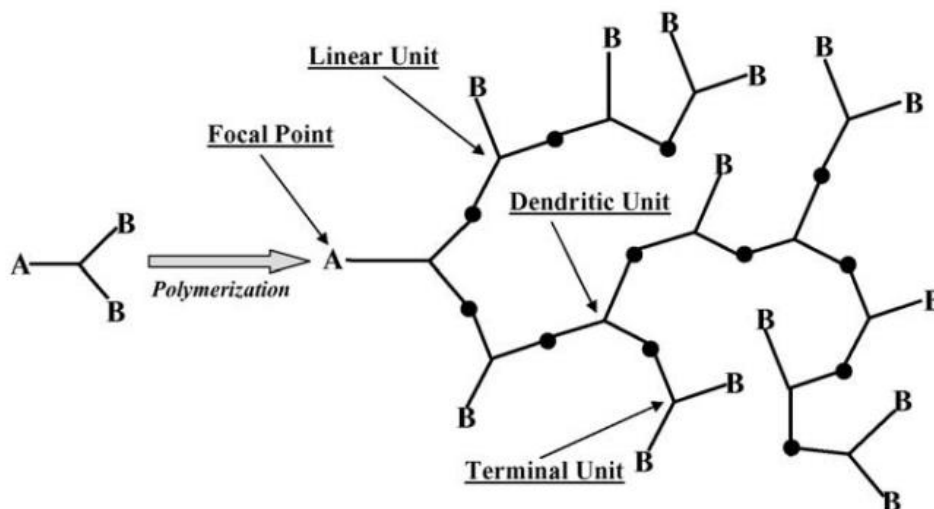
Figure 2.15 A hyperbranched polymer with its different segment types from the polymerization of AB_2 monomers [16]

The degree of branching of a linear polymer equals 0, while a perfect dendrimer has a DB of 1. The DB is the ratio of the sum of integration of dendritic and terminal units to the sum of integration of all repeating units in the structure, from ^{13}C NMR technique, as shown in Eq. (2.27). [16].

$$DB \ (\%) = \frac{D + T}{D + T + L} \qquad (2.27)$$

Furthermore, glass transition temperature (T_g) is the most important thermal properties for a dendritic polymer. There is a relationship between DB and Tg. It can be found that Tg gradually decreased with increasing DB. This can be explained to the following two factors. Firstly, if DB increases, there are many junction points in the hyperbranched structure, increasing the number of inner cavities. Secondly, if terminal units are plentifully formed with increasing DB, free volume in the backbone increase [41, 42].

De and Karak [14, 15] synthesized and characterized the hyperbranched epoxy resins by $A_2 + B_3$ polycondensation reaction between triethanol amine and in situ prepared diglycidyl ether of bisphenol A (DGEBA) as shown in Figure 2.16 [14], and by $A_2 + B_4$ polycondensation reaction between pentaerythritol and in situ prepared DGEBA as shown in Figure 2.17 [15]. They formulated the hyperbranched epoxy

resins to be adhesives for testing physical, thermal, and mechanical properties. They found that the unison of the aliphatic-aromatic moiety in hyperbranched structure offered a high-performance tough thermoset. The comparison of the properties between the best optimum from both pieces of research as shown in Table 2.5. It was seen that the properties of hyperbranched epoxy from the $A_2 + B_4$ polycondensation reaction is better than that from the $A_2 + B_3$ polycondensation reaction.
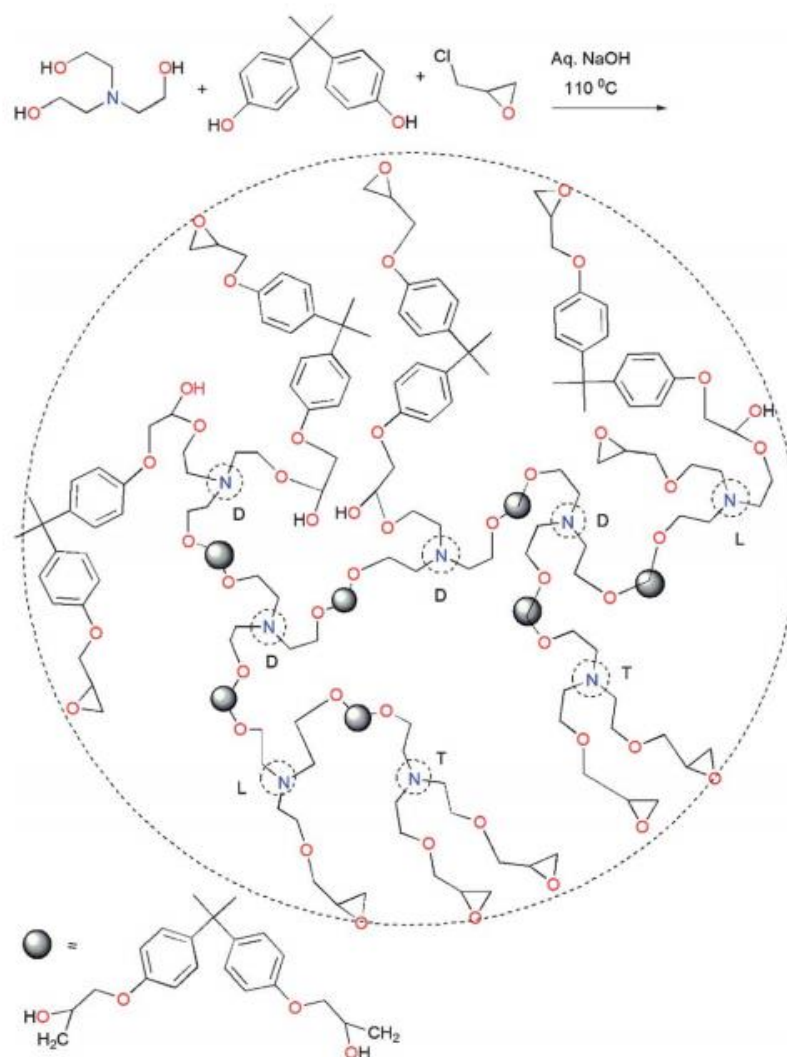
Figure 2.16 $A_2 + B_3$ polycondensation reactions between triethanol amine and in situ prepared diglycidyl ether of bisphenol A (DGEBA) [14]
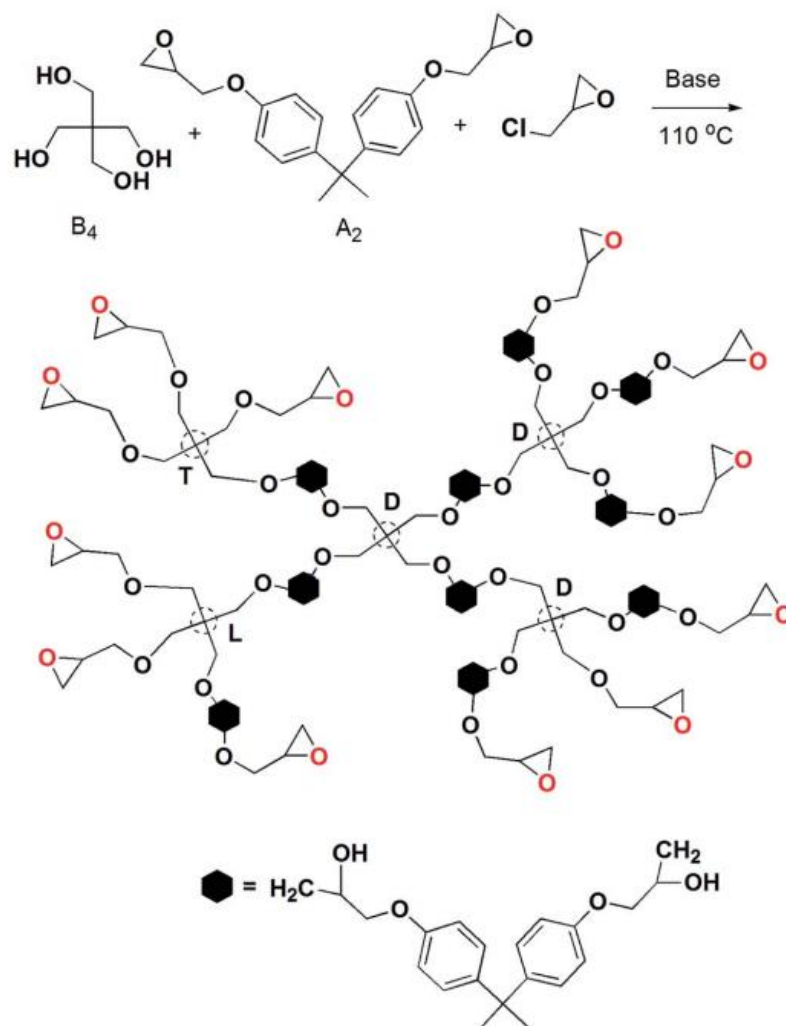
Figure 2.17 A$_2$ + B$_4$ polycondensation reactions between pentaerythritol and in situ prepared DGEBA [15]

Table 2.5 The properties of adhesive based on hyperbranched epoxy resin

Properties	$A_2 + B_3$ [14]	$A_2 + B_4$ [15]
Epoxy equivalent (g/eq)	358	394
Hydroxyl value (mg KOH per g)	100	102
Degree of branching	0.79	0.78
Curing at 100°C (min)	45	35 ± 2
Swelling value (%)	16	22 ± 1
Tensile strength (MPa)	47	51 ± 1.5
Elongation at break (%)	21	37.5 ± 1.6
Toughness (MPa)	758	1,432
Scratch hardness (kg)	9.0	>10.0
Impact strength (cm)	>100	>100
Bending (mm)	<1	<1
Adhesion strength (metal-metal) (MPa)	2,662	3,429 ± 17
Adhesion strength (wood-wood) (MPa)	1,319	>2,911
Initial degradation temperature (°C)	298	296

CHAPTER 3
EXPERIMENTS

3.1 Materials

Bisphenol A (BPA), (Tokyo Chemical Industry Co., Ltd., Japan) is one of the most widely used to synthesized DGEBA resin and was used as a reactant for preparing in-situ generated DGEBA monomer (A_2). It should purify BPA by recrystallization from toluene (Merck, India) before use. Epichlorohydrin (ECH), (Tokyo Chemical Industry Co., Ltd., Japan) was the most reactant to synthesize DGEBA resin. ECH was used to prepare A_2 monomer (in-situ generated DGEBA) and substitution of end terminal hydroxyl groups to transform to epoxy groups of hyperbranched epoxy resin. Pentaerythritol (PE), (Tokyo Chemical Industry Co., Ltd., Japan) was a tetraol and was the common branched generating moiety used to synthesize hyperbranched polymers. Therefore, PE was used as the B_4 branch generating unit for reacting with in-situ generated DGEBA. PE should be purified by recrystallization from ethanol (Merck, India) before use. Polyethylene glycol (PEG400, $M_w = 400$ g/mol), (Sigma-Aldrich) was used as the aliphatic A_2 monomer. Sodium hydroxide (NaOH), (Ajax Finechem, Australia) was used as a base catalyst for the synthesis of hyperbranched epoxy resins. Sodium chloride (NaCl), (Ajax Finechem, Australia) was used to prepare an aqueous solution for purifying the synthesized epoxy resins. Hydrobromic acid (HBr), acetic acid, potassium acid phthalate, methyl violet, and chlorobenzene, (Tokyo Chemical Industry Co., Ltd., Japan) were used to determine the epoxy equivalent weight (EEW) of the hyperbranched epoxy resins. Diglycidyl ether of bisphenol A (DGEBA), (Sigma-Aldrich, USA) was used as the main base of epoxy resin in formulated adhesives. Diethylenetriamine (DETA), (Tokyo Chemical Industry Co., Ltd., Japan) was used as a curing agent for thermal curing. Triarylsulfonium hexafluorophosphate (Sigma-Aldrich, USA) was used as a photoinitiator for UV curing.

3.2 Synthesis of hyperbranched epoxy resin

These hyperbranched epoxy resins were synthesized by the polycondensation reaction of BPA blended with PEG400 as A_2 monomer (mass ratio of 100:0, 95:5,

90:10, and 85:15), and PE (10 wt% respect to A_2, BPA and PEG400) with ECH (1:2 mole ratio to a hydroxyl group) at 110°C under continuous stirring. For example, preparation of hyperbranched epoxy resin without PEG, an amount of 5.0 g of BPA, 0.5 g of PE (for 10 wt%), and 10.82 g of ECH were taken in two necked round bottom flasks equipped with a water condenser and a dropping funnel. The reaction mixture was stirred with a magnetic stirrer continuously. 5N aqueous solution of NaOH (1.852 g, equivalent to the hydroxyl group) was slowing dropped into the mixture by a dropping funnel. The addition of NaOH solution was started at 60 °C to the mixture and it took about 30 min and the reaction temperature was set at 110 °C for 4 hr. When the desired time was completed, the reaction was terminated by immediately quenching the mixture. The mixture was then settled in a separation funnel in order to separate the aqueous layer (the residual reactants) from the organic layer. The organic layer was purified with 15% NaCl solution followed by distilled water until the washer's pH was 8-9 and dried under vacuum at 70 °C until the mass of the sample was constant and viscous transparent liquid was observed. The composition for the synthesis of hyperbranched epoxy resins is tabulated in Table 3.1.

Table 3.1 The composition for the synthesis of hyperbranched epoxy resins

Resin	B_4	A_2		End Group
	PE (g)	BPA (g)	PEG (g)	ECH (g)
HBE	0.50	5.00	-	10.82
HBE5P	0.50	4.75	0.25	10.65
HBE10P	0.50	4.50	0.50	10.48
HBE15P	0.50	4.25	0.75	10.30

3.3 Characterization of hyperbranched epoxy resin

FTIR spectra of the hyperbranched epoxy resin were recorded by a PerkinElmer FT-IR System in a wavenumber range of 400 – 4000 cm^{-1}, attenuated total reflectance (ATR) mode and resolution of ±2 cm^{-1}. NMR (500 MHz) spectrometer from Varian Unity Inova was used to record the H^1 NMR and ^{13}C NMR spectra of the resin by using TMS as reference and CDCl$_3$ as the solvent. The degree of branching (DB) was measured by ^{13}C NMR technique [14-16, 43] and was

calculated by Eq. (2.24). EEW of the resins was evaluated by using the standard test methods (ASTM D 1652) [44]. The molecular weight of the resins was measured by gel permeation chromatography (GPC), Shimadzu/LC-10ADvp, using a refractive index (RI) detector and CH_3Cl as mobile phase operated at 40 °C with rate of 1 mL/min. For the standard calibration, there was the use of the Mark–Houwink calibration curve correction method.

3.4 Preparation of the epoxy mixture

There were five epoxy mixtures: namely, DGEBA combined with hyperbranched epoxy resin consisting of various PEG contents. The mixtures of each system are shown in Table 3.2. Moreover, there were eight formulations of combined epoxy, DGEBA and HBE10P resins, as shown in Table 3.3. The weight of the combined resins was 10 g. The DGEBA and the synthesized resins were homogenously blended for 10 min at 40 °C. Subsequently, either 0.5 g of triarylsulfonium hexafluorophosphate salts (5 wt% of resin) for UV curing or DETA curing agent (1:1 molar ratio of active functional groups) for thermal curing were added into the resin. The mixture was mechanically stirred at room temperature for 10 min.

Table 3.2 The mixture for DGEBA combined with hyperbranched epoxy resin consisting of various PEG contents

Sample name	Composition (70 wt%/30 wt%)
D	DGEBA (100 wt%)
DH	DGEBA + HBE
DH5P	DGEBA + HBE5P
DH10P	DGEBA + HBE10P
DH15P	DGEBA + HBE15P

Table 3.3 The mixture of DGEBA combined with HBE10P

DGEBA:HBE10P (wt%/wt%)	100:0	90:10	80:20	70:30	60:40	50:50	30:70	0:100

Sample name	DGEBA	D90H10	D80H20	D70H30	D60H40	D60H50	D30H70	HBE10P

3.5 Thermal curing behavior and thermal properties

The thermal curing behavior of the resins was characterized by differential scanning calorimetry (DSC), DSC 1 STARe Mettler-Toledo, under a nitrogen atmosphere. First, the non-isothermal curing behavior was measured in a range of 25 – 200 °C with a heating rate of 10 °C/min in order to evaluate onset temperature, peak temperature, and suitable curing temperature [34]. Isothermal curing kinetics was performed at various curing temperatures ranging from 70 to 100 °C. Moreover, the glass transition temperature (T_g) of the cured epoxy adhesive was also measured by non-isothermal DSC measurement from (-30) to 200 °C at a heating rate of 10 °C/min.

3.6 UV curing behavior and thermal property

The UV curing behavior and thermal properties of the UV-curable epoxy systems were investigated by photo-differential scanning calorimetry (photo-DSC), PerkinElmer: DSC8500, under nitrogen atmosphere. The UV source and high-pressure mercury lamp were from Omicure Series2000 (Excelitas Technologies). The uncured samples (8.0 ± 0.2 mg) were placed in aluminum pans and under the desired isothermal condition for 1 min before and 3 min after UV exposure. For the first scanning, UV curing was performed at various isothermal temperatures (30, 60 and 80 °C) for 1 min following by UV irradiation of 10, 20, 30, 40, and 50 mW/cm^2 with various irradiation times (10, 20, 30 and 60 s). After shutting off UV light, the dark reaction proceeded at the same isothermal temperature for 3 min, as shown in Figure 3.1a. The residual heat of reaction (ΔH_{res}) of the cured samples was measured in the second scan in a range of 30 – 180 °C with a heating rate of 10 °C/min. Finally, the second protocol was repeated to determine the glass transition temperature (T_g) of cured samples. Conversion (α) or degree of cure of the cured samples was evaluated, as in Eq. (2.10).

3.7 Photo-rheological property

The photo-rheological property of the epoxy systems was determined by the photo-rheometer, MCR-302WEPS (Anton-Paar). The UV source and high-pressure mercury lamp were as same as the photo-DSC technique. The rheological properties of the uncured samples were investigated by using a parallel plate (PP12-Dispo, d = 12 mm) with the gap between parallel plates of 0.1 mm, frequency of 10 Hz, strain of 0.1%, and various isothermal temperature (30, 60 and 80 °C) , as shown in Figure 3.1b. Before UV irradiation, the uncured samples were held under isothermal condition for 1 min, in order to maintain initial viscosity and initial modulus of the uncured samples. The UV curing experiments were performed with five UV intensities i.e. 10, 20, 30, 40, and 50 mW/cm^2 and with four irradiation times i.e. 10, 20, 30 and 60 s.
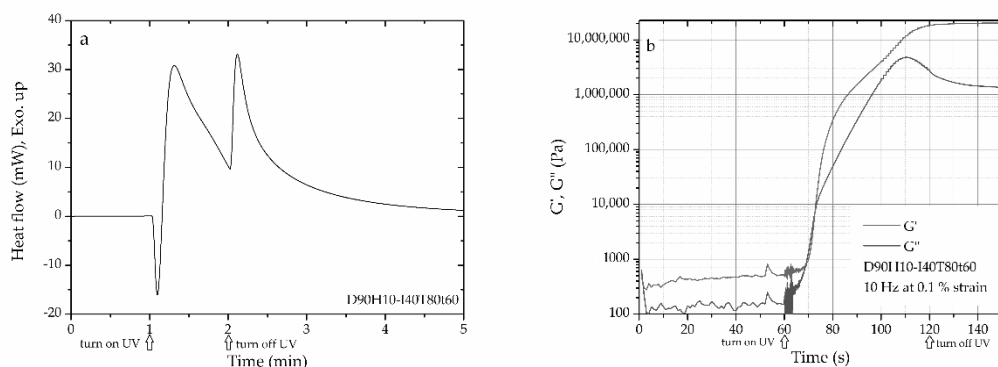
Figure 3.1 The representative data of (a) differential scanning calorimetry (DSC) and (b) rheological measurements.

3.8 Radius of gyration of the network segment

The radius of gyration of the network segment was determined via small-angle X-ray scattering (SAXS) technique (Nano Viewer RA-MICRO7HFM, Rigaku). The wavelength of the incident X-ray (CuKα) was 0.154 nm and the camera length, the sample-to-detector distance, was 700 mm. The range of scattering vector length (q) was 0.014 – 0.355 nm^{-1}. The size of the imaging plate (IP) detector was 125 × 125 mm. The cured samples, obtained from photo-DSC experiments, were measured under isothermal condition (25 °C).

The radius of gyration (R_g) was determined by the Zimm plot ($1/I$ vs q^2). The Ornstein-Zernike model [45] was assumed for the q-dependence of the scattering intensity $I(q)$, as in Eqs. (3.1 and 3.2):

$$I(q) = \frac{I_0}{1 + \xi^2 q^2}$$

(3.1)

$$\frac{1}{I} = \frac{1}{I_0} + \frac{\xi^2 q^2}{I_0}$$

(3.2)

where ξ is the correlation length and I_0 is the absolute intensity. A plot of $1/I$ vs q^2 (Eq. (3.2)) produces $1/I_0$ (intercep) and ξ^2/I_0 (slope). At low q, the radius of gyration was calculated, as shown in Eq. (3.3):

$$R_g = \sqrt{3}\xi$$

(3.3)

3.9 Audit of adhesive between slider and suspension in HGA

The audit of adhesive between slider and suspension in HGA was performed in the quality control (QC) process for checking the adhesive before use in the real process at Western Digital (Thailand) Company Limited, Thailand. The adhesives for the test were DGEBA and D90H10 systems having triarylsulfonium hexafluorophosphate salts (5 wt% of resin) as the photoinitiator. These adhesives were contained in a black syringe. Two dots of adhesive were shot on a suspension through a nozzle (dimension of 180 μm) by the air pressure (100 – 700 kPa) for shoot time of 50 ms. During the dispense of the adhesive, there was a heater to control the temperature (20 – 50 °C) at the syringe as shown in Figure 3.2. The dot size of the adhesive was captured by a camera through an electron microscope in order to check the dot size. The slider was placed on the adhesive's area and UV rays were radiated on the adhesives through the bottom of suspension. There were three times of UV exposure. UV source and high-pressure mercury lamp were from Omicure Series2000, Excelitas Technologies, and the UV curing procedures were shown in Table 3.4. First exposure, there were UV intensity of 10 W/cm^2 and irradiation time of 0.5 s. The second time, there were UV intensity of 4 W/cm^2 and an irradiation time of 2 s. Finally, UV curing was under isothermal temperature of 160 °C by hot nitrogen gas in an oven for 15 min. However, the final cure used UV LED bars for

radiating UV rays for 33 s. For the pull strength test, it was performed via the Accuforce machine which inspects the pull strength of the adhesives. As in Table 3.5, the specification limits of adhesive for the HGA process were tabulated.
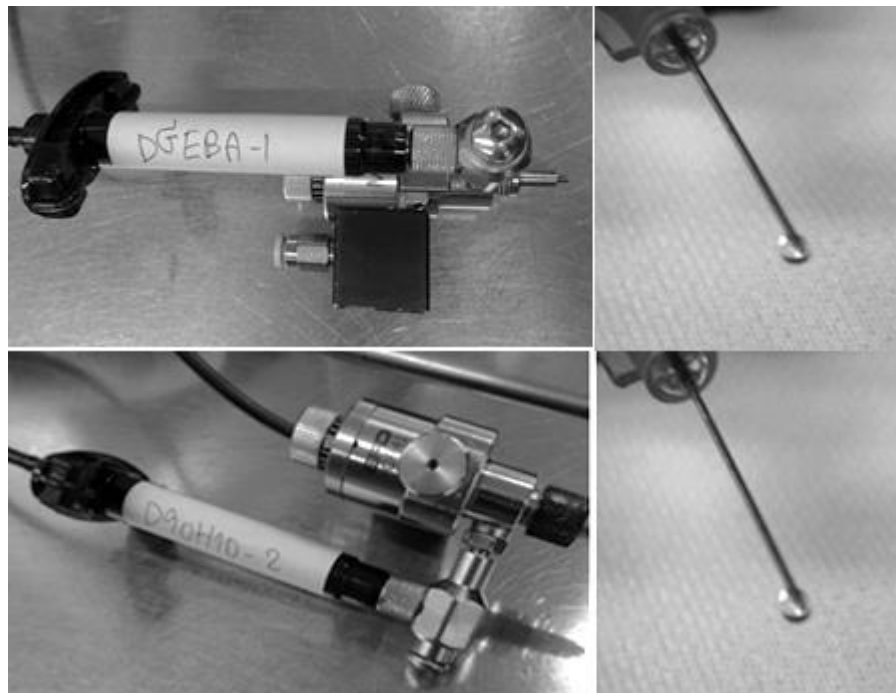
Figure 3.2 Setting up of adhesive for peel strength audit

Table 3.4 UV exposure of the quality control process for checking the adhesive before use in the real process

UV exposure	UV intensity (W/cm^2)	Irradiation time (s)	Temperature (°C)
1	10	0.5	20
2	4	2	20
3	N/A	33	160

Table 3.5 The process specification limits of adhesive for HGA process

Viscosity (cP)	Dot size of adhesive (μm)	Pull strength without solder jet bonding (gram-force, gf)
400,000 ± 2 %	~ 230 (min. = 160, max. = 280)	> 200

CHAPTER 4
RESULTS AND DISCUSSION

4.1 Synthesis and characterization of the hyperbranched epoxy resins

The synthesis of hyperbranched epoxy resins began with the formation of in situ diglycidyl ether of polyethylene glycol (DGEPEG), in situ diglycidyl ether of bisphenol A, and in situ diglycidyl ether copolymer of bisphenol A and polyethylene glycol (DGECBAPEG) [19], as shown in Figure 4.1. These in situ products were synthesized by polymerization of BPA and PEG catalyzed by NaOH at a reaction temperature of 60 °C. As shown in Figure 4.2, when the mixture was heated to 110 °C, the hyperbranched epoxy resin was subsequently synthesized by $A_2 + B_4$ polycondensation reaction. At the same time, the terminal hydroxyl groups of the synthesized resins were changed to terminal epoxy groups by epichlorohydrin.

The important chemical bond of the resins was identified by FTIR and NMR techniques. The FT-IR spectra showed the important functional groups of all synthesized resins (Figure 4.3). There were the stretching vibrations (v_{max}/cm^{-1}) of the following feature: 3450 (O–H), 3050 (aromatic C–H), 2970 (aliphatic C-H), 1620 (aromatic C=C), 1249 (C–O), 1040 (C–C), and 915 (oxirane) [14, 15]. The FT-IR results of all synthesized resins were similar, and it was hardly identifying new chemical bonds and the difference between with and without PEG. Therefore, it should additionally identify the chemical bond via NMR technique.

The ^{1}H-NMR spectra (Figure 4.4), δ_H (ppm), of HBE and HBE5P resins indicated the structural feature in Table 4.1 and the ^{13}C-NMR spectrum (Figure 4.5), δ_C (ppm), of HBE and HBE5P resins indicated the structural feature in Table 4.2. For the ^{1}H-NMR and ^{13}C-NMR spectra of HBE10P and HBE15P resins, there was the same peak indicating the important chemical bonding, therefore this research shows only the spectrum of HBE5P resins.

Diglycidyl ether of polyethylene glycol (DGEPEG)

Diglycidyl ether of bisphenol A (DGEBA)

Diglycidyl ether copolymer of bisphenol A and polyethylene glycol (DGECBAPEG)
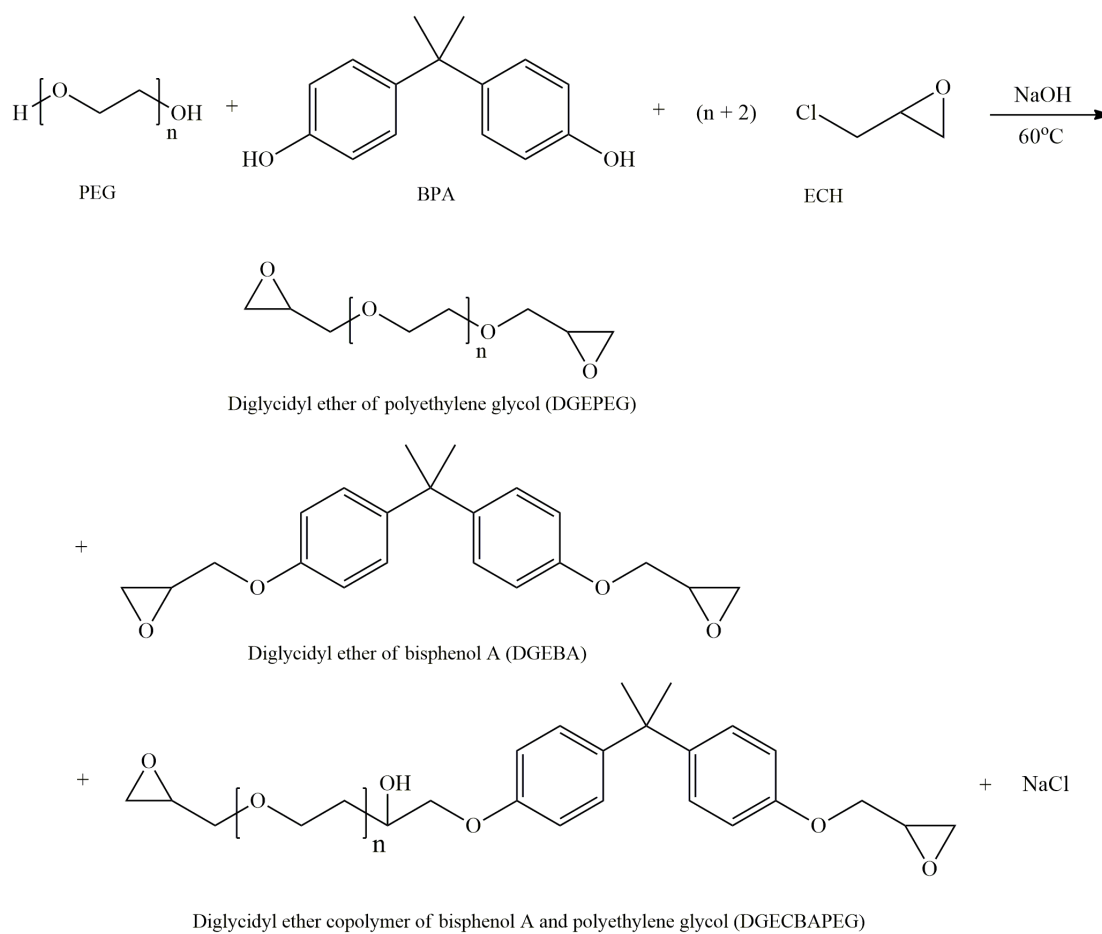
Figure 4.1 The formation of in situ diglycidyl ether of polyethylene glycol (DGEPEG), in situ diglycidyl ether of bisphenol A, and in situ diglycidyl ether copolymer of bisphenol A and polyethylene glycol (DGECBAPEG)
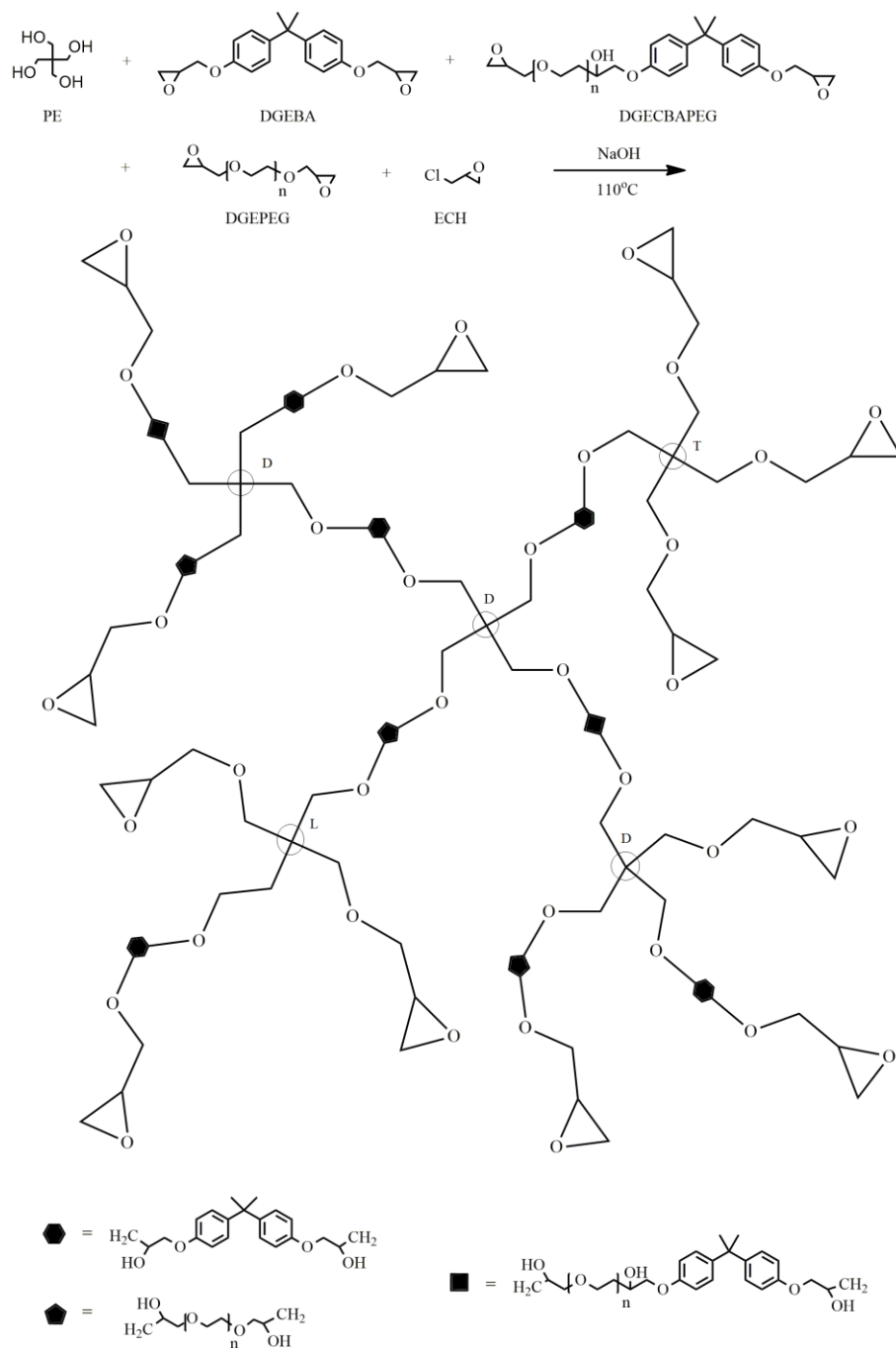
Figure 4.2 Synthesis of the hyperbranched epoxy resin and its possible structure
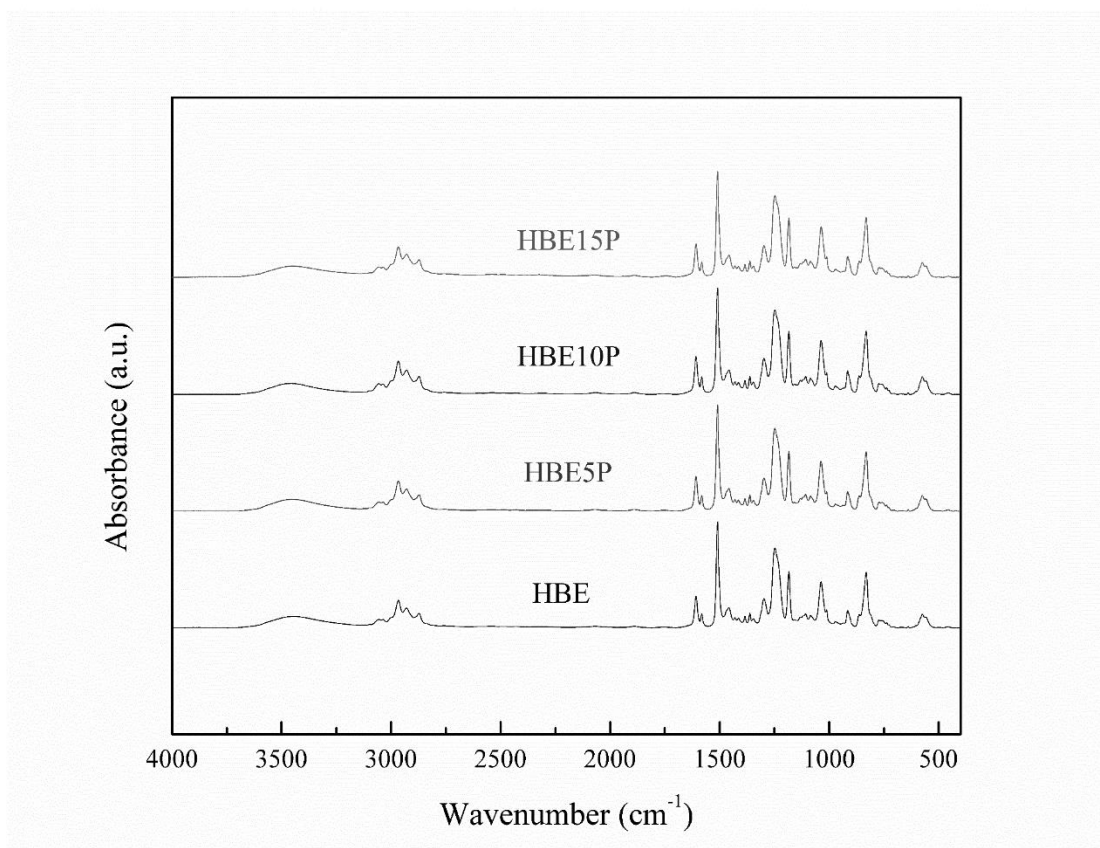
Figure 4.3 FT-IR spectra of hyperbranched epoxy resins (HBE) at various PEG contents
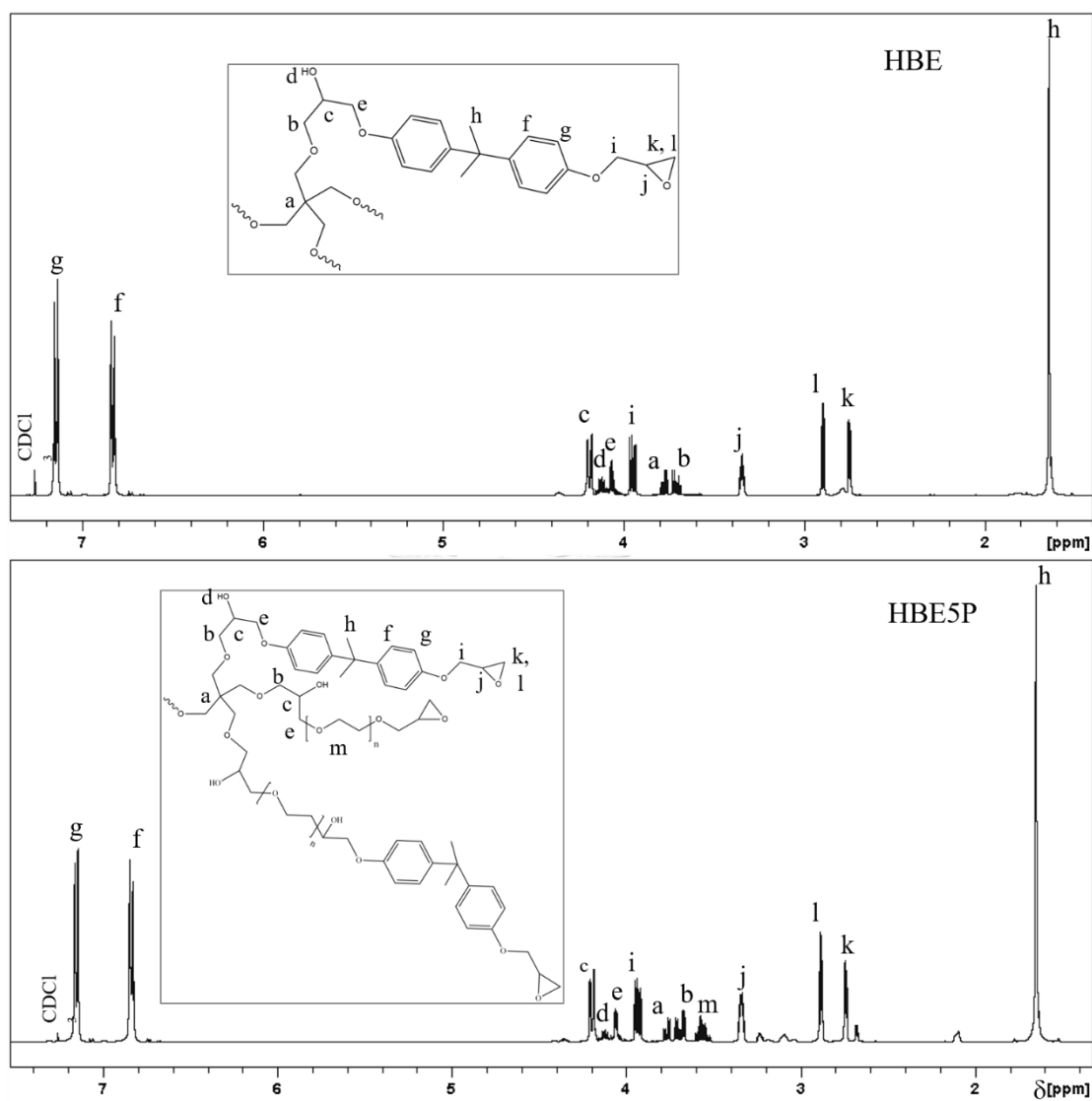
Figure 4.4 ^{1}H-NMR spectra of HBE and HBE5P resins
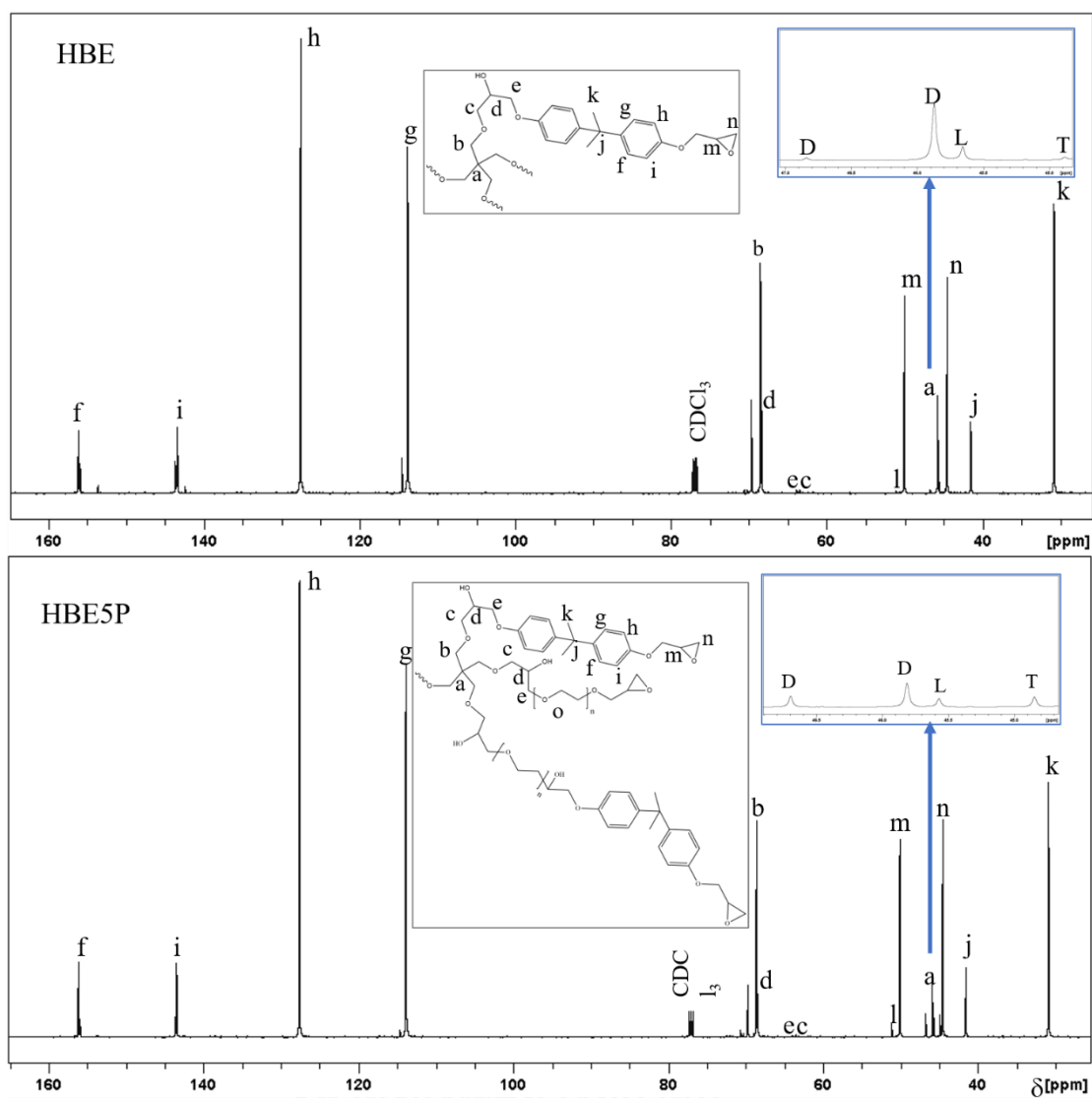
Figure 4.5 ^{13}C-NMR spectra of HBE and HBE5P resin

Table 4.1 The ^{1}H-NMR spectra, δ_H (ppm), of HBE and HBE5P resins

δ_H (ppm)	HBE	HBE5P
3H, CH$_3$	1.62	1.62
2H, oxirane	2.76, 2.90	2.78, 2.90
1H, oxirane	3.38	3.38
2H, CH$_2$ of PE	3.65	3.65
2H, 4CH$_2$ of the substituted and unsubstituted PE	3.70–3.80	3.70–3.80
2H, CH$_2$–oxirane	3.9	3.9
2H, CH$_2$ of BPA	4.10	4.08
1H, OH	4.15	4.15
1H, CHOH	4.20	4.20
4H, Ph	6.82, 7.08	6.82, 7.08
2H, CH$_2$ of PEG	-	3.60

Table 4.2 The ^{13}C NMR spectrum, δ_C (ppm), of HBE and HBE5P resins

δ_C (ppm)	HBE	HBE5P
CH$_3$, BPA	31	31
C, isopropylidene of BPA	41	41
CH$_2$, oxirane	44	44
central C of PE	44 – 47	44 – 47
CH, oxirane	50	50
CH$_2$–oxirane	51	51
CH$_2$–O and CHOH	62 – 67	62 – 67
CH$_2$, PE	68	68
4C, Ph	114, 127, 143, 156	114, 127, 143, 156

From the ^{13}C-NMR spectra (Figure 4.5), it could be determined the degree of branching (DB), Eq. (2.27) of the hyperbranched epoxy resins with various ratios of BPA and PEG from the four units of central carbon atoms of pentaerythritol [15]

($\delta_{C(HBE)}$ = 44.90, 45.65, 45.87, and 46.84 ppm and $\delta_{C(HBE5P)}$ = 44.85, 45.58, 45.83, and 46.70 ppm). As tabulated in Table 4.3, DB was calculated by Eq. (2.27). It was found that DB of all synthesized resins was more than 0.5 and it could conclude that the synthesized resins were hyperbranched resin [16]. DB of each system with and without PEG in their structure was hardly different. However, dendritic units decreased and terminal units increased because when the in situ DGECBAPEG was formed, the amount of in situ epoxide group might be reduced, resulting in reducing the generation of branching units. Furthermore, the glass transition temperature of the resins with PEG decreased due to the internal plasticized effect of PEG and the influence of braching density [46], namely high free volume in the structure.

Table 4.3 Dendritic (D), linear (L), and terminal (T) units, degree of branching (DB), and physical properties of HBE, HBE5P, HBE10P, and HBE15P resins

Resin	Branching Structure				M_W (g mol^{-1})	T_g (°C)	EEW (g eq^{-1})
	D (%)	L (%)	T (%)	DB			
HBE	77.80	18.14	4.06	0.82	4148	-9	697
HBE5P	64.65	17.23	18.12	0.83	4014	-14	663
HBE10P	73.13	10.15	16.72	0.90	4049	-19	564
HBE15P	76.86	10.92	12.23	0.89	4124	-20	468

4.2 Thermal curing behavior of hyperbranched epoxy

The thermal curing study of the hyperbranched epoxy resins cured with diethylenetriamine (DETA) was investigated by DSC technique. Firstly, the onset temperature (To), peak temperature (Tp), and the heat of reaction ($\Delta Hrxn$) of the epoxy mixtures should be determined by non-isothermal DSC method, as shown in Figure 4.6 and Table 4.4. Increase in PEG (0–10 wt.%) in the resins, T_o and T_p decreased due to the long-chain structure of PEG acting as a plasticizer, resulting in increasing the mobility of the polymer chains. However, for HBE15P system, the effects of chain entanglement and branching chains during crosslinking predominated: therefore, T_o and T_p of HBE15P system obviously increased [47]. Besides, at high content of PEG chains in the system could delay the curing reaction [48].

Furthermore, epoxy equivalent weight (EEW) of the synthesized resins decreased with an increase in PEG content: namely, an increase in active epoxide ring. Therefore, the heat of reaction increased. Also, T_g of the hyperbranched epoxy thermosets with 0 – 10 wt% of PEG decreased due to more flexible PEG chains and high DB [41, 42, 49]. However, T_g of HBE15P thermoset greatly increased due to the highest heat of reaction, resulting in high crosslink density [50].
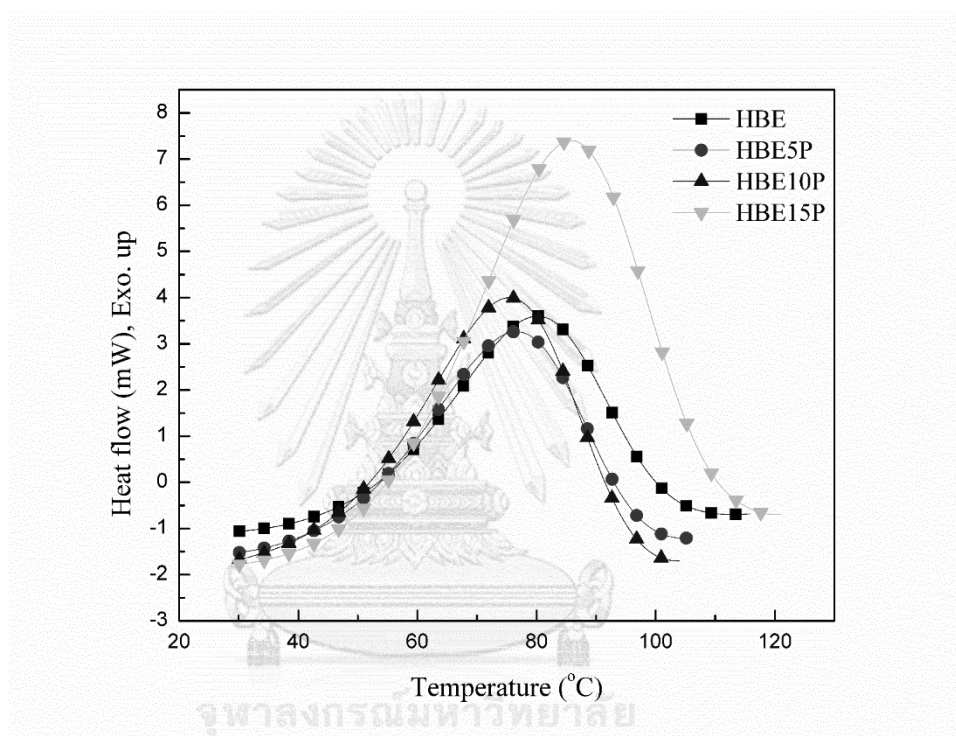
Figure 4.6 The thermal curing behavior of HBE, HBE5P, HBE10P, and HBE15 systems

Table 4.4 The curing behavior and thermal properties of HBE, HBE5P, HBE10P, and HBE15P systems

Parameter	HBE	HBE5P	HBE10P	HBE15P
Onset temperature (°C)	50.74	48.10	46.16	53.44
Peak temperature (°C)	79.96	76.95	75.47	85.43
Heat of reaction (J g^{-1})	205.16	242.65	258.19	307.13
Curing time at 70 °C (sec)	1,058	1,055	872	1,173
Curing time at 80 °C (sec)	933	968	817	997
Curing time at 90 °C (sec)	870	911	700	735
Curing time at 100 °C (sec)	613	773	597	515
T$_g$ (°C)	77.90	72.79	51.82	109.41

The curing time of the hyperbranched epoxy at 70, 80, 90, and 100 °C as tabulated in Table 4.4 was monitored by isothermal DSC method. The curing time of all cured hyperbranched epoxy mixtures decreased with increasing curing temperature due to high kinetic energy and high mobility of epoxy molecules which resulted in low viscosity, accelerated the cure rate, and reduced the curing time [1].

The kinetic parameters (k, m, n, and E$_a$) were evaluated by fitting the experimental data (cure rate dα/dt and degree of cure α) with Eq. (2.16) via MATLAB program. The fitting of the data and the equation model are shown in Table 4.5 and Figure 4.7. The degree of cure should be selected in a range of 0.05 – 0.95 [37] to avoid the relative experimental errors for the fitting. The results were found that the experimental data could fit well with the theoretical model because the coefficient of determination (r^2) of all results was high enough (>0.90). The rate had the accelerating and decreasing mechanisms at the initial and final stages, respectively. For the rate constant (k), it was a function of curing temperature (Arrhenius equation) in which it increased when the temperature increased.

Table 4.5 The curing kinetic parameters of the hyperbranched epoxy at several curing temperatures

Parameter	HBE	HBE5P	HBE10P	HBE15P
70 °C				
k	0.115	0.297	0.145	0.118
n	0.894	1.288	0.882	0.944
m	0.040	0.281	0.059	0.064
r^2	0.999	0.990	0.998	0.999
80 °C				
k	0.201	0.899	0.349	0.268
n	1.143	1.630	1.120	1.253
m	0.050	0.278	0.122	0.142
r^2	0.999	0.987	0.998	0.998
90 °C				
k	0.311	1.943	0.631	0.410
n	1.321	2.060	1.302	1.242
m	0.047	0.490	0.160	0.061
r^2	0.999	0.991	0.996	0.997
100 °C				
k	0.725	2.401	1.308	0.889
n	1.646	1.928	1.622	1.493
m	0.257	0.262	0.147	0.136
r^2	0.994	0.947	0.927	0.982
E_a (kJ mol^{-1})	63.38	75.56	76.52	69.02
r^2	0.975	0.936	0.996	0.987

Moreover, the rate constant (k) of the hyperbranched epoxy with PEG was higher than those without PEG due to high degree of branching [51]. The rate constant (k) of HBE5P system was the highest: namely, its initial cure rate was very fast. However, its curing time was not the lowest due to high crosslink network structures, resulting in hindering the cure reaction. Furthermore, n and m orders of each cured hyperbranched epoxy at the same isothermal temperature were

insignificantly different, except HBE5P. The n and m values of the HBE5P system were the highest. It implied that the cure rate of the HBE5P system was the fastest in the initial stage and then the rate was the slowest at the final stage because the reaction was controlled by the diffusion-reaction due to high crosslink structure [52, 53]. Besides, the activation energy (E_a) of the epoxy thermoset at several curing temperatures was calculated from Eq. (2.17) and listed in Table 4.5. The E_a increased with the increase of PEG due to the steric hindrance of PEG and hyperbranched structure [54, 55], whereas the activation energy of HBE15P decreased due to its a large amount of equivalent active epoxy group per mass sample (low EEW) in which it could facilitate the curing reaction, and the low interaction of the molecular chain [56, 57].
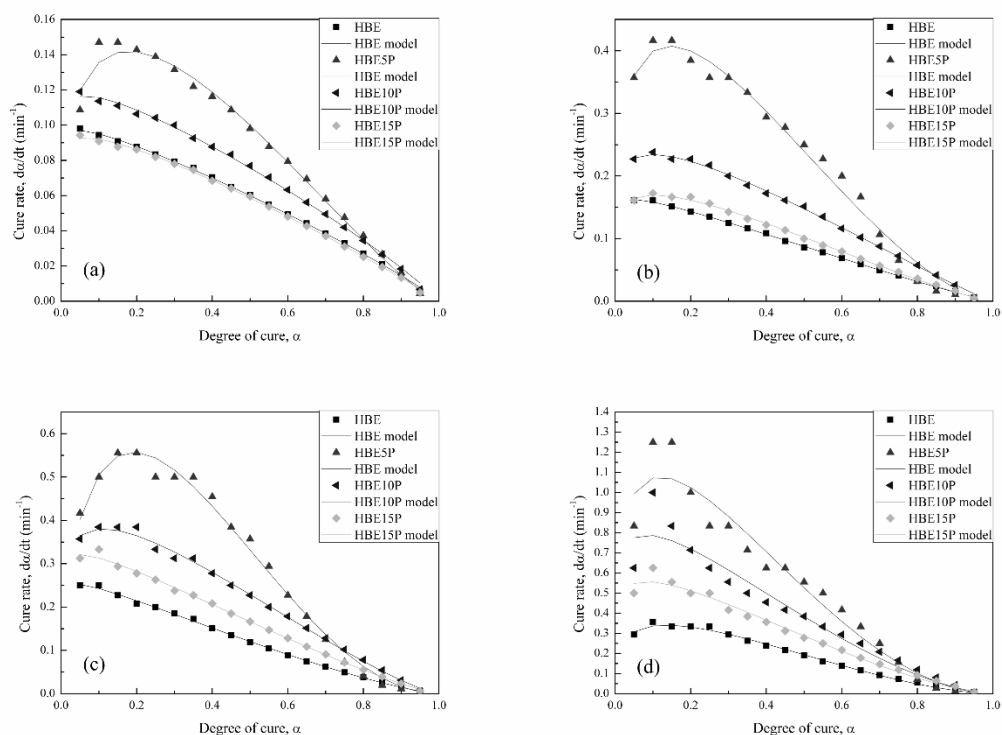
Figure 4.7 The cure rate and degree of cure of HBE with various PEG contents at (a) 70 °C, (b) 80 °C, (c) 90 °C, and (d) 100 °C. The symbol shows the experimental result and the solid line is model fitting.

4.3 Thermal curing behavior of DGEBA with hyperbranched epoxy resin

Firstly, curing behavior (T_o, T_p and ΔH_{rxn}) of the epoxy mixtures was investigated by non-isothermal DSC method, as shown in Figure 4.8 and Table 4.6. It was found that when PEG increased, the T_o and T_p decreased due to the long-chain structure and ether group of PEG acting as the plasticizer. For ΔH_{rxn} of the resins, it increased when PEG increased because EEW decreased, increasing the active epoxide ring and inducing more curing reaction. Moreover, T_g of the epoxy thermoset with the hyperbranched resins increased due to high crosslink density [50].
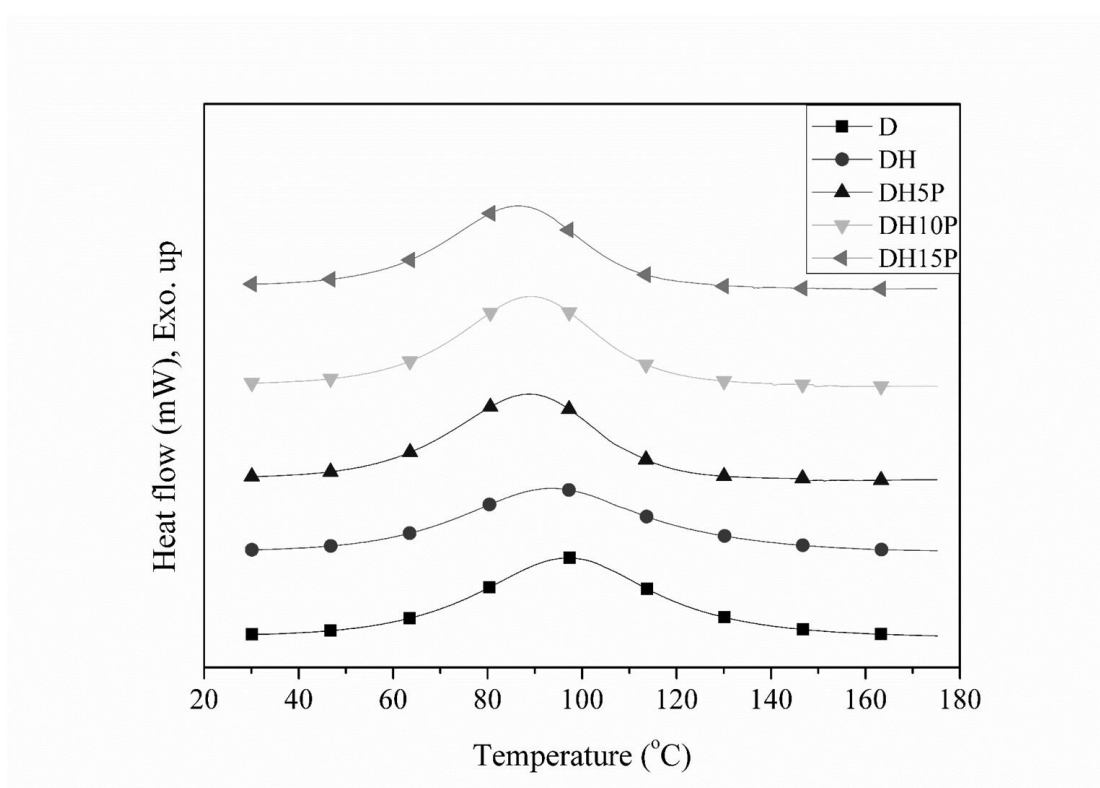
Figure 4.8 The curing behavior of D, DH, DH5P, DH10P and HD15P

Table 4.6 The curing behavior and thermal properties of D, DH, DH5P, DH10P, and DH15P systems

Parameter	D	DH	DH5P	DH10P	DH15P
Onset temperature (°C)	61.79	58.80	57.98	60.70	57.12
Peak temperature (°C)	97.00	93.54	88.85	89.22	86.64
Heat of reaction ($J\ g^{-1}$)	447.35	379.32	388.26	393.25	392.31
Curing time at 70 °C (sec)	1,398	1,427	1,427	1,424	1,398
Curing time at 80 °C (sec)	1,101	1,118	1,186	1,048	1,038
Curing time at 90 °C (sec)	744	881	828	780	900
Curing time at 100 °C (sec)	695	825	761	718	771
T_g (°C)	140.70	110.91	114.26	116.15	122.72
EEW ($g\ eq^{-1}$)	170.205	220.114	219.050	215.304	210.362

As tabulated in Table 4.6, the curing time of all systems at 70, 80, 90, and 100 °C was determined by the isothermal DSC method. When curing temperature increased, the curing time of all cured epoxy mixtures decreased because of high mobility of epoxy molecules which accelerated the cure rate, decreased viscosity, and reduced the curing time [1]. Moreover, curing time of DH10P system was lower than other systems when the curing temperature increased due to its optimal rate of reaction following the autocatalytic model or Šesták-Berggren model [35], as shown in Figure 4.9 and Table 4.7, The cure rate of the DH10P system had the accelerating and decreasing behaviors at the initial and final stages, respectively. The DH10P system provided the optimum kinetic parameters and these resulted in the lowest activation energy.
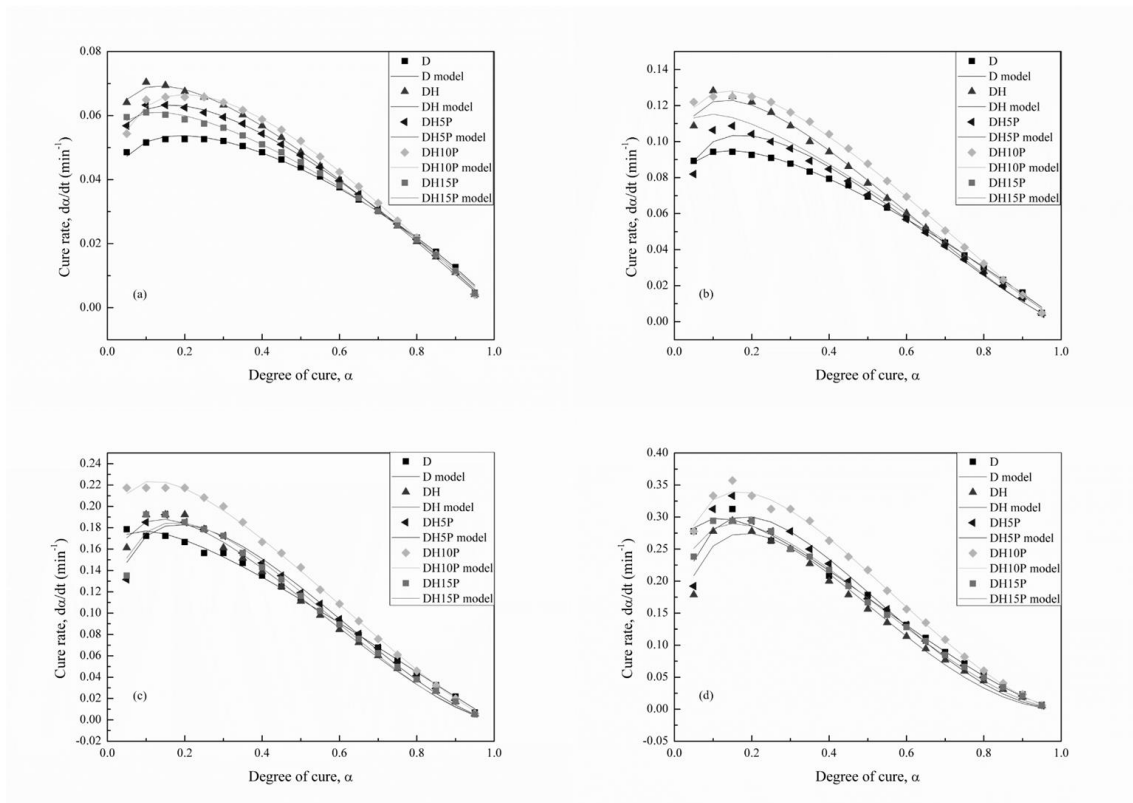
Figure 4.9 The cure rate and degree of cure of DGEBA with various hyperbranched epoxy resins at (a) 70 °C, (b) 80 °C, (c) 90 °C, and (d) 100 °C. The symbol shows the experimental result and the solid line is model fittin

จุฬาลงกรณ์มหาวิทยาลัย

CHULALONGKORN UNIVERSITY

Table 4.7 The curing kinetic parameters of the hyperbranched epoxy systems at several curing temperatures

Parameter	D	DH	DH5P	DH10P	DH15P
70 °C					
k	0.089	0.111	0.106	0.130	0.089
n	0.846	1.025	0.975	1.067	0.871
m	0.198	0.161	0.190	0.266	0.126
r^2	0.997	0.999	0.999	0.999	0.998
80 °C					
k	0.152	0.221	0.209	0.220	0.165
n	0.979	1.294	1.268	1.155	1.050
m	0.164	0.197	0.262	0.185	0.108
r^2	0.999	0.996	0.992	0.999	0.999
90 °C					
k	0.255	0.375	0.441	0.382	0.449
n	1.065	1.473	1.487	1.278	1.570
m	0.109	0.237	0.340	0.175	0.336
r^2	0.998	0.994	0.988	0.998	0.988
100 °C					
k	0.528	0.866	0.901	0.792	0.666
n	1.418	1.969	1.880	1.574	1.644
m	0.184	0.441	0.422	0.312	0.298
r^2	0.996	0.981	0.973	0.997	0.996
E_a (kJ mol^{-1})	62.15	71.35	76.10	63.53	74.94
r^2	0.988	0.990	0.998	0.989	0.978

4.4 Effect of hyperbranched epoxy on UV curing, thermal- and rheological-properties of DGEBA

The UV curing behavior, thermal and rheological properties of the blended epoxy system (having DGEBA and hyperbranched epoxy) using triarylsulfonium hexafluorophosphate salts acting as photoinitiator were investigated by photo-DSC and photo-rheometer, respectively. The curing behavior and thermal property were studied with UV intensity of 30 mW cm^{-2}, the irradiation time of 120 s and temperature of 30 °C, while the rheological properties were studied by UV intensity of 30 mW cm^{-2}, the irradiation time of 120 s and temperature of 30 °C.

The conversion and cure rate of each sample are shown in Figure 4.10 – 4.11 and Table 4.8. As shown in Figure 4.12 – 4.13, it was seen that the cure rate decreased when the content of hyperbranched epoxy resin increased because it could act as a delaying agent by the H-bond affecting to increase viscosity and the obstacle of hyperbranched structure [1, 35, 50, 58]. However, the cure rate of D90H10 and D80H20 systems early decreased and the conversion value of these systems showed lower than that of others because of a high rate at the initial stage, Therefore, their reaction was finally controlled by diffusion due to high crosslink density. Moreover, the systems with higher 30 wt% HBE10P could not achieve complete curing reaction because the hyperbranched polymers can act as a delaying agent due to its non-entanglement structure [59-63].

The fully-cured glass transition temperature of each sample is shown in Table 4.8. It was found that the glass transition temperature decreased when the content of hyperbranched resins increased due to the hyperbranched resins' structure having branching point and free volume. However, the growth of the viscosity of these systems increased gradually as shown in Figure 4.13. Besides, the system with more than 30% of HBE10P could not be fully cured after measurement because of a non-entangled molecule of hyperbranched resin.

For the suitable ratio of DGEBA and HBE10P, there is the consideration of the operating temperature (25 – 80 °C) in a hard disk drive to select the suitable ratio. There are only two systems, D90H10 and D80H20, in which their glass transition temperatures were more than 80 °C. Moreover, the conversion after UV and dark curing of both systems was very high value, (> 0.95) and the residual heat of reaction

was minimal value. Also, the cure rate of D90H10 was not only higher than that the cure rate of D80H20 but the change of heat capacity (ΔC_p) of D90H10 (0.248 J/g ^{o}C) at glass transition state was also less than that of D80H20 (0.369 J/g ^{o}C). Therefore, D90H10 resin was selected for studying the influence of UV curing conditions.

Table 4.8 Curing behavior, thermal and rheological properties of each epoxy systems

Resin	EEW (g eq^{-1})	Photo-DSC[a]				Photo-rheometer	
		α_{UV}	α	T_g (^{o}C)	ΔC_P (J g^{-1} ^{o}C^{-1})	Initail viscosity (cP)	t_{gel} (s)
DGEBA	170.21	0.43	0.57	113.54	113.54	6,001	- (parallel)
D90H10	182.98	0.49	0.63	96.54	96.54	45,923	174
D80H20	197.83	0.52	0.67	87.34	87.34	27,680	78
D70H30	215.30	0.50	0.72	78.04	78.04	23,602	93
HBE10P	564.00	-	-	-	-	7,955	-

α_{UV}: UV conversion, α: UV and dark conversions
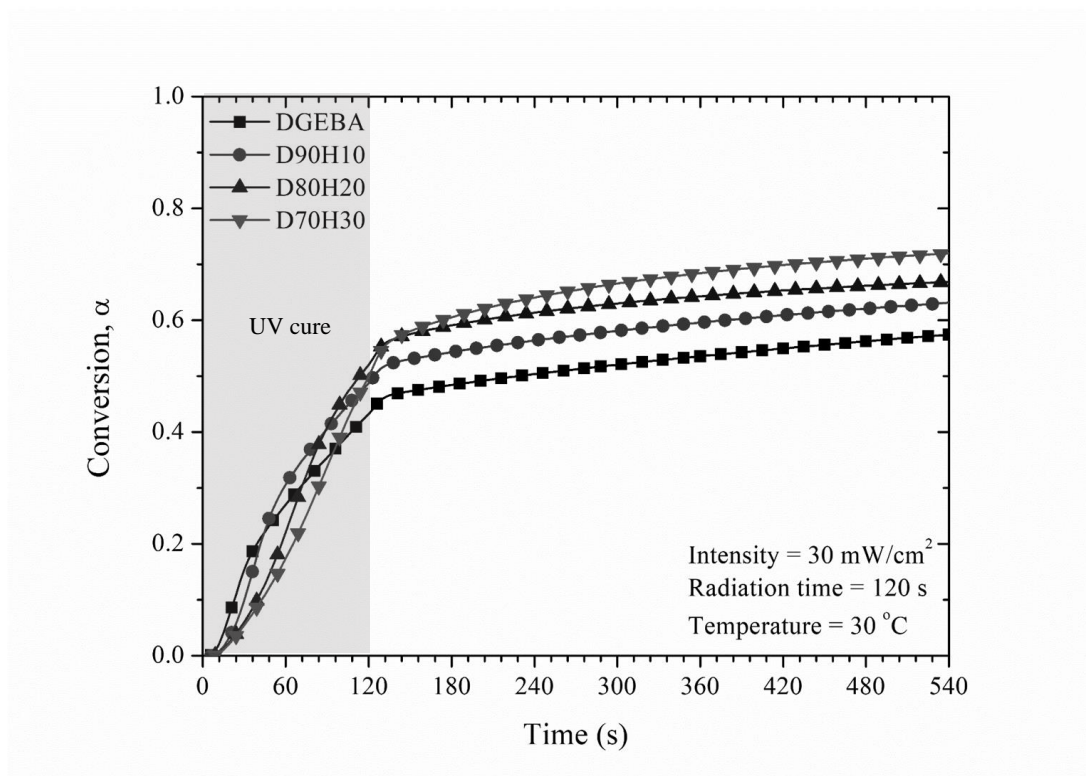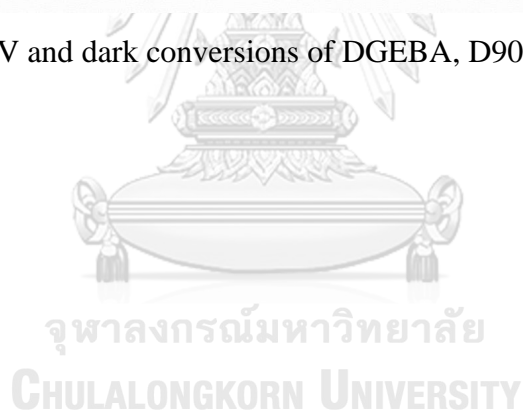
Figure 4.10 The UV and dark conversions of DGEBA, D90H10, D80H20, and D70H30 systems
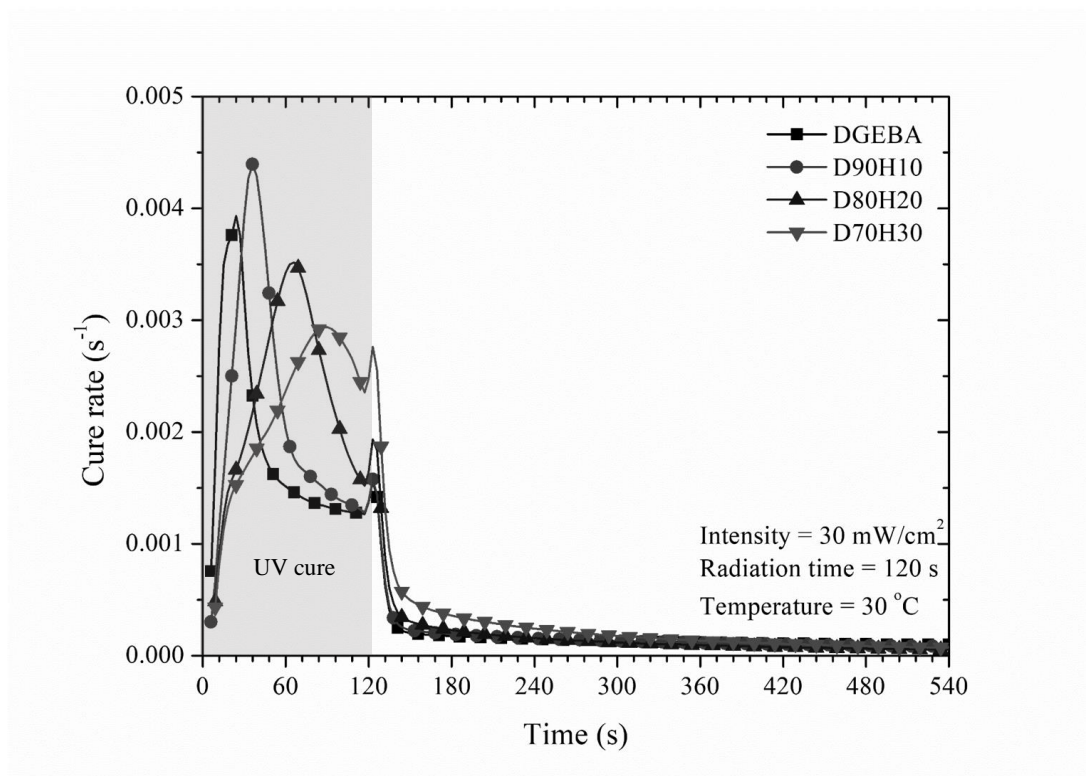
Figure 4.11 The UV and dark conversions of DGEBA, D90H10, D80H20, and D70H30 systems
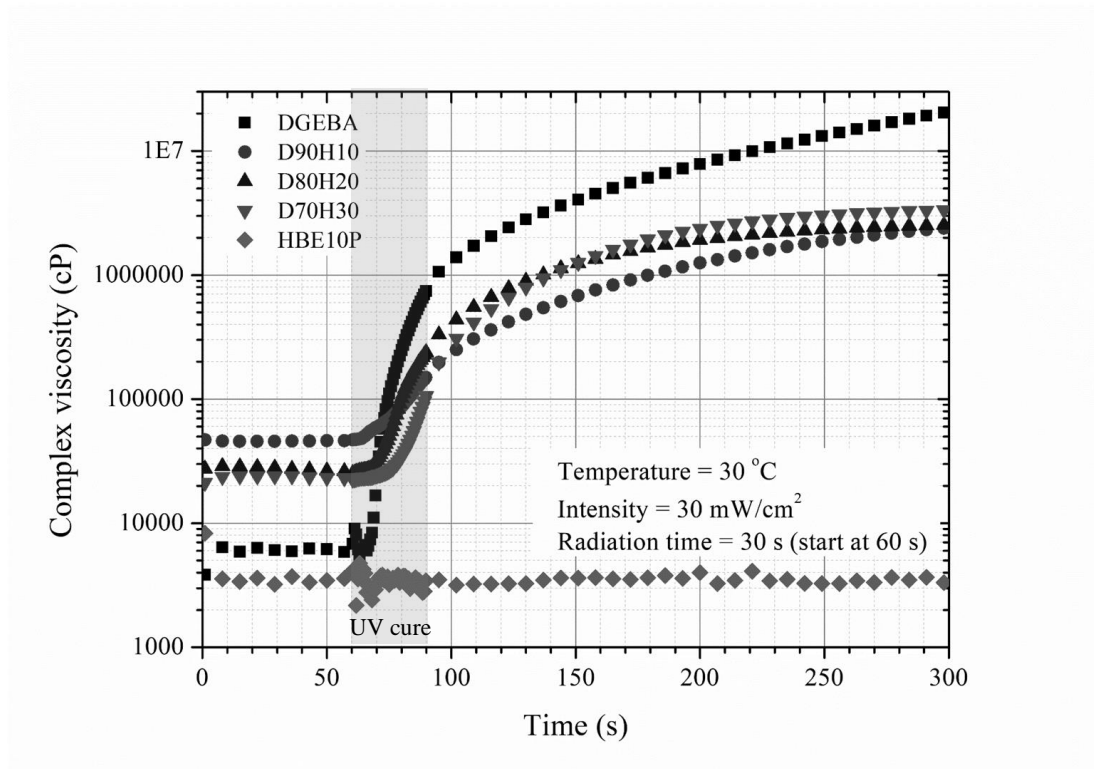
Figure 4.12 The growth of complex viscosity of DGEBA, D90H10, D80H20, D70H30, and HBE10P systems
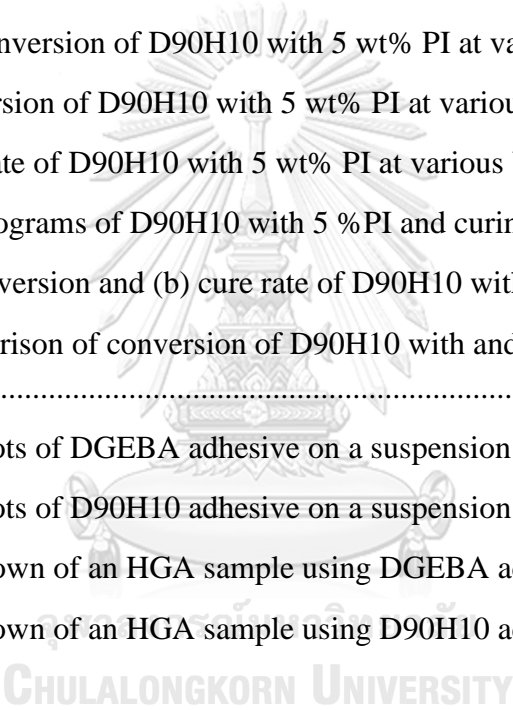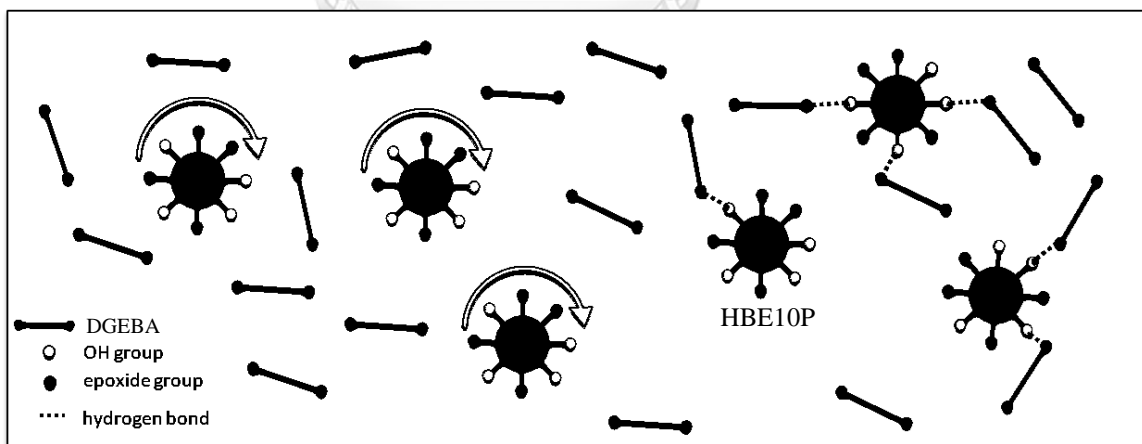
Figure 4.13 The effects of ball-bearing, globular and non-entanglement structure, and hydrogen bond on the epoxy system

4.5 Effect of photoinitiator content on UV curing, thermal- and rheological-properties

This experiment was performed to study the effect of photoinitiator (PI) content (3, 5, and 10 wt% of resin) on UV and dark curing behavior of the D90H10 system. The curing behavior and flow behavior were investigated by photo-DSC and photo-rheometer, respectively. The curing properties were studied by UV intensity of 30 mW cm^{-2}, the irradiation time of 120 s and temperature of 30 °C, while the rheological properties were studied by UV intensity of 30 mW cm^{-2}, the irradiation time of 120 s and temperature of 30 °C.

The curing behavior of each sample is shown in Figure 4.14 – 4.15 and Table 4.9. It was found that the conversion after UV and dark curing and the cure rate of the system with 5 wt% PI were the maximum values whereas the minimum values were of the system with 10 wt% PI. At 10 wt% PI, there were excessively activated PI molecules, resulting in an excess of protonated epoxide molecules. Therefore, it resulted in high crosslink density at the irradiated surface of the sample and it blocked the UV penetration as shown in Figure 4.16.

For fully-cured glass transition temperature (T$_g$) as shown Table 4.9, T$_g$ of the system with 3 wt% PI was less than 80 °C and there was higher ΔC$_p$ value than others because of low PI content resulting in low crosslink density. Therefore, there were only two systems that were suitable for HDD. However, the cure rate and the conversion after UV and dark curing of the system with 5 wt% PI were the maximum values, so D90H10 with 5 wt% PI was the suitable mixture for the next study.
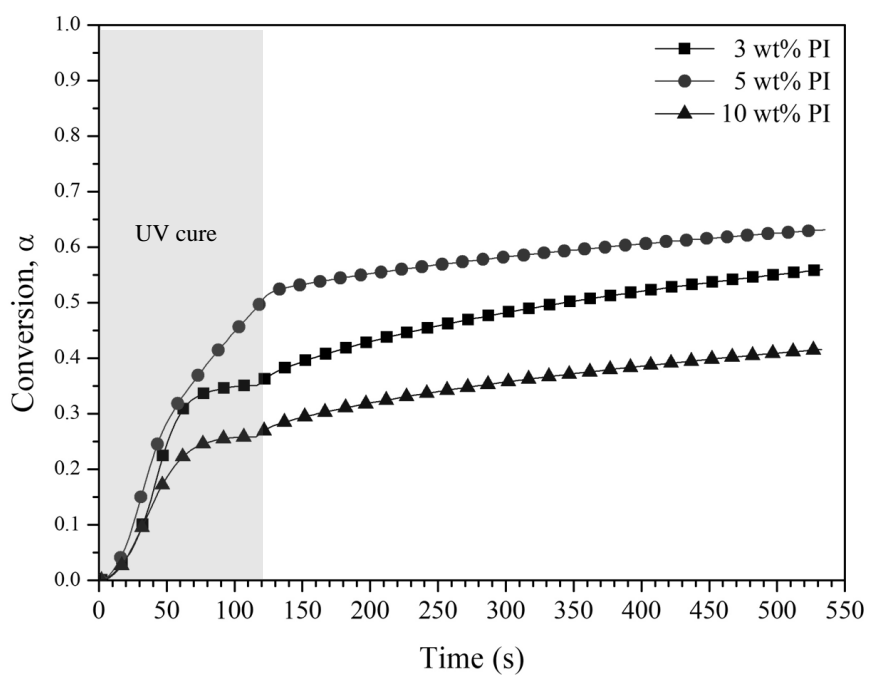
Figure 4.14 The conversion of D90H10 with 3, 5 and 10 wt% photoinitiator
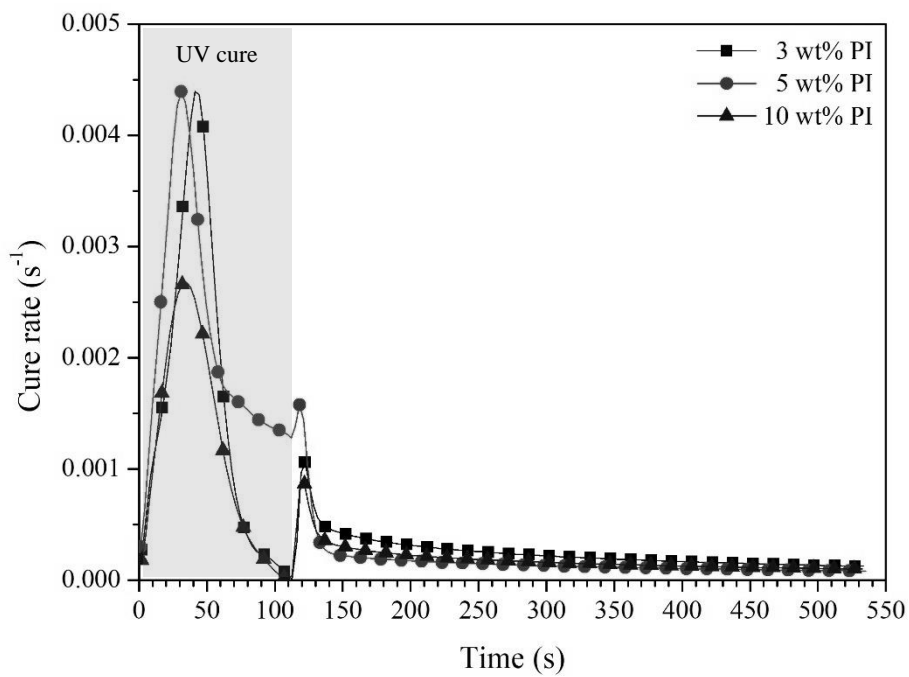
Figure 4.15 The cure rate of D90H10 with 3, 5 and 10 wt% photoinitiator

Table 4.9 Heat of reaction and conversion of each sample by UV and dark curing

PI content (wt%)	α_{UV}	α	T_g (°C)	ΔC_P at T_g (J g^{-1} °C^{-1})	t_{gel} (s)
3	0.35	0.56	76.01	0.414	440
5	0.49	0.63	96.54	0.248	174
10	0.26	0.42	91.57	0.267	-
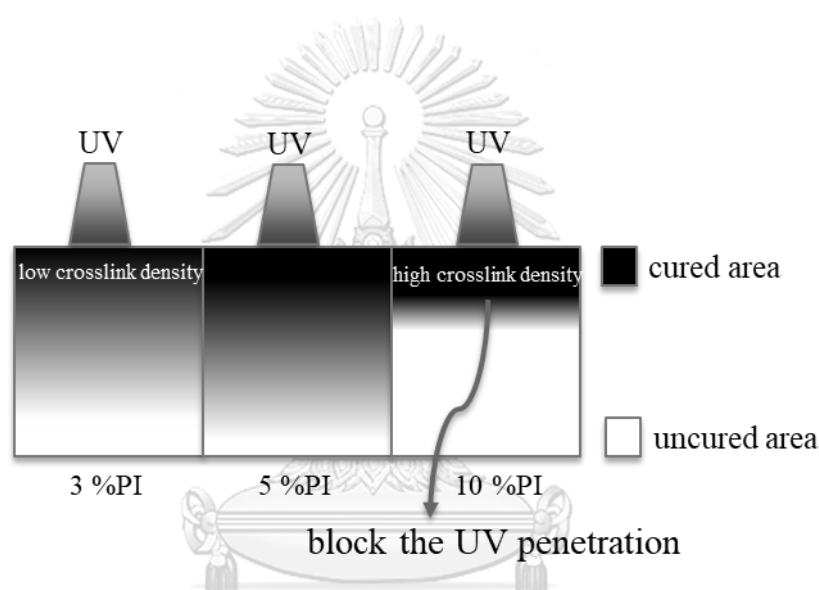
Figure 4.16 The effect of photoinitiator concentration on UV cure

4.6 Effect of temperature and irradiation time on UV curing, thermal- and rheological-properties

The curing condition is a factor that can affect curing behaviors and rheological properties, such as UV intensity, irradiation time (t_{ir}), and temperature. This part shows the effects of irradiation time and temperature on the curing behaviors and the rheological properties with a UV intensity of 30 mW/cm^2 only.

Figure 4.17 shows the effect of irradiation time and temperature on the storage modulus (G'). The G' increased when irradiation time and temperature increased because there were more initiated molecules and more mobility. This result could relate to complex viscosity that increased when these influences increased as shown in Figure 4.18. Furthermore, the irradiation time and temperature affected the gelation

time (t_{gel}) as shown in and Table 4.10. The gelation time can be determined from the crossover of G' and G'' and it was found that the gelation time decreased when the radiation time and temperature increased because the sample obtained higher energy and UV penetration, except I30T30t10, I30T30t60, and I30T80t10 conditions in which there was no the gelation time.

For the I30T30t10 condition, the state of the sample after the test was high viscous liquid due to low initiated molecules resulting in that cannot achieve the formation of network structure.

For I30T30t60 and I30T80t10 conditions, there were very high rate and high crosslink density resulting in high brittleness. This occurrence may cause the failure of network structure forming due to shear force from the rheometer [39]. Moreover, it can be explained by the time-temperature-transformation (TTT) diagram [64]. If the temperature is not more than $T_{g, gel}$, the curing reaction will be restrained, and the state of the sample will be a sol glass resulting in no the crossover of G' and G''. This occurrence is called vitrification.

For UV curing behavior by photo-DSC technique. According to Figure 4.19 and Table 4.10, it was seen that UV conversion (α_{UV}) increased when the radiation time and temperature increased because of more initiated molecules and high mobility. For the thermal property of samples in various curing conditions as shown in Table 4.10, glass transition temperature increased when the radiation time and temperature increased due to high curing reaction. However, the total conversion after UV and dark curing (α) decreased when the irradiation time or the temperature was too much, especially I30T30t60 and I30T80t10 conditions. According to the time-temperature-transformation (TTT) diagram, the reaction was hindered by vitrification ($T_{g, gel} > T_{curing}$) and it resulted in low glass transition temperature due to low conversion and low crosslink density.
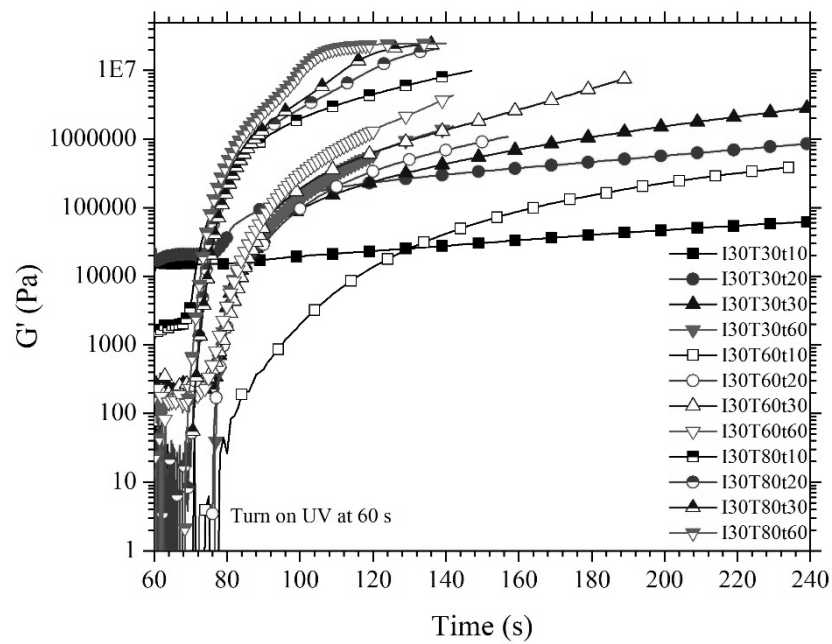
Figure 4.17 Storage modulus in various curing condition with UV intensity of
30 mW/cm^2
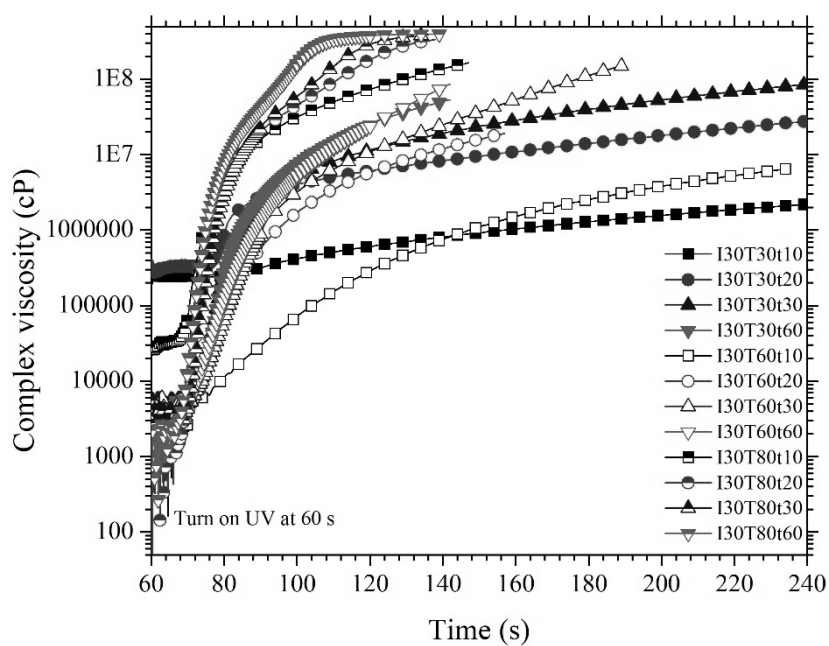
Figure 4.18 Complex viscosity in various curing condition with UV intensity of 30 mW/cm^2
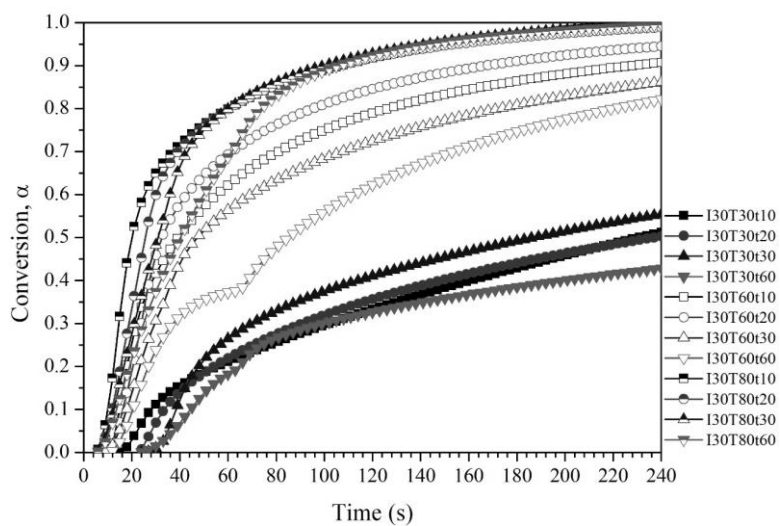
Figure 4.19 The conversion of D90H10 with 5 wt% PI at various curing conditions

Table 4.10 Gelation time in various curing condition with UV intensity of 30 mW/cm^2

Curing condition	UV curing		Dark curing	α	ΔH (J g^{-1})	T_g (°C)	t_{gel} (s)
	ΔH_{UV} (J g^{-1})	α_{UV}	ΔH_{dark} (J g^{-1})				
I30T30t10	-	-	38.02	-	38.02	-	-
I30T30t20	-	-	71.67	-	71.67	-	437.0
I30T30t30	1.68	0.01	86.86	0.67	88.54	57.43	266.8
I30T30t60	37.84	0.18	51.32	0.43	89.16	64.80	-
I30T60t10	-	-	107.73	0.91	107.73	57.46	56.0
I30T60t20	29.46	0.22	99.79	0.94	129.25	129.27	25.7
I30T60t30	57.87	0.31	104.88	0.86	162.75	81.41	23.8
I30T60t60	58.76	0.37	69.10	0.82	127.86	67.75	22.5
I30T80t10	7.99	0.06	116.98	1.00	124.97	50.00	-
I30T80t20	64.72	0.36	111.02	0.99	175.74	57.50	13.0
I30T80t30	99.54	0.48	106.4	0.99	205.94	60.00	13.0
I30T80t60	184.59	0.69	82.79	0.99	267.38	96.50	11.2

4.7 Effect of UV intensity on UV curing, thermal- and rheological-properties

The curing and rheological properties of D90H10 system with 5 wt% photoinitiator were investigated via photo-DSC and photo-rheometer, respectively. These properties were studied by varying UV intensity (10, 20, 30, 40, and 50 mW/cm^2), the irradiation time of 60 s, and a temperature of 80 °C.

As tabulated in Table 4.11, it was found that the t_{gel} of the D90H10 system decreased when UV intensity increased due to high activated photoinitiator and monomer molecules, generating a high reaction rate. Moreover, the photo-rheological properties were seen to be complementary to the UV conversion (α_{UV}) from DSC's heating profile, as shown in Figure 4.20 – 4.21. Higher UV conversion of epoxy with low t_{gel} was observed; therefore, the increase in UV intensity can accelerate the curing reaction.

This study used the molecular weight between crosslinking points (M_c) and the radius of gyration (R_g), which were calculated from Eq. (2.26) and Eq. (3.3), to explain the curing reaction, as shown in Table 4.11. Increase in UV intensity from 10 to 30 mW/cm^2, M_c and R_g increased because of high molecular weight and structure of hyperbranched resin. Moreover, high activated photoinitiator molecules can generate more protonated epoxide molecules in the hyperbranched resin, and it resulted in creating a large molecule between the crosslinking points.

However, the occurrence was reversed when the UV intensity increased from 30 to 50 mW/cm^2, the M_c and R_g greatly decreased. With excessive UV intensity, there were exceedingly activated photoinitiator molecules and protonated epoxide molecules. Therefore, each active chain quickly encountered each other, resulting in very low M_c and very high cross-link density. Furthermore, the cure rate and t_{gel} slightly decreased and increased, respectively. It can be denoted by high storage modulus at the gel point (G'_{gel}), as shown in Table 4.11. Moreover, it resulted in low mobility and low cure rate during the UV reactions.

Table 4.11 The properties of D90H10 system at various UV intensity

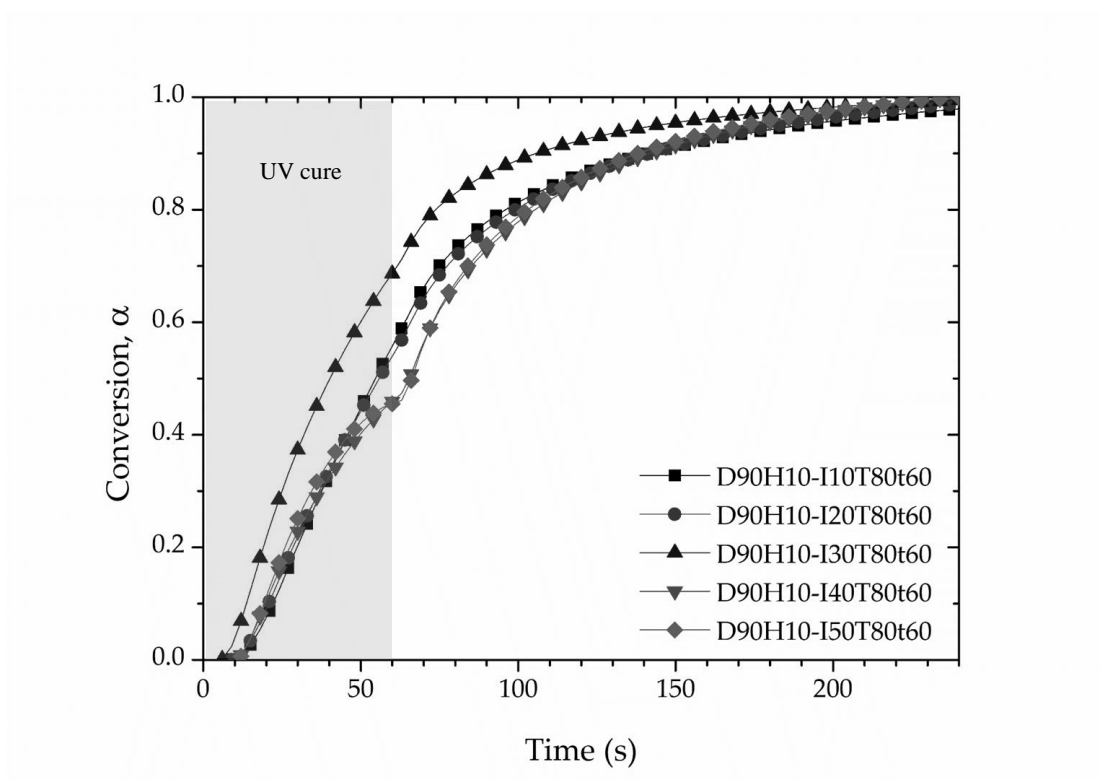| UV intensity (mW/cm^2)	Photo-rheometer					Photo DSC	SAXS
	t_{gel} (s)	G'_{gel} (Pa)	M_c (g mol^{-1})	α_{UV}	α	T_g (°C)	R_g (nm)
10	22.5	2,630	942,493	0.56	0.98	132.50	8.39
20	18.8	1,890	1,311,507	0.54	0.99	121.62	9.06
30	11.0	1,870	1,325,520	0.69	0.99	102.95	18.00
40	12.5	7,000	354,104	0.46	1.00	103.58	10.8
50	12.2	9,180	270,179	0.45	1.00	107.48	8.78

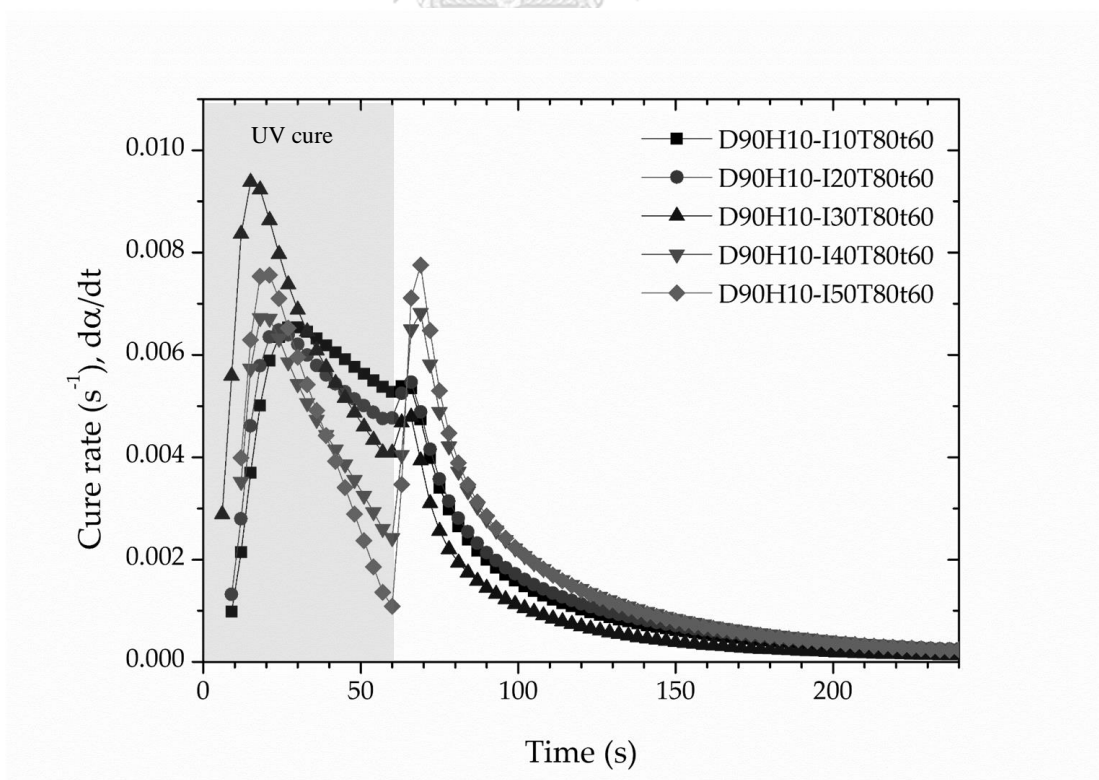Figure 4.20 Conversion of D90H10 with 5 wt% PI at various UV intensities

Figure 4.21 Cure rate of D90H10 with 5 wt% PI at various UV intensities

Interestingly, as shown in Figure 4.21, there were double peaks in the cure rate profile. The UV curing reaction was the first peak and the dark curing reaction was the second peak (after shutting off UV light). Owing to the presence of hydroxyl group in the DGEBA and hyperbranched resins, these phenomena can be explained in that there are two propagation mechanisms of the ring-opening cationic polymerization of epoxy in the presence of hydroxyl group: ACE and AM mechanisms, as shown in Figure 2.6 [26]. The ACE mechanism predominated until the reaction passes the maximum rate during the UV reaction, whereas the AM mechanism further predominated because of the concentration of hydroxyl, (OH) group, which is larger than that of initiator, $[I^+]$.

After shutting off UV light, there is no activation of the initiator; therefore, the dark reaction follows the AM mechanism which is the chain transfer reaction resulting in the activated monomer and the consumption of OH group to produce another OH group. These reactions release heat as same as the curing reaction; therefore, the exothermic heat could be observed by the photo-DSC technique, resulting in the second peak in the dark curing period. Besides, the second peak at high UV intensity was higher than the second peak at low UV intensity due to greater initiator concentration.

4.8 Effect of curing agent on UV curing behavior of D90H10 system

This section studied the effect of curing agent (CA) for thermal cure on UV curing behavior by photo-DSC technique. Firstly, it should investigate the thermal curing behavior of sample, D90H10 with 5 %PI and DETA, by scanning temperature as shown in Figure 4.22 and Table 4.12. It was found that there were onset and peak temperatures of 60 °C and 95 °C, respectively. Moreover, there were two glass transition temperatures of 58 °C and 138 °C. It means that there was phase separation due to dual resins, DGEBA and HBE10P resins, however, there was only a glass temperature for the system without photoinitiator, around 115 °C.
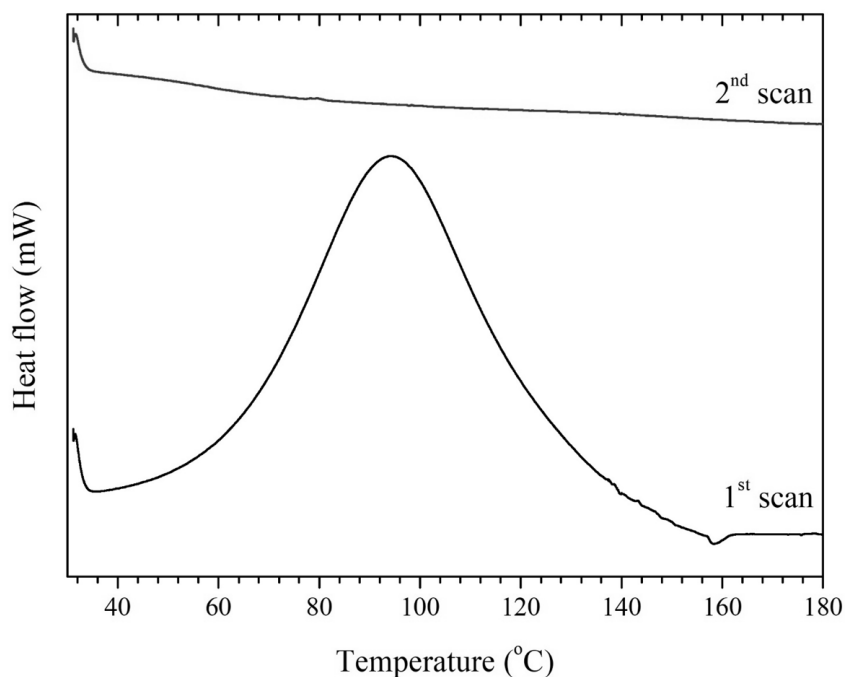
Figure 4.22 Thermograms of D90H10 with 5 %PI and curing agent

Table 4.12 Curing behavior and thermal properties of D90H10 with 5 %PI and DETA curing agent

Sample	1st scan			2nd scan
	T_o (°C)	T_p (°C)	ΔH_{rxn} (J g^{-1})	T_g (°C)
D90H10 + 5 %PI + CA	60	95	402.35	58, 138

Furthermore, there were the study and investigation of conversion and cure rate of the samples that consist of the different compositions, as shown in Figure 4.23 and Table 4.13. The curing method was using a UV intensity of 30 mW/cm^2, the irradiation time of 10 s, thermal curing time (t_{curing}) of 4 min after UV radiation and temperature of 80 °C. It was found that the conversion decreased when CA was added. Moreover, there were two T_gs of the samples with photoinitiator and CA because there were two reactions concurrently, UV and thermal curing reactions.

However, there was a study of the effect of curing condition on curing behavior for this system as shown in Table 4.14. There were four thermal curing times (1, 2, 3, and 4 min) after UV cure and the same DSC method as the previous

experiment. It was found that the conversion increased and the residual heat of reaction (ΔH_{res}) decreased with an increase in curing time and it resulted in increasing peak temperature due to obstacle from a cured molecule. Furthermore, the T_g increased until the curing time exceeding 2 min and there were two T_gs because the thermal curing predominated. Besides, Figure 4.24 shows the conversion at various curing conditions. It was found that the conversion of the systems with curing agent was very low value when it was compared with the conversion of the system without curing agent because the Brønsted acid (H^+) from photoinitiator can react with a lone pair of the electron in nitrogen atom of amine group ($R-NH_2$) from curing agent, resulting in ammonium salts ($R-NH_4^+$) [30]. Therefore, it should not use the amine curing agent for photo-cationic polymerization because it can inhibit the reaction and it is not necessary to use the thermal initiator in the UV cure because the reaction can continue by heating.

Figure 4.23(a) Conversion and (b) cure rate of D90H10 with various compositions

Table 4.13 Conversion (α) and glass transition temperature of samples at various compositions and curing conditions (t_{curing} = 4 min)

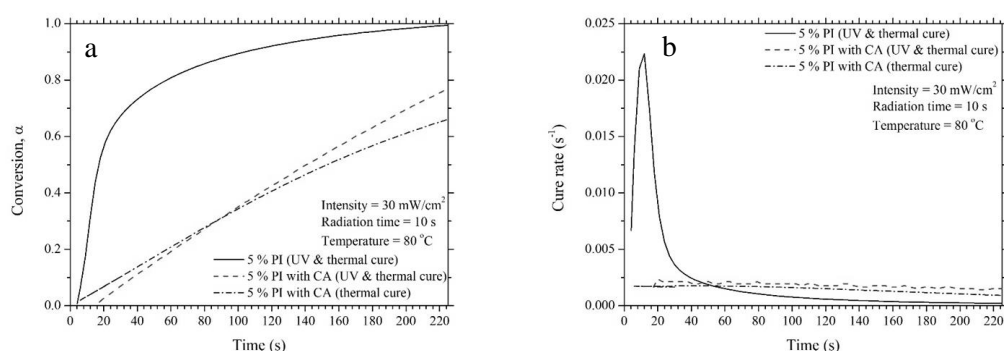| Sample	α	T_g (°C)
5 %PI (I30T80t10)	0.99	50.00
5 %PI + CA (80 °C)	0.67	102.91
5 %PI + CA (I30T80t10)	0.77	110, 150

Table 4.14 Curing behavior and thermal properties of D90H10 with 5 %PI and curing agent at various curing conditions

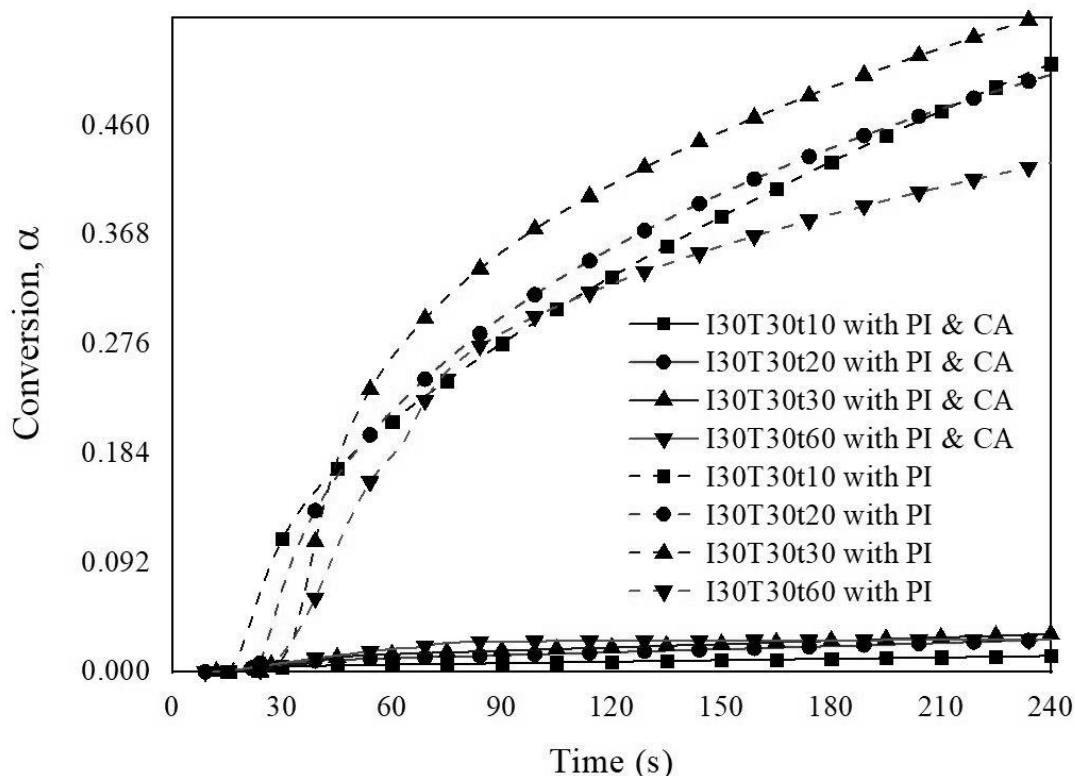| Curing condition	α	Residual reaction (2nd scan)			T_g (°C) (3rd scan)
		T_o (°C)	T_p (°C)	ΔH_{res} (J g^{-1})	
I30T80t10 (t_{curing} = 1 min)	0.12	54	90	300.75	95
I30T80t10 (t_{curing} = 2 min)	0.28	53	89	201.83	98
I30T80t10 (t_{curing} = 3 min)	0.48	52	95	164.99	65, 153
I30T80t10 (t_{curing} = 4 min)	0.77	54	97	123.02	110, 150

Figure 4.24 Comparison of conversion of D90H10 with and without CA at various curing conditions

4.9 Audit of DGEBA and D90H10 systems for HGA process

Before using an adhesive, it must inspect the adhesive's properties how they are suitable for the HGA process. This section studied viscosity, dot size and pull strength of DGEBA and D90H10 systems. In Table 4.15, the viscosity of DGEBA and D90H10 systems are 6,001 cP and 45,923 cP, respectively. Their results did not qualify for the process specification limits, as shown in Table 3.5; however, as shown in Figure 4.25 and Figure 4.26, dot sizes of both DGEBA and D90H10 systems on the suspension were appropriate because the air pressure and temperature can be adjusted.

For the pull strength test, it could not perform the test because of the incomplete reaction of both systems. As Figure 4.27 and Figure 4.28, the slider was torn down after the UV radiation for 4 hr. It was seen that the adhesives were not dry; therefore, the pull strength was not performed because there were not enough irradiation time and UV intensity in the QC process. Especially the third curing, there

is no direct focus of UV radiation on the adhesives, but the UV radiation is scattering. According to sections 4.6, it could compare the curing conditions of the experiments and the QC process. It was found that the UV conversion of these adhesives might be only 0.01-0.06, resulting in an incomplete reaction. However, the pull strength may be the same trend as glass transition temperature and storage modulus of the samples, viz. when these properties increase, the pull strength will also increase.
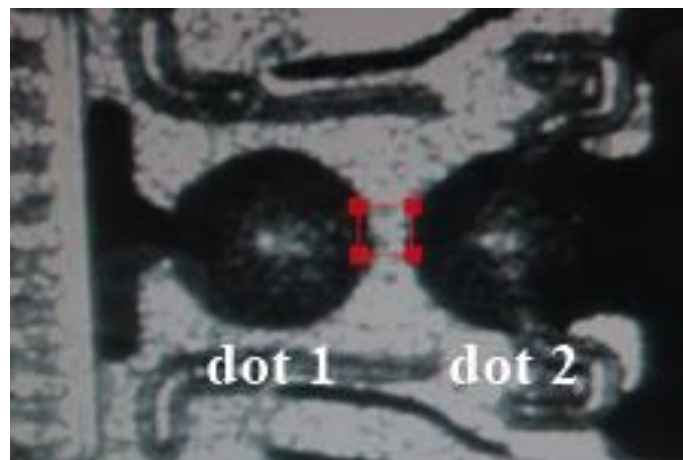
Figure 4.25 Two dots of DGEBA adhesive on a suspension

Figure 4.26 Two dots of D90H10 adhesive on a suspension

Table 4.15 Viscosity and dot size of DGEBA and D90H10 systems

System	Viscosity (cP)	Dot size (μm)	
		Dot 1	Dot 2
DGEBA	6,001	258	237
D90H10	45,923	244	268

Figure 4.27 Tear down of an HGA sample using DGEBA adhesive

Figure 4.28 Tear down of an HGA sample using D90H10 adhesive

CHAPTER 5
CONCLUSIONS AND RECOMMENDATIONS

5.1 Conclusions

The hyperbranched epoxy resin could be synthesized by A_2 + B_4 polycondensation reaction consisting of bisphenol A (BPA) and polyethylene glycol (PEG) as A_2 monomers, pentaerythritol as B_4 branching monomer, and epoxide end group. There were v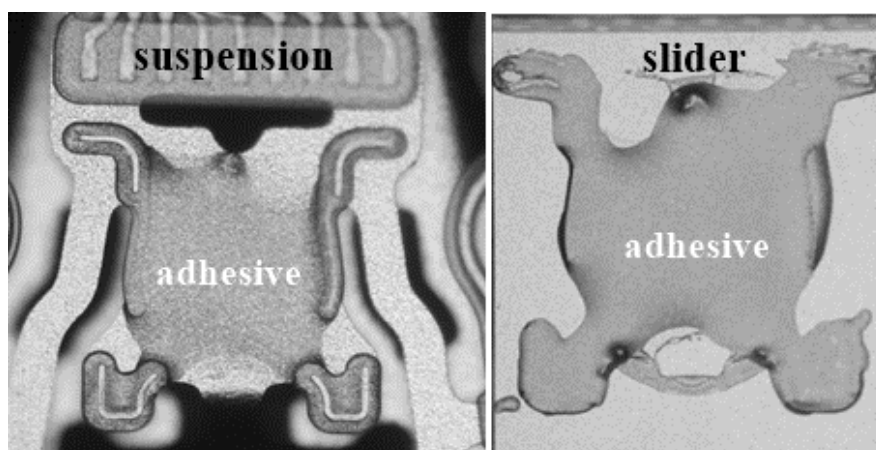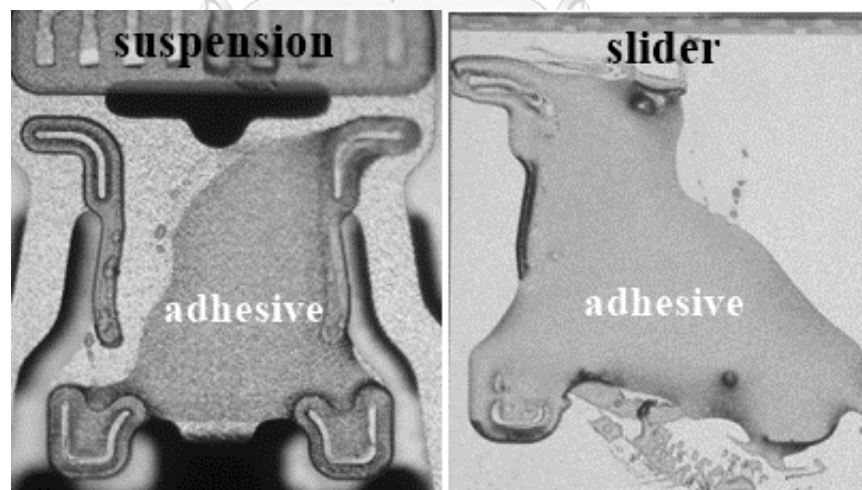arying PEG contents of 0, 5, 10, and 15 wt% of BPA. The synthesized resins could be confirmed by identifying the important chemical bond and possible structure by Fourier-transform infrared spectroscopy (FTIR) and H- and ^{13}C-nuclear magnetic resonance (H-NMR and ^{13}C-NMR) techniques. The ^{13}C-NMR technique could identify the degree of branching (DB) of the synthesized resins. It was found that the degree of branching of the synthesized resins was higher than 0.5 in which it meant they were the hyperbranched polymers. There was a high degree of branching when the content of PEG increased from 0.82 to 0.90.

The study of thermal cure with diethylenetriamine (DETA) as a curing agent, both the synthesized hyperbranched epoxy systems and combined resins between the hyperbranched polymer and diglycidyl ether of bisphenol A (DGEBA) had the curing behavior following auto-catalytic reaction of Šesták-Berggren equation. The hyperbranched epoxy resin system with 10 wt% PEG (HBE10P) and the combined resin system between DGEBA and hyperbranched epoxy with 10 wt% PEG (DH10P) provided thermal curing behavior and thermal properties appropriately.

Moreover, there was the study of UV cure of DH10P system with varying ratio of the combined resin (DGEBA:HBE10P = 100:0, 90:10, 80:20, 70:30, 60:40, 50:50, 30:70 and 0:100 wt/wt) and there were triarylsulfonium hexafluorophosphate salts as photoinitiator with varying of concentration of 3, 5 and 10 %wt of resin. It was found that the ratio of DGEBA to HBE10P of 90:10 (D90H10) with 5 wt% photoinitiator provided high UV conversion, low gelation time, and suitable rheological and thermal properties. Furthermore, high temperature and high irradiation time provided the conversion; however, when the irradiation time was too much, the conversion decreased. Also, increase in UV intensity from 10 to 30

mW/cm^2 provided high UV conversion, low gelation time, and decrease in glass transition temperature due to large network structure resulting in a decrease in crosslink density in which it was confirmed by the radius of gyration of network segment measured by small-angle X-ray scattering (SAXS) technique. However, when an increase in the UV intensity from 30 to 50 mW/cm^2, it resulted in low UV conversion and high gelation time because there was a very high initial reaction rate and then the reaction was controlled by diffusion. Besides, the glass transition temperature increased due to the high crosslink density.

Finally, DGEBA and D90H10 systems were inspected at the QC process of WD company in order to check dot size and pull strength. It was seen that the dot size of both systems was suitable for the HGA process. However, the pull strength of both systems could be not measured due to inappropriate irradiation time and UV intensity, resulting in incomplete curing reaction of the adhesives.

5.2 Recommendations

It should study the effect of UV and thermal curing conditions on bond strength at the real process in order to know the relationship of the curing condition, thermal and rheological properties, and the bond strength.

REFERENCES

1. Golaz, B., et al., *UV intensity, temperature and dark-curing effects in cationic photo-polymerization of a cycloaliphatic epoxy resin.* Polymer, 2012. 53(10): p. 2038-2048.

2. Kotch, T.G., et al., *Luminescent organometallic complexes as visible probes in the isothermal curing of epoxy resins.* Chemistry of materials, 1992. 4(3): p. 675-683.

3. Yu, J., et al., *Preparation of hyperbranched aromatic polyamide grafted nanoparticles for thermal properties reinforcement of epoxy composites.* Polymer Chemistry, 2011. 2(6): p. 1380-1388.

4. Jagadeesh, K.S., et al., *Cure kinetics of multifunctional epoxies with 2, 2'-dichloro-4, 4'-diaminodiphenylmethane as hardener.* Journal of applied polymer science, 2000. 77(10): p. 2097-2103.

5. Liaw, D.J. and W.C. Shen, *Curing of acrylated epoxy resin based on bisphenol-S.* Polymer Engineering & Science, 1994. 34(16): p. 1297-1303.

6. Montserrat, S. and J. Málek, *A kinetic analysis of the curing reaction of an epoxy resin.* Thermochimica acta, 1993. 228: p. 47-60.

7. Roşu, D., F. Mustată, and C.N. Caşcaval, *Investigation of the curing reactions of some multifunctional epoxy resins using differential scanning calorimetry.* Thermochimica Acta, 2001. 370(1-2): p. 105-110.

8. Guo, Q., et al., *Miscibility, crystallization kinetics and real-time small-angle X-ray scattering investigation of the semicrystalline morphology in thermosetting polymer blends of epoxy resin and poly (ethylene oxide).* Polymer, 2001. 42(9): p. 4127-4140.

9. Horng, T.J. and E.M. Woo, *Effects of network segment structure on the phase homogeneity of crosslinked poly (ethylene oxide)/epoxy networks.* Polymer, 1998. 39(17): p. 4115-4122.

10. Kalogeras, I.M., et al., *Dielectric properties of cured epoxy resin+ poly (ethylene oxide) blends.* Journal of non-crystalline solids, 2005. 351(33-36): p. 2728-2734.

11. Luo, X., et al., *Miscibility of epoxy resins/poly (ethylene oxide) blends cured with phthalic anhydride.* Polymer, 1994. 35(12): p. 2619-2623.

12. Sixun, Z., et al., *Epoxy resin/poly(ethylene oxide) blends cured with aromatic amine.* Polymer, 1995. 36(18): p. 3609-3613.

13. Gan, Y. and X. Jiang, *Photo-cured Materials from Vegetable Oils.* 2014.

14. De, B. and N. Karak, *Novel high performance tough hyperbranched epoxy by an*

A 2+ *B* 3 *polycondensation reaction.* Journal of Materials Chemistry A, 2013. 1(2): p. 348-353.

15. De, B. and N. Karak, *Ultralow dielectric, high performing hyperbranched epoxy thermosets: synthesis, characterization and property evaluation.* RSC Advances, 2015. 5(44): p. 35080-35088.

16. Seiler, M., *Hyperbranched polymers: Phase behavior and new applications in the field of chemical engineering.* Fluid Phase Equilibria, 2006. 241(1): p. 155-174.

17. Ebnesajjad, S. and A.H. Landrock, *Adhesives technology handbook.* 2 0 1 4 : William Andrew.

18. Ebnesajjad, S. and A.H. Landrock, *Chapter* 1 *- Introduction and Adhesion Theories*, in *Adhesives Technology Handbook (Third Edition)*, S. Ebnesajjad and A.H. Landrock, Editors. 2015, William Andrew Publishing: Boston. p. 1-18.

19. Petrie, E.M., *Epoxy adhesive formulations.* 2005: McGraw Hill Professional.

20. Moon, J.H., et al., *A study on UV-curable adhesives for optical pick-up: I. Photo-initiator effects.* International journal of adhesion and adhesives, 2 0 0 5 . 25(4): p. 301-312.

21. Decker, C., *Photoinitiated crosslinking polymerisation.* Progress in polymer science, 1996. 21(4): p. 593-650.

22. Decker, C. and K. Moussa, *Kinetic study of the cationic photopolymerization of epoxy monomers.* Journal of Polymer Science Part A: Polymer Chemistry, 1990. 28(12): p. 3429-3443.

23. Crivello, J.V., *UV and electron beam-induced cationic polymerization.* Nuclear Instruments and Methods in Physics Research Section B: Beam Interactions with Materials and Atoms, 1999. 151(1-4): p. 8-21.

24. Ficek, B.A., A.M. Thiesen, and A.B. Scranton, *Cationic photopolymerizations of thick polymer systems: Active center lifetime and mobility.* European polymer journal, 2008. 44(1): p. 98-105.

25. Sasaki, H., *Curing properties of cycloaliphatic epoxy derivatives.* Progress in organic coatings, 2007. 58(2-3): p. 227-230.

26. Vidil, T., et al., *Control of reactions and network structures of epoxy thermosets.* Progress in Polymer Science, 2016. 62: p. 126-179.

27. Crivello, J.V. and U. Bulut, *Dual photo-and thermally initiated cationic polymerization of epoxy monomers.* Journal of Polymer Science Part A: Polymer Chemistry, 2006. 44(23): p. 6750-6764.

28. Mariani, A., et al., *UV-ignited frontal polymerization of an epoxy resin.* Journal of Polymer Science Part A: Polymer Chemistry, 2004. 42(9): p. 2066-2072.

29. Chiang, T.H. and T.E. Hsieh, *A study of monomer's effect on adhesion strength of UV-curable resins.* International journal of adhesion and adhesives, 2006. 26(7): p. 520-531.

30. Chiang, T.H. and T.E. Hsieh, *A study of UV-curable epoxide resins containing thermal accelerator–Tertiary amines.* Reactive and Functional Polymers, 2008. 68(2): p. 601-612.

31. Decker, C., *UV-radiation curing of adhesives*, in *Handbook of Adhesives and Surface Preparation*. 2011, Elsevier. p. 221-243.

32. Peeters, S., *Overview of dual-cure and hybrid-cure systems in radiation curing.* Radiation Curing in Polymer Science and Technology, 1993. 3: p. 177-217.

33. Sbirrazzuoli, N. and S. Vyazovkin, *Learning about epoxy cure mechanisms from isoconversional analysis of DSC data.* Thermochimica Acta, 2002. 388(1-2): p. 289-298.

34. Ghaffari, M., et al., *The kinetic analysis of isothermal curing reaction of an epoxy resin-glassflake nanocomposite.* Thermochimica acta, 2012. 549: p. 81-86.

35. Vyazovkin, S., et al., *ICTAC Kinetics Committee recommendations for performing kinetic computations on thermal analysis data.* Thermochimica acta, 2011. 520(1-2): p. 1-19.

36. Perez-Maqueda, L.A., J.M. Criado, and P.E. Sanchez-Jimenez, *Combined kinetic analysis of solid-state reactions: a powerful tool for the simultaneous determination of kinetic parameters and the kinetic model without previous assumptions on the reaction mechanism.* The Journal of Physical Chemistry A, 2006. 110(45): p. 12456-12462.

37. Kamal, M.R., *Thermoset characterization for moldability analysis.* Polymer Engineering & Science, 1974. 14(3): p. 231-239.

38. Chambon, F. and H.H. Winter, *Linear viscoelasticity at the gel point of a crosslinking PDMS with imbalanced stoichiometry.* Journal of Rheology, 1987. 31(8): p. 683-697.

39. Winter, H.H., *Can the gel point of a cross-linking polymer be detected by the G'–G "crossover?* Polymer Engineering & Science, 1987. 27(22): p. 1698-1702.

40. Rubinstein, M. and R.H. Colby, *Polymer physics.* Vol. 23. 2003: Oxford university press New York.

41. Luo, X., et al., *The relationship between the degree of branching and glass transition temperature of branched polyethylene: experiment and simulation.* Polymer Chemistry, 2014. 5(4): p. 1305-1312.

42. Luo, X., et al., *Effect of branching architecture on glass transition behavior of*

hyperbranched copolystyrenes: the experiment and simulation studies. Chinese Journal of Polymer Science, 2016. 34(1): p. 77-87.

43.   Gong, W., et al., *Effect of the degree of branching on atomic-scale free volume in hyperbranched poly [3 -ethyl-3 -(hydroxymethyl) oxetane]. A positron study.* Macromolecules, 2005. 38(23): p. 9644-9649.

44.   Astm, D., 1 6 5 2 -9 7 . Standard Test Methods for Epoxy Content of Epoxy Resins.''June, 1997.

45.   Hammouda, B., *A tutorial on small-angle neutron scattering from polymers.* Gaithersburg: National Institute of Standards and Technology, 1995.

46.   Svoboda, P., *Influence of branching density in ethylene-octene copolymers on electron beam crosslinkability.* Polymers, 2015. 7(12): p. 2522-2534.

47.   Beamish, J.A., et al., *The effects of monoacrylated poly(ethylene glycol) on the properties of poly(ethylene glycol) diacrylate hydrogels used for tissue engineering.* Journal of biomedical materials research. Part A, 2010. 92(2): p. 441-450.

48.   Zhang, C., et al., *Multi-walled carbon nanotube in a miscible PEO/PMMA blend: Thermal and rheological behavior.* Polymer Testing, 2019. 75: p. 367-372.

49.   Shi, Y., et al., *Investigate the glass transition temperature of hyperbranched copolymers with segmented monomer sequence.* Macromolecules, 2016. 49(12): p. 4416-4422.

50.   Samthong, C., R.M. Laine, and A. Somwangthanaroj, *Synthesis and characterization of organic/inorganic epoxy nanocomposites from poly(aminopropyl/phenyl)silsesquioxanes.* Journal of Applied Polymer Science, 2013. 128(6): p. 3601-3608.

51.   Nabae, Y. and M.-a. Kakimoto, *Design and Synthesis of Hyperbranched Aromatic Polymers for Catalysis.* Polymers, 2018. 10(12): p. 1344.

52.   Cai, H., et al., *Curing kinetics study of epoxy resin/flexible amine toughness systems by dynamic and isothermal DSC.* Thermochimica Acta, 2008. 473(1-2): p. 101-105.

53.   Deng, Y. and G.C. Martin, *Diffusion and diffusion-controlled kinetics during epoxy-amine cure.* Macromolecules, 1994. 27(18): p. 5147-5153.

54.   Lin, M.-S., et al., *Optically clear simulataneous interpenetrating polymer networks based on poly(ethylene glycol) diacrylate and epoxy. II. Kinetic study.* 1993. 31(13): p. 3317-3325.

55.   Yu, A.Z., J.M. Sahouani, and D.C. Webster, *Highly functional methacrylated bio-based resins for UV-curable coatings.* Progress in Organic Coatings, 2 0 1 8 .

122: p. 219-228.

56. El-hefian, E.A., M.M. Nasef, and A.H. Yahaya, *Rheological and morphological studies of chitosan/agar/ poly (vinyl alcohol) blends.* Journal of Applied Sciences Research, 2010. 6(5): p. 460-468.

57. Wang, Y., et al., *Controllability of epoxy equivalent weight and performance of hyperbranched epoxy resins.* Composites Part B: Engineering, 2019. 160: p. 615-625.

58. Bulut, U. and J.V. Crivello, *Investigation of the Reactivity of Epoxide Monomers in Photoinitiated Cationic Polymerization.* Macromolecules, 2005. 38(9): p. 3584-3595.

59. Ganjaee Sari, M., et al., *Dynamic mechanical behavior and nanostructure morphology of hyperbranched-modified polypropylene blends.* Polymer International, 2014. 63(2): p. 195-205.

60. Han, K., et al., *Study on hyperbranched polyesters as rheological modifier for Spandex spinning solution.* Polymer international, 2006. 55(8): p. 898-903.

61. Jafarifard, S., et al., *The chemo-rheological behavior of an acrylic based UV-curable inkjet ink: Effect of surface chemistry for hyperbranched polymers.* Progress in Organic Coatings, 2016. 90: p. 399-406.

62. Li, T., et al., *Hyperbranched polyester as additives in filled and unfilled epoxy-novolac systems.* Polymer, 2012. 53(25): p. 5864-5872.

63. Sari, M.G., et al., *Modification of poly (propylene) by grafted polyester-amide-based dendritic nanostructures with the aim of improving its dyeability.* Journal of Applied Polymer Science, 2012. 124(3): p. 2449-2462.

64. Ebewele, R.O., *Polymer additives and reinforcements.* Polymer science and technology. Boca Raton: CRC Press, 2000: p. 483.

APPENDIX

Appendix A
Preparation of epoxy mixture for thermal cure

The ratio of epoxy to DETA curing agent was 1:1 molar ratio of active functional groups. The weight of amine curing agent of each system could be calculated by Eq. (A.1). Epoxy Wt is the weight of epoxy and phr amine is evaluated by Eq. (A.2). Moreover, epoxy equivalent weight (EEW) of the mixture and NH-group equivalent can be calculated by Eq. (A.3) – (A.4), respectively.

$$\text{curing agent Wt} = \frac{\text{epoxy Wt} \times \text{phr amine}}{100} \tag{A.1}$$

$$\text{phr amine} = \frac{\text{NH equivalent}}{\text{EEW}} \times 100 \tag{A.2}$$

$$\text{EEW of mixture} = \frac{\text{Total Wt}}{\dfrac{\text{Wt}_a}{\text{EEW}_a} + \dfrac{\text{Wt}_b}{\text{EEW}_b}} \tag{A.3}$$

$$\text{NH equivalent} = \frac{\text{Mw of amine curing agent}}{\text{Amount of NH-group}} \tag{A.4}$$

จุฬาลงกรณ์มหาวิทยาลัย

CHULALONGKORN UNIVERSITY

Appendix B
Data of photo-rheological properties
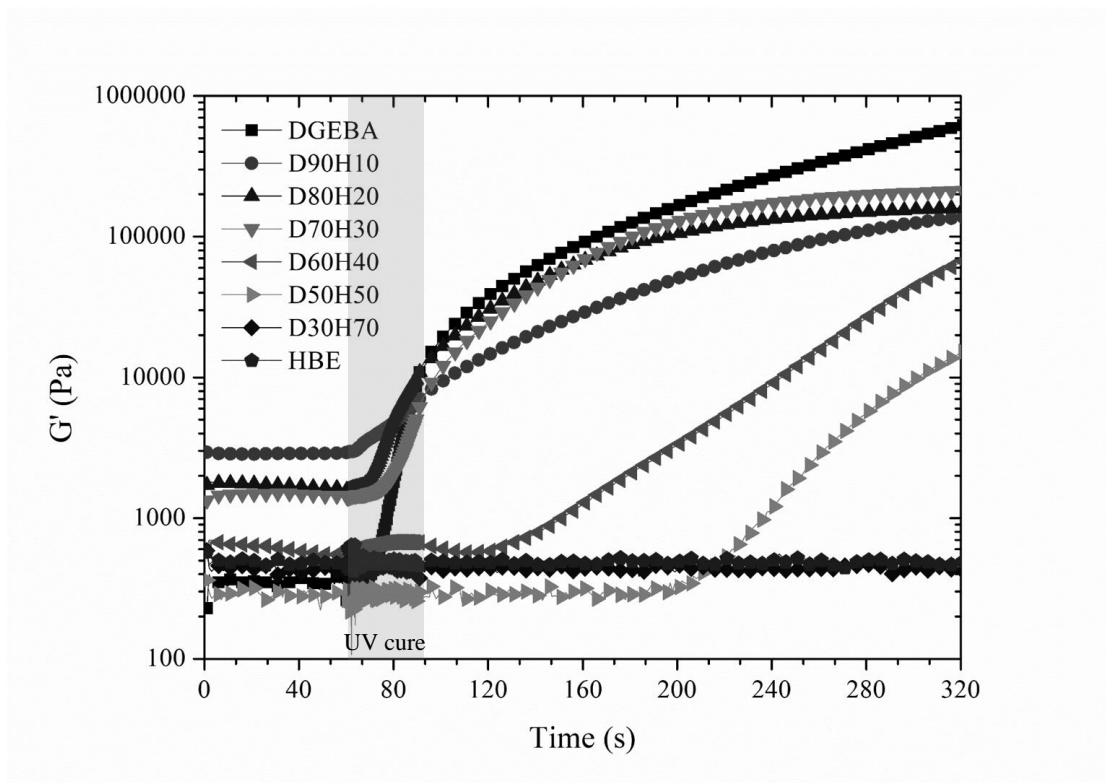
Figure B.1 Growth of storage modulus at the various ratio of DGEBA and hyperbranched epoxy resins
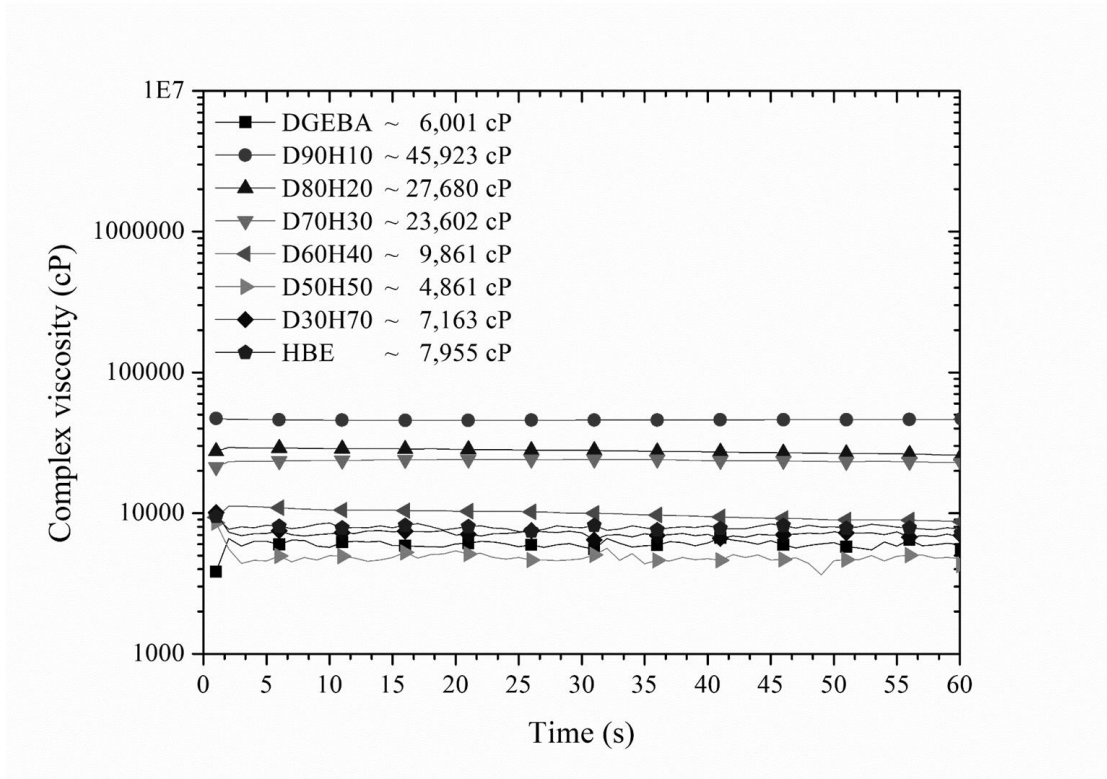
Figure B.2 The initial complex viscosity at the various ratio of DGEBA and hyperbranched epoxy resins
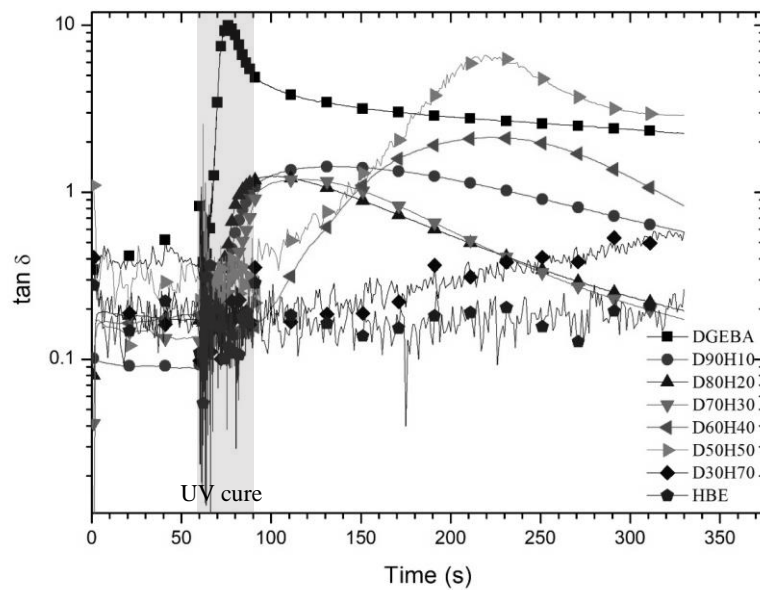
Figure B.3 tanδ at the various ratio of DGEBA and hyperbranched epoxy resins

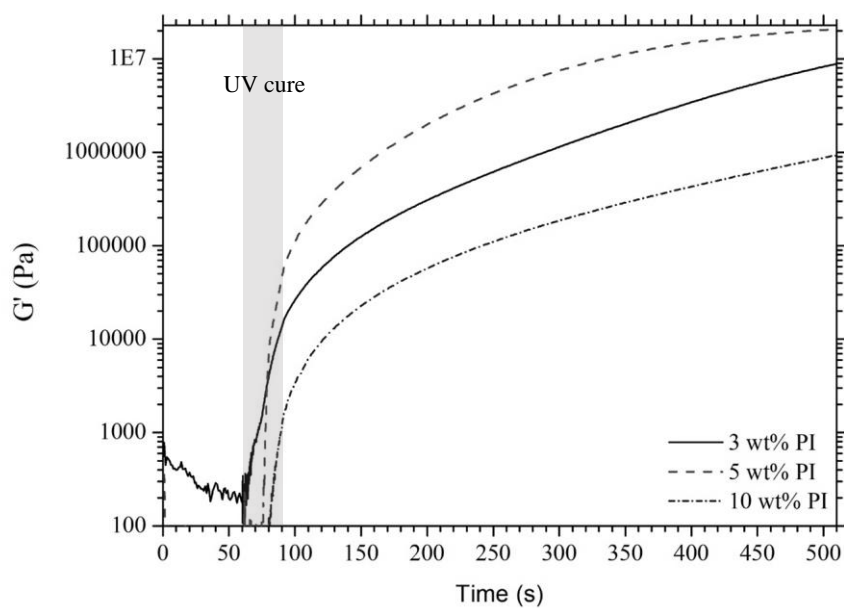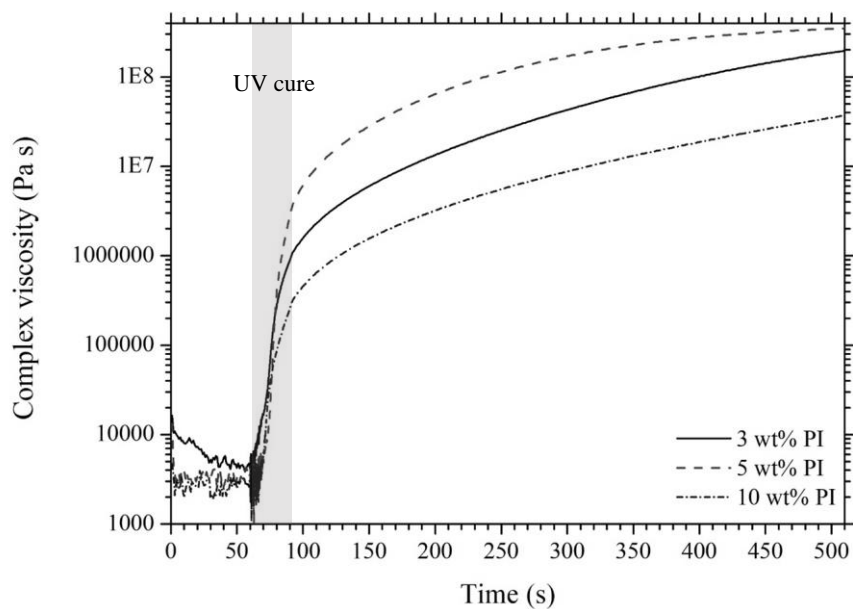Figure B.4 Growth of storage modulus of D90H10 with various PI contents
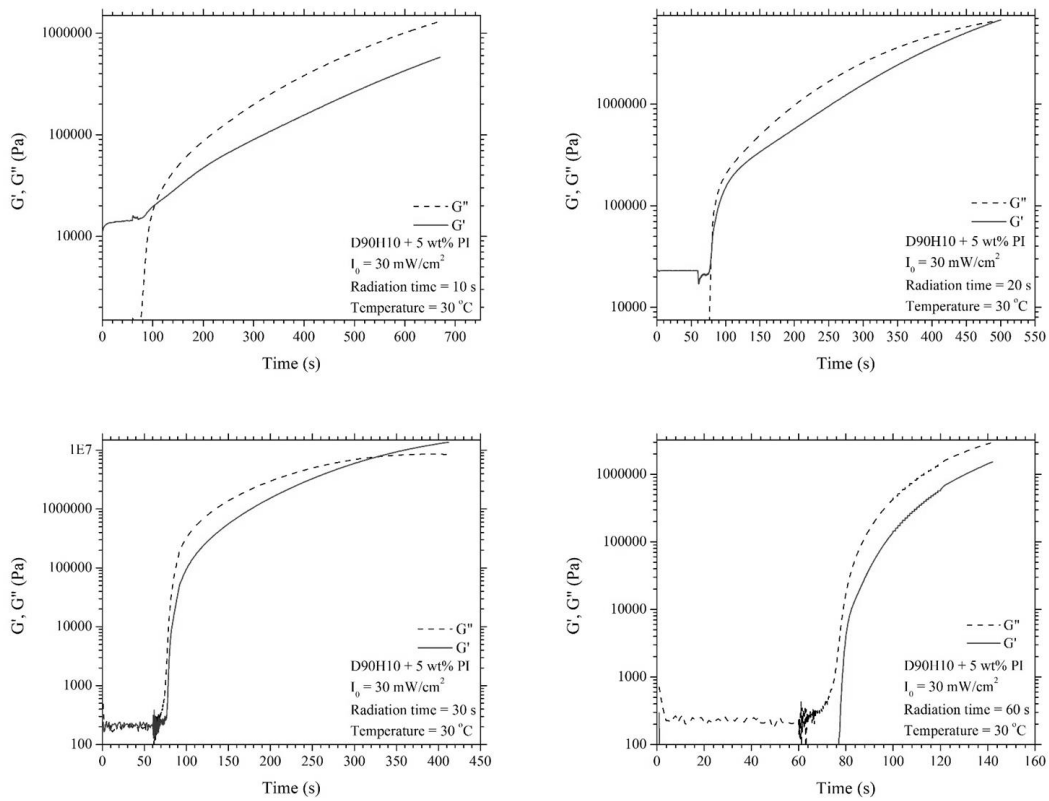

Figure B.5 Growth of complex viscosity of D90H10 with various PI contents

Figure B.6 G' and G" of D90H10 with 5 wt% PI at UV intensity of 30 mW/cm^2, the temperature of 30 °C, and various irradiation time
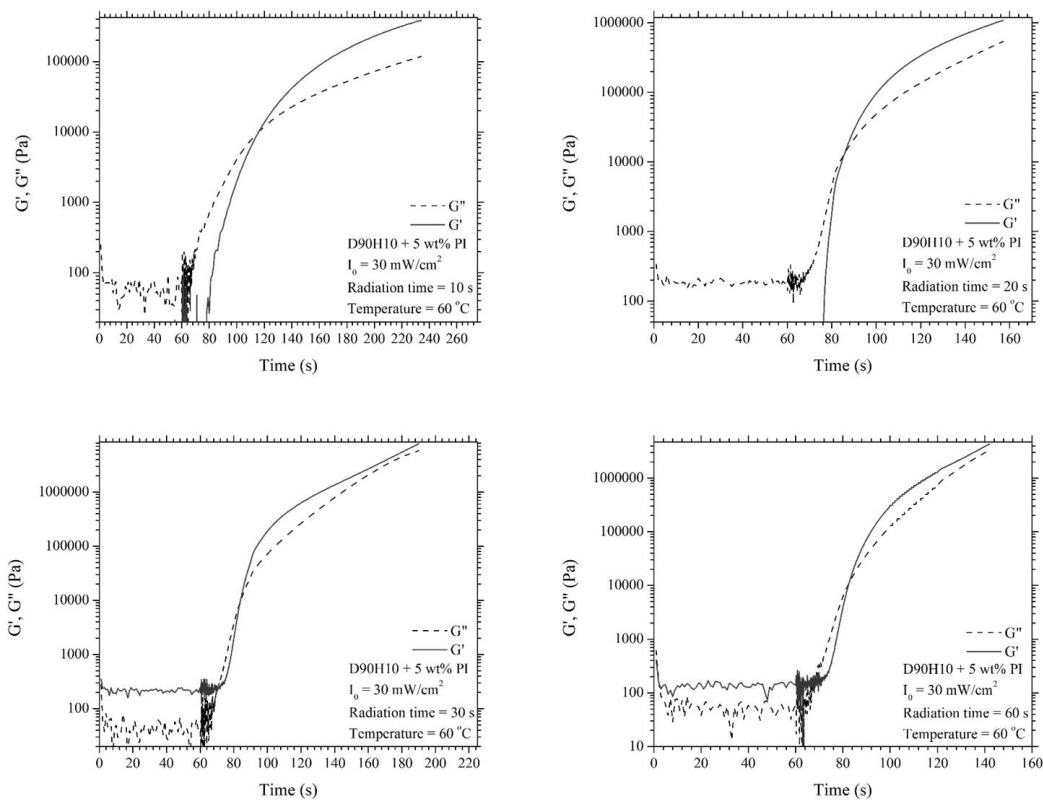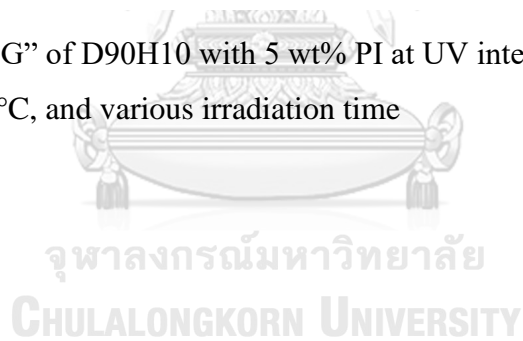
Figure B.7 G' and G" of D90H10 with 5 wt% PI at UV intensity of 30 mW/cm^2, the temperature of 60 °C, and various irradiation time
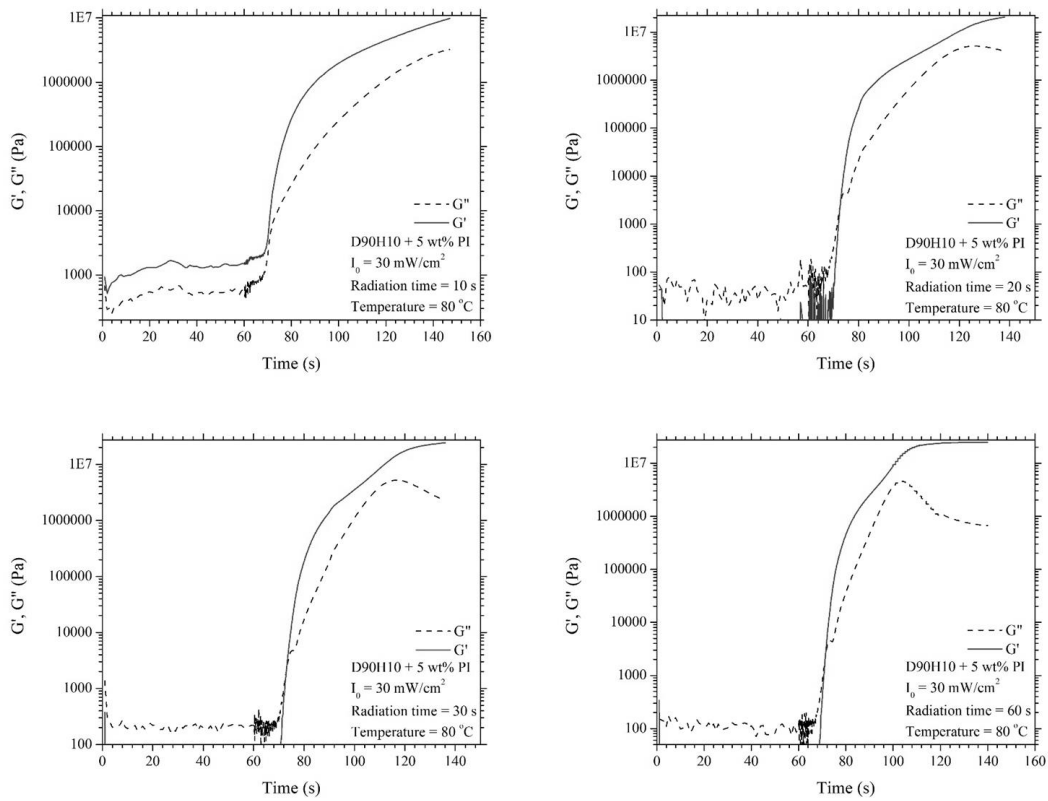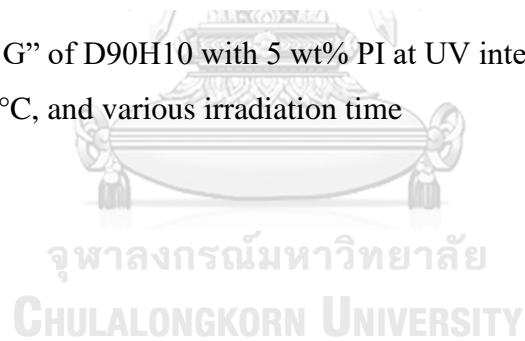
Figure B.8 G' and G" of D90H10 with 5 wt% PI at UV intensity of 30 mW/cm^2, the temperature of 80 °C, and various irradiation time
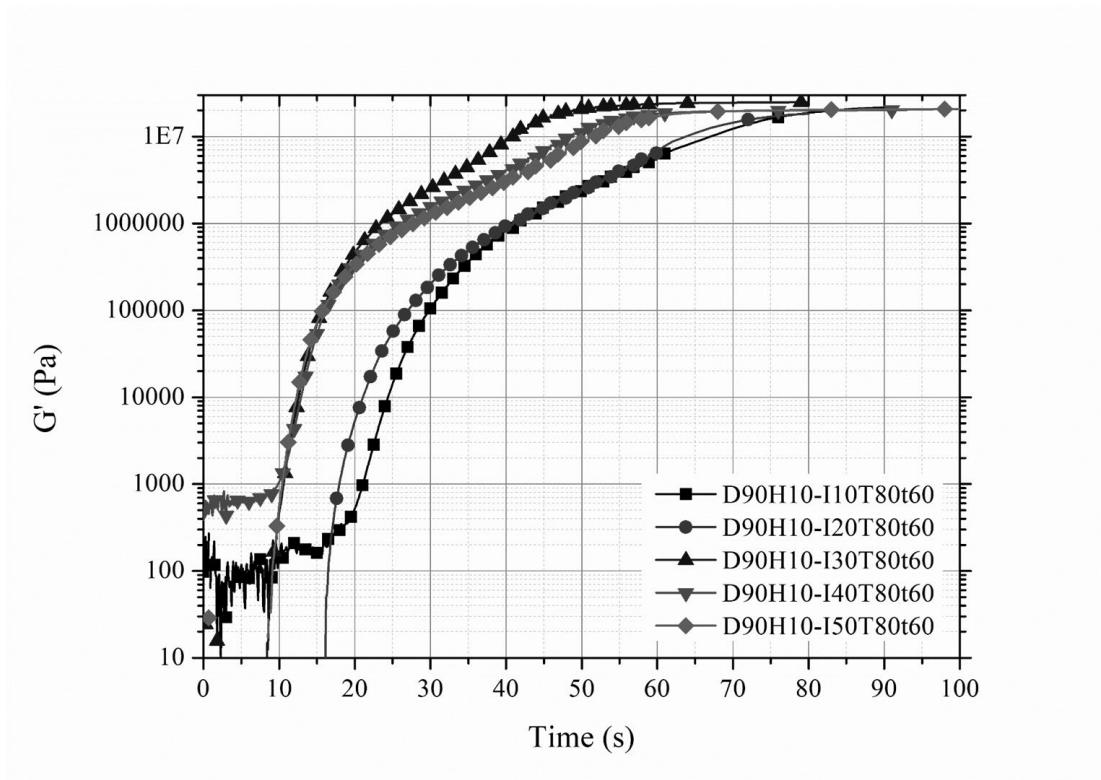
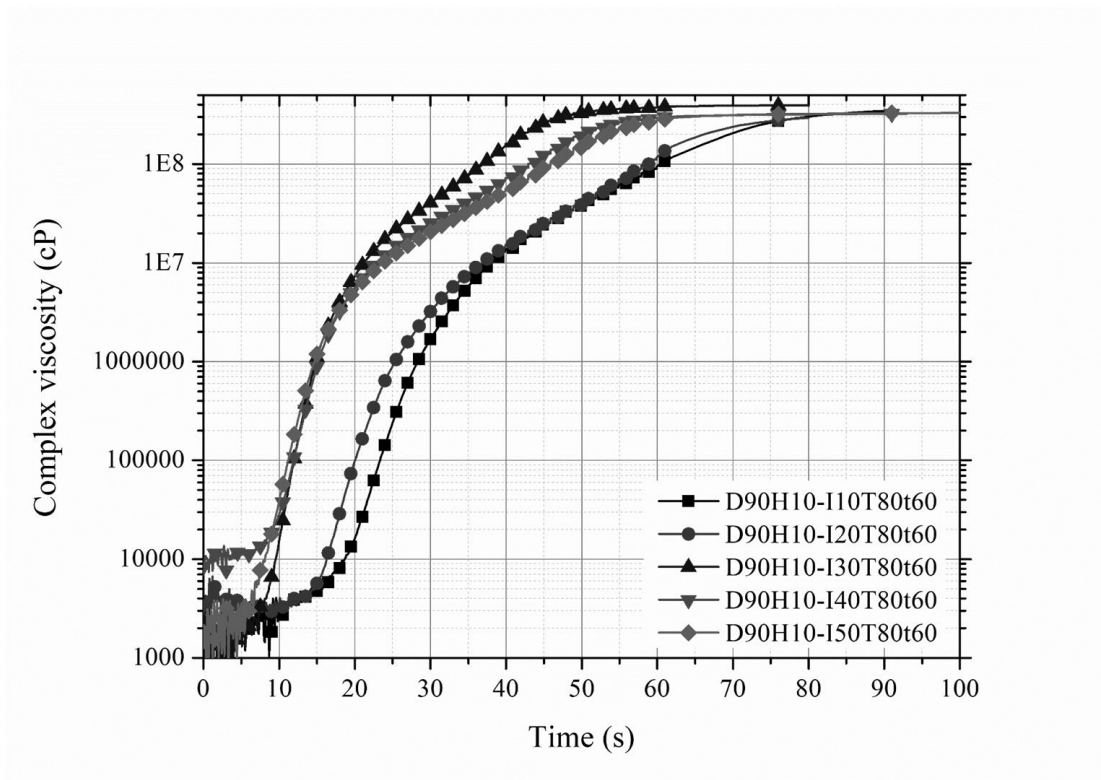Figure B.9 Growth of storage modulus of D90H10 with 5 wt% PI at various UV
intensities

Figure B.10 Growth of complex viscosity of D90H10 with 5 wt% PI at various UV intensities
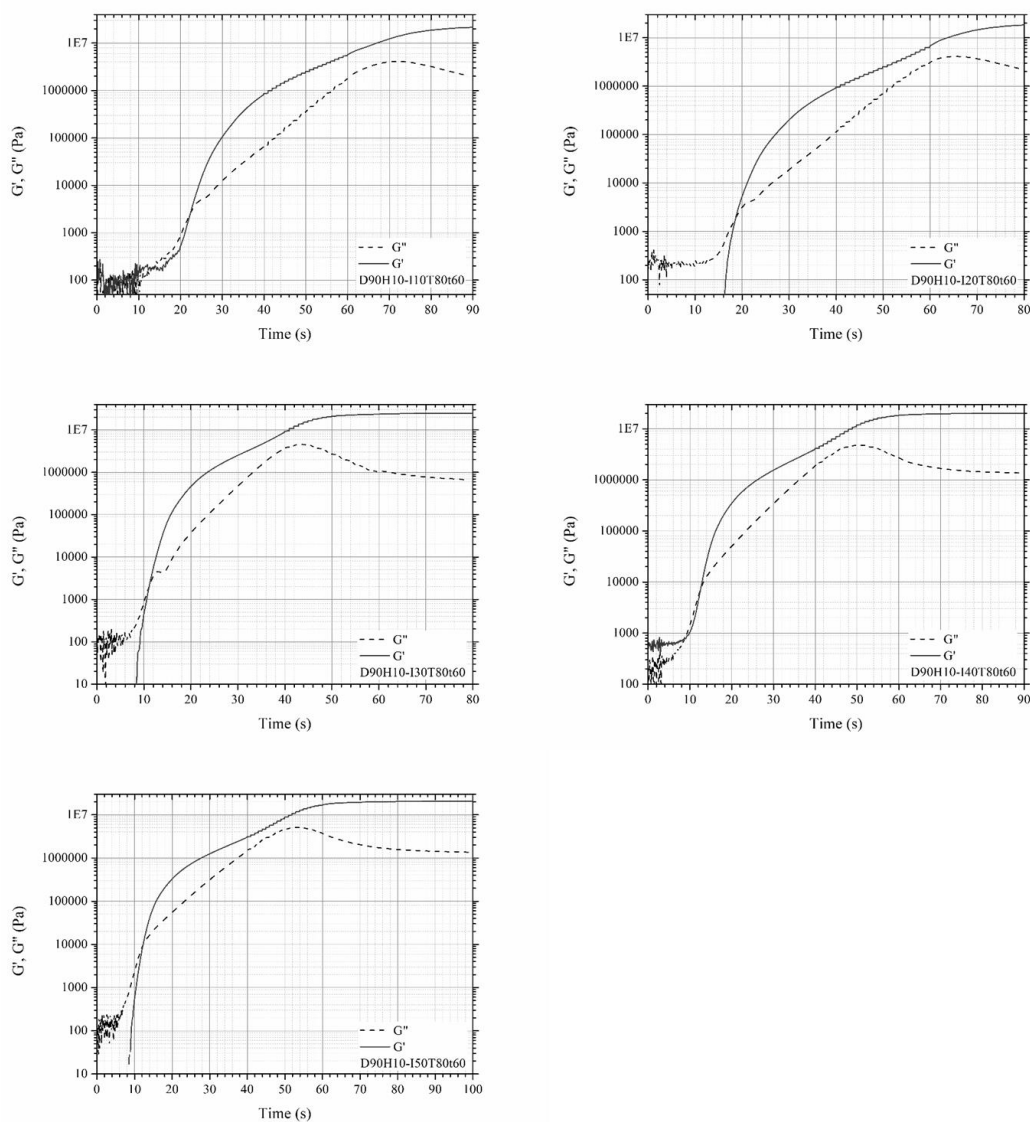
Figure B.11 G' and G" of D90H10 with 5 wt% PI at various UV intensities
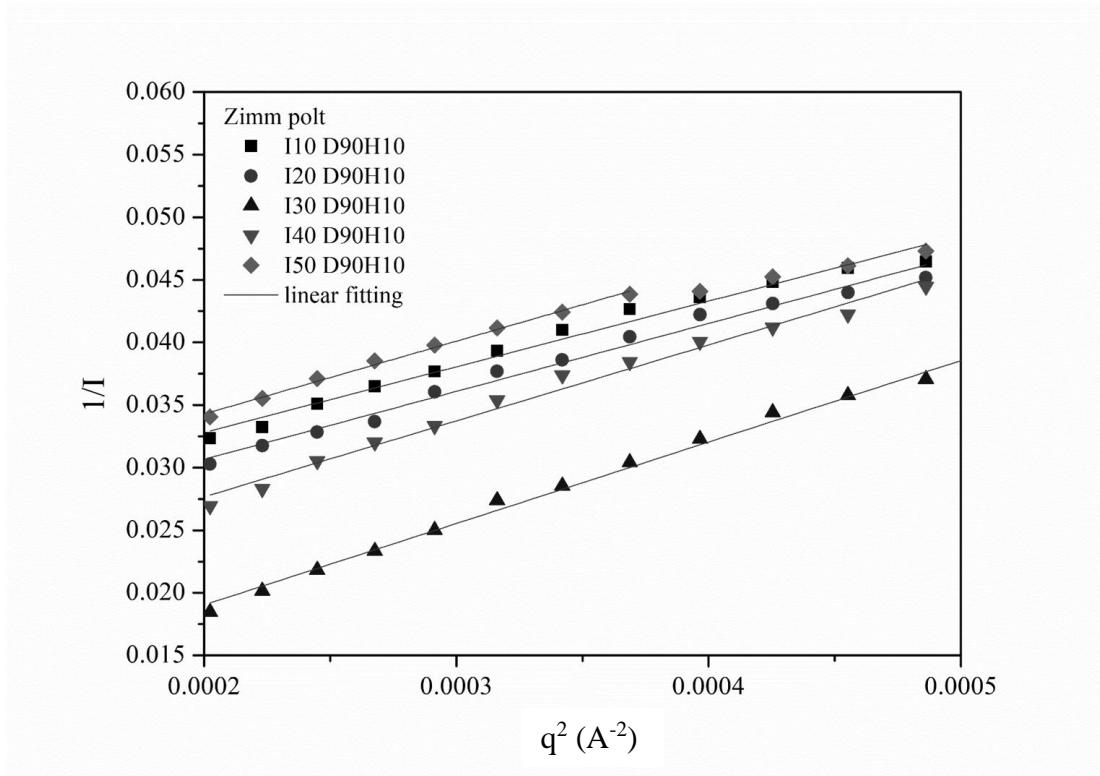
Appendix C

Data of SAXS measurement

Figure C.1 Zimm plot of D90H10 at various UV intensities

Table C.1 The parameter from Zimm plot and Ornstein-Zernike model

UV intensity (mW/cm^2)	Low q (Zimm plot [1/I - q^2])*				
	slope	intercept	I$_0$	ξ (nm)	R$_g$ (nm)
10	52.44	0.0223	44.78	4.846	8.39
20	54.26	0.0198	50.45	5.232	9.06
30	65.04	0.0060	165.84	10.386	18.00
40	60.65	0.0155	64.35	6.247	10.80
50	58.16	0.0227	44.13	5.066	8.780

VITA

NAME   Tossapol Boonlert-uthai

DATE OF BIRTH   27 June 1988

PLACE OF BIRTH   Bangkok, Thailand

INSTITUTIONS   Bachelor's degree and master's degree in Chemical
ATTENDED   Engineering at Chulalongkorn University
HOME ADDRESS   33 (99/24) Ramintra Road, Kannayao, Bangkok, Thailand
                          10230

PUBLICATION   Boonlert-uthai, T.; Samthong, C.; Somwangthanaroj, A.
Synthesis, Thermal Properties and Curing Kinetics of
Hyperbranched BPA/PEG Epoxy Resin. Polymers 2019,
11, 1545.